Vol. 68 • No. 3

March 2025

# Microwave Journal

## CAUTION Going Terahertz Test Carefully

**SPECIAL FOCUS: Cables & Connectors**

horizon house®

Founded in 1958

mwjournal.com

## MILLER MMIC — Advancing RF MMIC Design Through Human-AI collaboration and competition

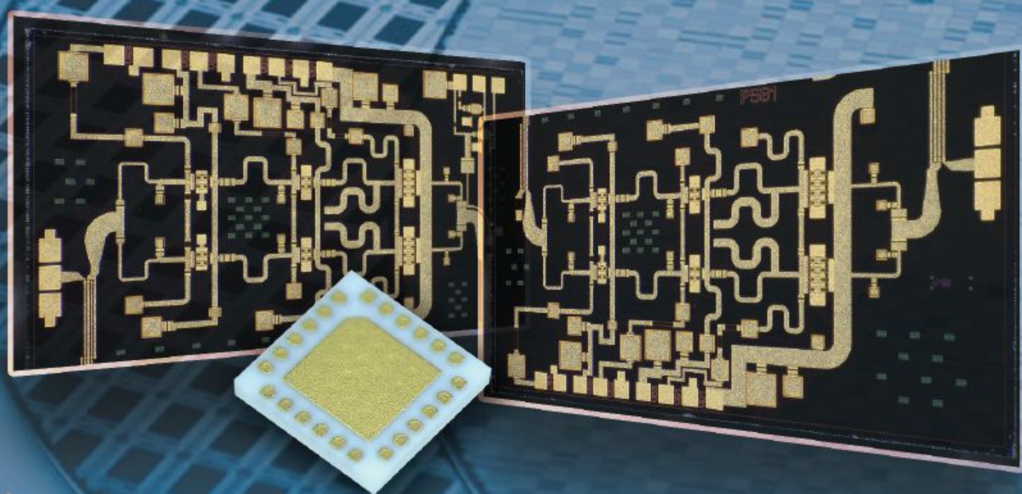

**Miller MMIC** is a global provider of RF semiconductor solutions with expertise in GaAs and GaN processes. We offer a diverse range of products tailored to various wireless applications. Our product lineup encompasses a wide array of offerings, including Low Noise Amplifiers, Distributed Amplifiers, Power Amplifiers, Driver Amplifiers, RF Switches, RF PIN Diode Switches, and numerous other voltage- and digitally-controllable RF components.

## RapidRF MILLER MMIC RapidRF AI Platform for RF MMIC Design

### RF Distributed Low Noise Amplifiers

| PN | Freq Low (GHz) | Freq High (GHz) | Gain (dB) | NF(dB) | P1dB (dBm) | Voltage (VDC) | Current (mA) | Package |
|---|---|---|---|---|---|---|---|---|
| MMW001T | DC | 20.0 | 17~19 | 1~3.5 | 23 @ 10GHz | 8.0 | 145 | die |
| MMW4FP | DC | 50.00 | 16.00 | 4.00 | 24.00 | 10 | 200 | die |
| MMW507 | 0.20 | 22.0 | 14.0 | 4 - 6 | 28.0 | 10.0 | 350 | die |
| MMW508 | DC | 30.0 | 14.0 | 2.5dB @ 15GHz | 24.5 | 10.0 | 200 | die |
| MMW509 | 30KHz | 45.0 | 15.0 | | 20.0 | 6.0 | 190 | die |
| MMW510 | DC | 45.0 | 11.0 | 4.5 | 15.5 | 6.0 | 100 | die |
| MMW510F | DC | 30.00 | 20.00 | 2.50 | 22.00 | | | die |
| MMW511 | 0.04 | 65.0 | 10.0 | 9.0 | 18.0 | 8.0 | 250 | die |
| MMW512 | DC | 65.0 | 10.0 | 5.0 | 14.5 | 4.5 | 85 | die |
| MMW5FN | DC | 67.00 | 14.00 | 2.00 | 19.00 | 4.5 | 81 | die |
| MMW5FP | DC | 67.00 | 14.00 | 4.00 | 21.00 | 8 | 140 | die |
| MMW011 | DC | 12.0 | 14.0 | | 30.5 | 12.0 | 350 | die |

### Low Noise Amplifiers

| PN | Freq Low (GHz) | Freq High (GHz) | Gain (dB) | NF(dB) | P1dB (dBm) | Voltage (VDC) | Current (mA) | Package |
|---|---|---|---|---|---|---|---|---|
| MML040 | 6.0 | 18.0 | 24.0 | 1.5 | 14.0 | 5.0 | 35 | die |
| MML058 | 1.0 | 18.0 | 15.0 | 1.7 | 17.0 | 5.0 | 35 | die |
| MML063 | 18.0 | 40.0 | 11.0 | 2.9 | 15.0 | 5.0 | 52 | die |
| MML080 | 0.8 | 18.0 | 16.5/15.5 | 1.9/1.7 | 18/17.5 | 5.0 | 65/40 | die |
| MML081 | 2.0 | 18.0 | 25/23 | 1.0/1.0 | 16/9.5 | 5.0 | 37/24 | die |
| MML083 | 0.1 | 20.0 | 23.0 | 1.6 | 11.0 | 5.0 | 58 | die |

### RF Driver Amplifier

| PN | Freq Low (GHz) | Freq High (GHz) | Gain (dB) | NF(dB) | P1dB (dBm) | Voltage (VDC) | Current (mA) | Package |
|---|---|---|---|---|---|---|---|---|
| MM3006 | 2.0 | 20.0 | 19.5 | 2.5 | 22.0 | 7.0 | 130 | die |
| MM3014 | 6.0 | 20.0 | 15.0 | - | 19.5 | 5.0 | 107 | die |
| MM3017T | 17.0 | 43.0 | 25.0 | | 22.0 | 5.0 | 140 | die |
| MM3031T | 20.0 | 43.0 | 20.0 | | 24.0 | 5.0 | 480 | die |
| MM3051 | 17.0 | 24.0 | 25.0 | - | 25.0 | 5.0 | 220 | die |
| MM3058 | 18.0 | 40.0 | 20/19.5 | 2.5/2.3 | 16/14 | 5/4 | 69/52 | die |
| MM3059 | 18.0 | 40.0 | 16/16 | 2.5/2.3 | 16/15 | 5/4 | 67/50 | die |

### GaAs Medium Power Amplifier

| PN | Freq Low (GHz) | Freq High (GHz) | Gain (dB) | P1dB (dBm) | Psat (dBm) | Voltage (VDC) | Current (mA) | Package |
|---|---|---|---|---|---|---|---|---|
| MMP107 | 17.0 | 21.0 | 19.0 | 30.0 | 30.0 | 6.0 | 400 | die |
| MMP108 | 18.0 | 28.0 | 14.0 | 31.5 | 31.0 | 6.0 | 650 | die |
| MMP111 | 26.0 | 34.0 | 25.5 | 33.5 | 33.5 | 6.0 | 1300 | die |
| MMP112 | 2.0 | 6.0 | 20.0 | 31.5 | 32.0 | 8.0 | 365 | die |
| MMP501 | 20.0 | 44.0 | 15.0 | 27 -- 32 | 29 - 34 | 5.0 | 1200 | die |
| MMP502 | 18.0 | 47.0 | 14.0 | 28.0 | 30.0 | 5.0 | 1500 | die |

### PN: MMW5FP
RF GaAs MMIC DC-67GHz

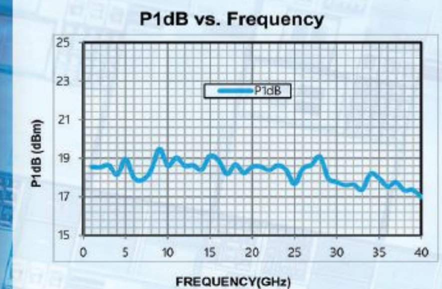


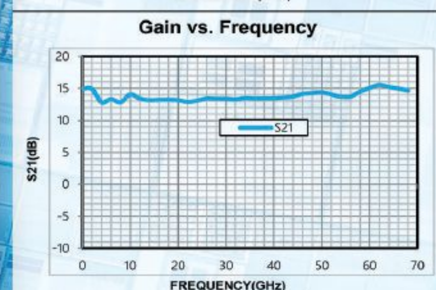


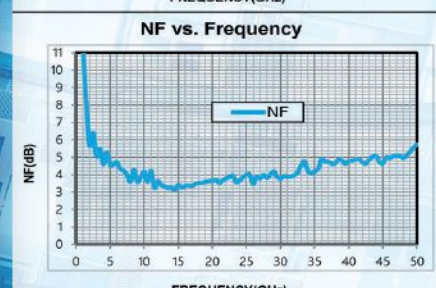


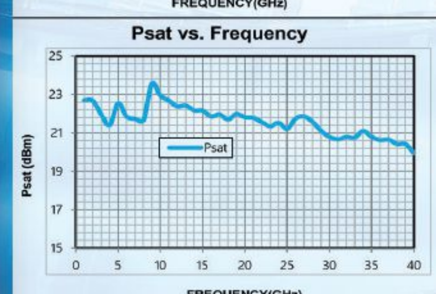



CALL US 1-833-2MILLER(264-5537)
WWW.MILLERMMIC.COM

RapidRF

sales@millermmic.com
support@millermmic.com


DC TO 110 GHz

# RF & Microwave Test Accessories

One-Stop Shopping from R&D to Production

LEARN MORE

**ADAPTERS**
Coax & Waveguide

**AMPLIFIERS**
DC to 110 GHz

**ATTENUATORS**
DC to 65 GHz

**GAUGES, CAL KITS & WRENCHES**

**BIAS TEES**
0.1 MHz to 54 GHz

**CABLES**
Test Leads
& System Cables

**COUPLERS**
0.005 MHz to 65 GHz

**DC BLOCKS**
0.1 MHz to 65 GHz

**EQUALIZERS**
DC to 40 GHz

**FILTERS**
DC to 86 GHz

**HYBRIDS, 90° & 180°**
0.01 to 4200 MHz

**IMPEDANCE MATCHING PADS**
DC to 3000 MHz

**LIMITERS**
0.2 to 8200 MHz

**MIXERS**
0.0005 MHz to 65 GHz

**MODULATORS & DEMODULATORS**
1 to 200 MHz

**MULTIPLIERS**
0.05 MHz to 20 MHz

**PHASE DETECTORS**
1 MHz to 100 MHz

**PHASE SHIFTERS**
250 MHz to 430 MHz

**POWER DETECTORS**
10 MHz to 43.5 GHz

**POWER SPLITTERS & COMBINERS**
DC to 67 GHz

**SWITCHES**
DC to 67 GHz

**TERMINATIONS**
DC to 65 GHz

**TRANSFORMERS & BALUNS**
DC to 2500 MHz

Mini-Circuits®


RF-LAMBDA
THE LEADER OF RF BROADBAND SOLUTIONS
BROADBAND SSPA / EMC BENCHTOP
SOLID STATE POWER AMPLIFIER
0.1-22GHZ
ULTRA BROADBAND SSPA
RFLUPA01M22GA
4W 0.1-22GHZ
RFLUPA0218GB
20W 1-19GHZ
300W 6-18GHZ SOLID STATE BROADBAND
400W 8-11GHZ
SOLID STATE BROADBAND
0.1-6GHZ VHZ,
UHF, L, S, C BAND
RFLUPA02G06GC
100W 2-6GHZ
RFLUPA0706GD
30W 0.7-6GHZ
MADE IN USA
6-18GHZ C, X, KU BAND
RFLUPA08G11GA
50W 8-11GHZ
RFLUPA0618GD
60W 6-18GHZ
RFLUPA06G12GB
25W 6-12GHZ
18-50GHZ K, KA, V BAND
RFLUPA18G47GC
2W 18-47GHZ
RFLUPA27G34GB
15W 27-34GHZ
RFLUPA47G53GA2
10W 47-53GHZ
RFLUPA27G34GB
30W 18-40GHZ
BENCHTOP RF MICROWAVE SYSTEM POWER AMPLIFIER
RAMP00G06GA- 30W 0.01-6GHZ
RAMP39G48GA- 4W 39-48GHZ
RAMP01G22GA- 8W 1-22GHZ
RAMP27G34GA- 8W 27-34GHZ
www.rflambda.com
sales@rflambda.com
1-888-976-8880
1-972-767-5998
San Diego, CA, US
Carrollton, TX, US
Ottawa, ONT, Canada
Frankfurt, Germany

# Microwave Journal CONTENTS

March 2025
Vol. 68 • No. 3
Test & Measurement +
Cables & Connectors
mwjournal.com


## Cover Feature


**18** **Optimizing D-Band Amplifiers: Diving Into RF Measurement Challenges**
*A. Engelmann*, B. Derat**, M. Lörner** and M. Dietz****
**Institute for Smart Electronics and Systems (LITES), Friedrich-Alexander-Universität; **Rohde & Schwarz; ***Fraunhofer Institute, Electronic Microsystems and Solid-State Technology (EMFT)*


## Special Report


**48** **Analysis of the Test and Measurement Equipment Market**
*Shrikant Mahankar and Kritee Das, MarketsandMarkets*


## Technical Feature


**54** **Recent Advancements in Terahertz Components Fabrication: A Step Toward Next-Generation Communication Systems**
*V. Manimala, Builders Engineering College and N. Gunavathi, National Institute of Technology*


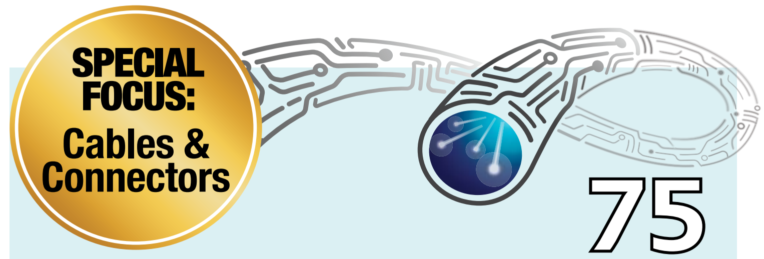



**78** **Evolution of Interconnects in Benchtop RF Test**
*Jim Alexander, Dan Birch and David Beraun, Samtec*

**86** **Supporting Commercial Vehicle Production Through Modular Innovation**
*Robert Weirauch, HUBER+SUHNER*

**94** **Proprietary Connector Design Enhances Quality and Phase Stability**
*Junkosha*

**96** **High-Density Connection Enhances PXIe Test & Measurement**
*The Phoenix Company of Chicago, Inc.*

**100** **Selecting the Right RF Cable Assembly**
*Smiths Interconnect*

**104** **Durable RF Cable Assemblies**
*Swift Bridge Technologies*

**105** **New Products**


## Application Note


**66** **Making Material Measurements with a VNA**
*Brian Walker, Copper Mountain Technologies*


**ACCESS NOW!**
**digital.microwavejournal.com**

eXclusive Digital Content >>>


**High-Selectivity SIW Filters with Controllable Transmission Zeros**
*Qingqing Ye, Institute of Microelectronics of the Chinese Academy of Sciences and University of the Chinese Academy of Sciences; Anmou Liao and Rui Guo, Institute of Microelectronics of the Chinese Academy of Sciences; Zheng Wang and Yongwen Gong, Beijing Smart-Chip Microelectronics Technology Co. Ltd.; Chong Li and Juchuan Guo, State Grid Hebei Marketing Service Center*

**Slotline Radial Stubs Improve the Bandwidth of Balun Bandpass Filters**
*Yubo Wang, Mi Lin and Guohua Liu, School of Electronics and Information, Hangzhou Dianzi University*


68 YEARS OF PUBLISHING EXCELLENCE

# Microwave Journal CONTENTS

mwjournal.com

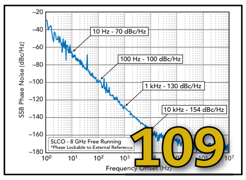



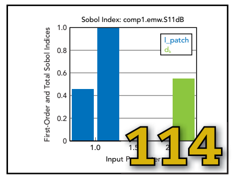


## Product Features


**109** **Sapphire Oscillators Deliver Next-Generation Phase Noise Performance**
*Saetta Labs*

**112** **Unlocking High Frequency Data Acquisition With a 12-bit Digitizer**
*Teledyne SP Devices*

**114** **Using Uncertainty Quantification to Predict Reliability in High Frequency Device Design**
*COMSOL*


## Tech Briefs


**120** **Test Cables Work to 110 GHz**
*Pasternack, an Infinite Electronics brand*

**120** **Antenna Range Spotlights 300 mm Apertures**
*Eravant (formerly Sage Millimeter Inc.)*

**121** **Quantum/Cryogenic Building Blocks**
*KRYTAR*

**122** **Analysis of Mobility and Interactions with Body-worn Devices**
*Remcom Inc.*


## Departments


| | | | |
|---|---|---|---|
| 17 | Mark Your Calendar | 124 | New Products |
| 37 | Defense News | 126 | Book End |
| 41 | Commercial Market | 128 | Ad Index |
| 44 | Around the Circuit | 128 | Sales Reps |
| 123 | Making Waves | 130 | Fabs & Labs |



*Microwave Journal* (USPS 396-250) (ISSN 0192-6225) is published monthly by Horizon House Publications Inc., 685 Canton St., Norwood, MA 02062. Periodicals postage paid at Norwood, MA 02062 and additional mailing offices.





**POSTMASTER:** Send address corrections to Microwave Journal, PO Box 1028, Lowell, MA 01853 or e-mail mwj@e-circ.net.com. Subscription information: (978) 671-0446. This journal is issued without charge upon written request to qualified persons working in the RF & microwave industry. Other subscriptions are: domestic, $130.00 per year, two-year subscriptions, $200.00; foreign, $225.00 per year, two-year subscriptions, $400.00; back issues (if available) and single copies, $20.00 domestic and $30.00 foreign. Claims for missing issues must be filed within 90 days of date of issue for complimentary replacement.





Posted under Canadian international publications mail agreement #PM40612608


## STAFF


**Group Director:** Carl Sheffres

**Associate Publisher:** Michael Hallman

**Media Director:** Patrick Hindle

**Brand & Content Director:** Jennifer DiMarco

**Technical Editor:** Eric Higham

**Associate Technical Editor:** Cliff Drubin

**Editorial & Media Specialist:** Kelley Roche

**Associate Editor:** Kaitlyn Joyner

**Multimedia Staff Editor:** Barbara Walsh

**Electronic Marketing Manager:** Chris Stanfa

**Senior Digital Content Specialist:** Lauren Tully

**Digital Content Specialist:** Vincent Carrabino

**Director of Production & Distribution:** Edward Kiessling

**Art Director:** Janice Levenson

**Graphic Designer:** Ann Pierce

### EUROPE

**Office Manager:** Nina Plesu

### CORPORATE STAFF

**CEO:** William M. Bazzy

**President:** Ivar Bazzy

**Vice President:** Jared Bazzy





**EXECUTIVE EDITORIAL OFFICE**
685 Canton Street, Norwood, MA 02062
Tel: (781) 769-9750
FAX: (781) 769-5037
e-mail: mwj@mwjournal.com

**EUROPEAN EDITORIAL OFFICE**
16 Sussex Street, London SW1V 4RW, England
Tel: Editorial: +44 207 596 8730 Sales: +44 207 596 8740
FAX: +44 207 596 8749

**SUBSCRIPTION SERVICES**
Send subscription inquiries and address changes to:
Tel: (978) 671-0446
e-mail: mwj@e-circ.net


**www.mwjournal.com**

Printed in the USA

# Microwave Journal ONLINE .COM

## eLEARNING CENTER

**Fraunhofer Demo (DD700)** 3/12

**Designing with Juliano and Katerina eLearning Series: Antenna Simulation and Optimization**
*Sponsored by: Ansys* 3/18
**microwavejournal.com/events/2304**

## Executive Interview

**Keith Barclay**, CEO at **Stellant Systems**, discusses his background, the heritage of Stellant Systems, the company's product, technology and market portfolio, along with his vision for the future.

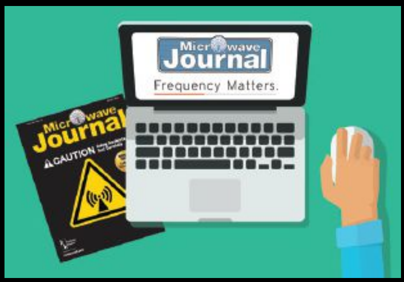


**Catch *Frequency Matters*, the industry update from *Microwave Journal*,**
**microwavejournal.com/FrequencyMatters**

## Join Us Online

Follow us
@Pathindle
@MWJEric
@MWJEditor

Join us at the RF and Microwave Community

Become a fan at facebook.com/microwavejournal

## WHITE PAPERS

Look for additional content from:

KEYSIGHT

## ONLINE PANELS

3/14 **Using AI in the Design of Electronic Systems**

3/28 **AI in RF**


**Microwave Journal podcasts include the RF/microwave update series, Frequency Matters, plus interviews with industry experts and executives.**

https://podcasts.microwavejournal.com

**Visit us @ mwjournal.com**


3H COMM
BPF
17 GHZ
3H 100-829
2018-1875
SN04
3H Communication Systems
SAMPLES



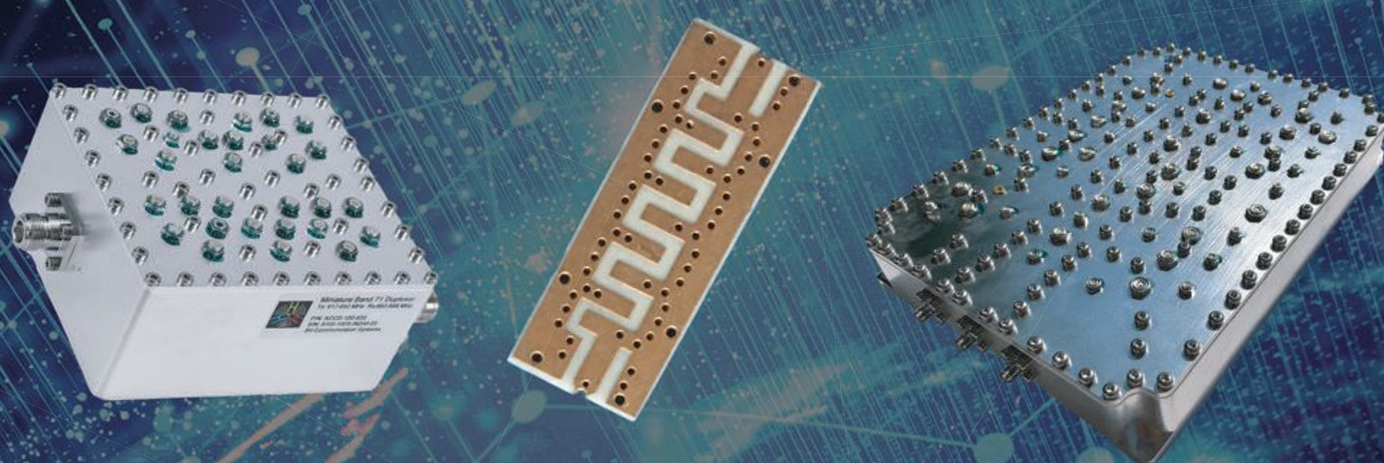

# STAY CONNECTED TO COMING EVENTS

# MARK YOUR CALENDAR

## MARCH

**15-20**
**IPC APEX EXPO 2025**
Anaheim, Calif.
www.ipcapexexpo.org

**25-27**
**EMV**
Stuttgart, Germany
https://emv.mesago.com/events/en.html

**30-4/4**
**EuCAP 2025**
Stockholm, Sweden
www.eucap2025.org

## APRIL

**8-9**
**IEEE Texas Symposium**
Waco, Texas
https://texassymposium.org

**14-15**
**WAMICON**
Cocoa Beach, Fla.
www.ieeewamicon.org

## JUNE

**2-4**
**Space Tech Expo USA**
Long Beach, Calif.
www.spacetechexpo.com

**15-17**
**RFIC 2025**
San Francisco, Calif.
https://rfic-ieee.org

**15-20**
**IMS2025**
San Francisco, Calif.
https://ims-ieee.org

**20**
**ARFTG**
San Francisco, Calif.
http://arftg.org/105-conference

## JULY

**13-18**
**IEEE AP-S/URSI**
Ottawa, Canada
https://2025.apsursi.org/

## ONLINE PANEL SERIES

**3/28**
**AI in RF**

## Call for Papers Deadlines

**3/30** IEEE RFID-TA

**5/9** BCICTS

FOR DETAILS VISIT MWJOURNAL.COM/EVENTS

Cover Feature
Invited Paper

# Optimizing D-Band Amplifiers: Diving Into RF Measurement Challenges

A. Engelmann*, B. Derat**, M. Lörner** and M. Dietz***

*Institute for Smart Electronics and Systems (LITES), Friedrich-Alexander-Universität, Erlangen, Germany

**Rohde & Schwarz, Munich, Germany

***Fraunhofer Institute, Electronic Microsystems and Solid-State Technology (EMFT), Munich, Germany

RF characterization up to D-Band (110 to 170 GHz) is increasingly necessary with the current drive toward 6G wireless communications, high speed digital links and advanced sensing technologies. Considering the sensing use case and the design and optimization of a D-Band power amplifier (PA), this article investigates the measurement challenges accompanying leading-edge RF technology development. The importance of measuring amplifiers with actual load conditions in an on-wafer test environment will be illustrated.

## MMWAVE SINGLE-CONNECT IS THE NEW NORMAL

In 1950, Rohde & Schwarz achieved a remarkable milestone: creating the first vector network analyzer (VNA). This instrument characterized single-port S-parameters to 300 MHz, a breakthrough in RF measurements. Seventy-five years of technological development later, RF design and testing have evolved to where mmWave characterization is the new normal. A single measurement setup captures more than S-parameters and provides a complete performance overview of the device under test (DUT) after one calibration and connection.

Single-touchdown is of the utmost relevance to IC design where costly and fragile die are measured with delicate probing systems. RF components and modules, typically made for matching 50 Ω conditions, are now used in complex, non-ideal environments. It is a common requirement for semiconductor foundries to provide 50 Ω reference specifications and accurate models to enable system integrators and IC designers to achieve the best system performance.

This article discusses challenges in large-signal characterization of D-Band PAs using a sub-THz load-tuning measurement setup.

## D-BAND AMPLIFIER FOR SENSING APPLICATIONS

Large channel bandwidths in D-Band create new possibilities for high-resolution imaging, radar and high data-rate communication systems. PAs are a key building block in these applications and are used before transmit chain antennas or as a driver stage for a frequency multiplier or mixer. Advanced silicon-on-insulator (SOI) CMOS technologies achieving an $f_T$ and $f_{max}$ of 350 GHz and 370 GHz, respectively, are suitable for low-power, high efficiency mmWave circuits. Despite the high performance of mmWave transistors, achieving high output power at D-Band frequencies is still challenging. The short gate length, which results in low operational and breakdown voltages, is a critical output power limiting factor.

Using transistors with longer gate widths and higher current swings can increase output power. However, this creates a significant gain reduction at high frequencies, caused mainly by increased parasitic gate-drain and gate-source capacitance. Enlarging the transistor gate width also decreases the optimum output impedance. The transformation ratio to 50 Ω becomes larger and may lead to lossier matching networks. Power-combining is a common approach to increase output power.

However, this requires additional complex dividers and combining structures, increasing loss, DC power and chip area.[1,2] SOI technology enables transistor stacking to increase the maximum voltage swing, which has already been successfully demonstrated at lower frequencies.[3] Nevertheless, this amplifier topology requires an increased nominal supply voltage, which can require special care and have disadvantages for integration into larger systems.

Two implementations of com-

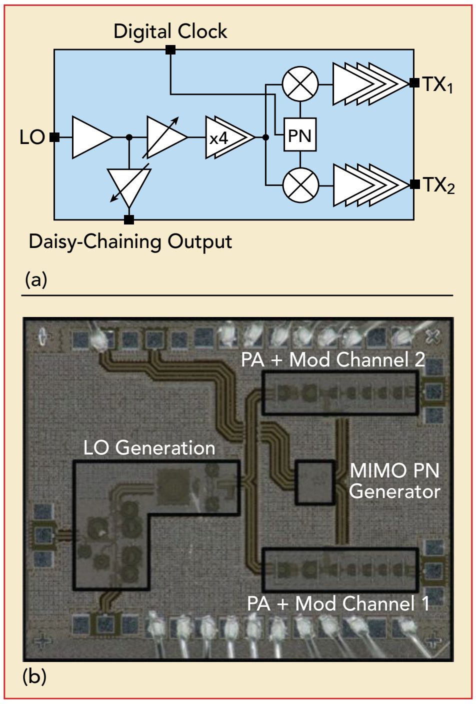


Fig. 1 **PMCW transmitter block diagram (a) and transmitter chip micrograph (b).**

pact, energy-saving and high efficiency D-Band PAs have been proposed.[4] These PAs operate at 0.8 V supply voltage on 22 nm fully-depleted SOI (FD-SOI) technology. The PAs are part of a gesture/motion recognition in a phase-modulated continuous wave (PMCW) radar transceiver system. This emerging application allows new man-machine interfaces and supports non-invasive vital sign assessment. The radar architecture was introduced by F. Probst et al.[5] ***Figure 1*** shows the Tx architecture and a micrograph of the chip and the relevant building blocks. Two broadband transmit antennas and the Tx chip are integrated into an embedded wafer-level ball grid array (eWLB) package.

The antenna/Tx interconnection has significant losses at D-Band frequencies. Chip placement and subsequent processing of the antenna redistribution layers are highly dependent on process tolerances, creating modeling and interconnection challenges. The PA design ensures sufficient output power to the antennas, even when manufacturing tolerances change antenna input impedances. Load sensitivity simulations and measurements are necessary to evaluate this essential capability of the PA.

The amplifier stages employ a pseudo-differential topology. ***Figure 2*** shows the differential common-source transistor pair schematic with cross-coupled neutralization capacitors ($C_N$). These capacitors boost gain and increase differential mode stability by compensating for the parasitic gate-drain capacitance ($C_{gd}$). $C_N$ overcompensates $C_{gd}$, resulting in a three to four dB gain increase instead of maximizing stability. Figure 2 shows the $C_N$ influence on the maximum available gain ($G_{max}$), $K$ and $\mu$ stability factors at 140 GHz. To limit compensation network losses, $C_N$ are alternated polarity metal-oxide-metal (APMOM) capacitors. The back-gate bias voltage feeds two resistors, $R_{BG}$ and aids operation point tuning.

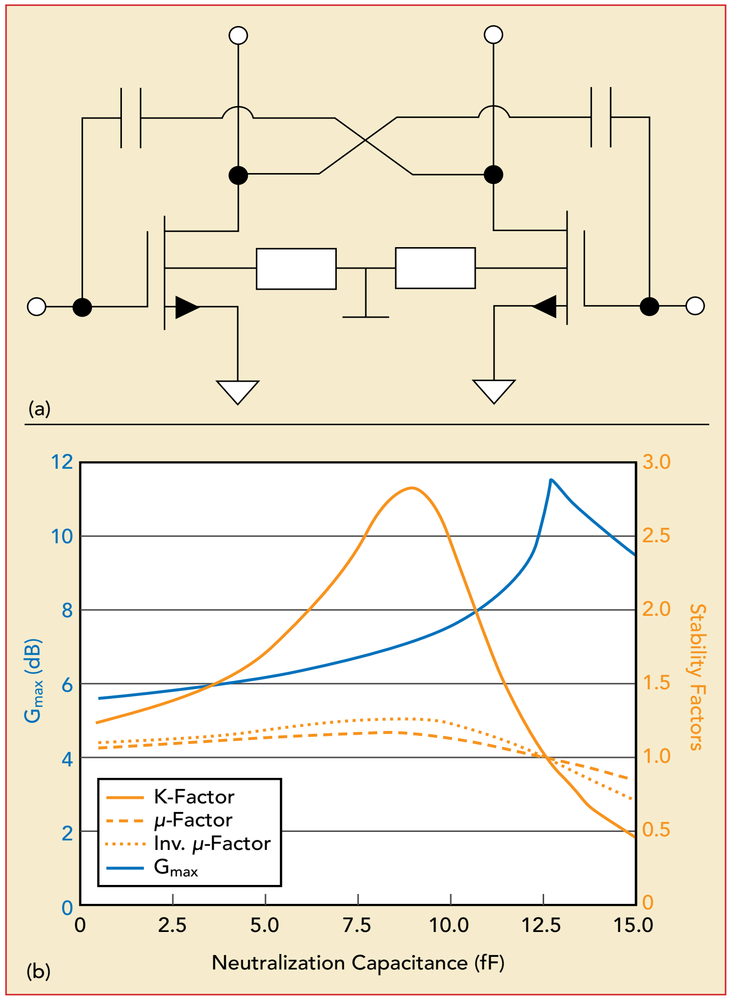


Fig. 2 **Pseudo-differential topology (a) and 140 GHz performance (b).**

Each PA has three drivers for sufficient gain and one high-power output stage. ***Figure 3*** shows a simplified block diagram of the two PAs. Tuning the driver gain to slightly different frequencies enhances amplifier bandwidth, while load-pull simulations optimize the output-matching network to maximize the available output power. Each stage uses super-low threshold voltage (SLVT) n-MOS transistors with double gate-pitch, double-sided gate connection and minimum channel length of 20 nm. Two parallel, 600 nm finger-width transistors are used as driver stages to account for the gate resistance/parasitic finger capacitance trade-off. Three parallel 800 nm finger-width transistors comprise the output stages. Output PA stages are biased for class AB operation for better efficiency, while the drivers are biased in class A for high gain. Two mmWave implementation methods were investigated for the input, output and interstage matching networks. The first uses stacked transformer-based (TB) matching, while the second uses T-line-based (LB) networks.

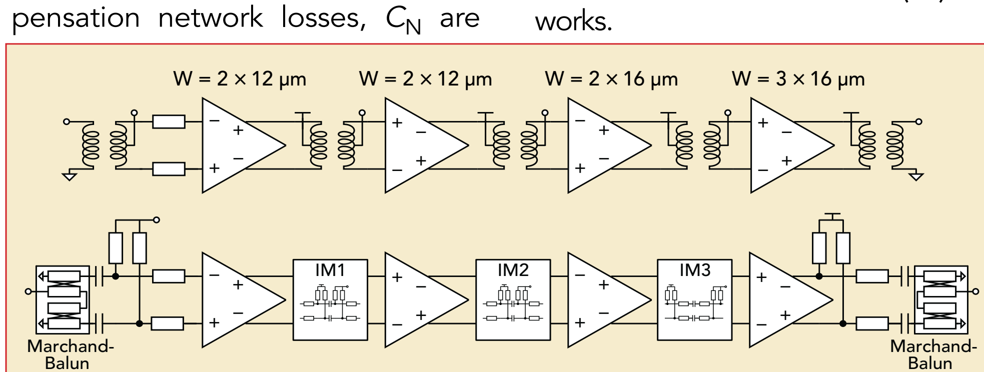


Fig. 3 **TB-PA (top) and LB-PA (bottom).**

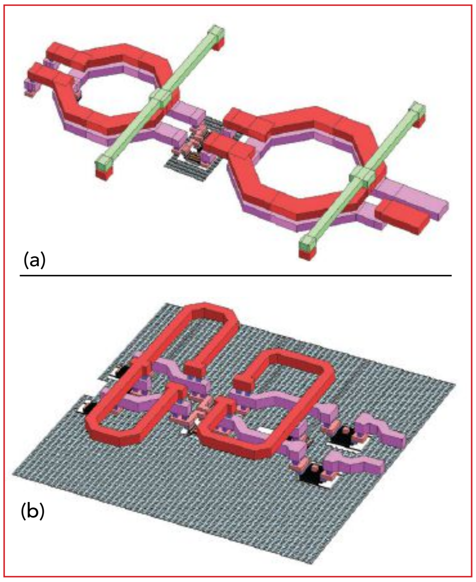


Fig. 4 **Input- and output-matching networks of the TB-PA (a) and LB-PA (b).**

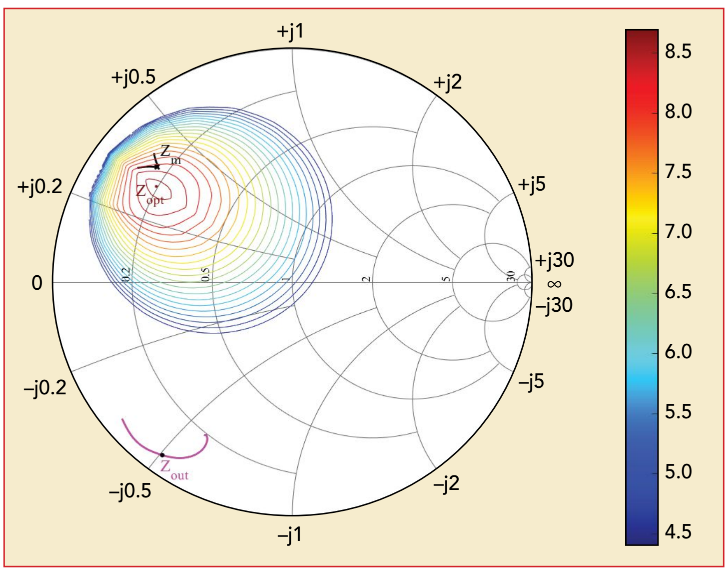


Fig. 5 **Simulated 140 GHz load-pull power contours.**

***Figure 4*** shows 3D views of the TB-PA and LB-PA output stages. The TB-PA benefits from the transformer's compact device size and the ease of routing the DC feed over the center tabs. Short T-lines between the input transformer and the first PA stage provide more efficient impedance matching. For measurement purposes, input and output transformers are baluns. The main drawback of this design is the increased effort to generate accurate circuit models encompassing all relevant D-Band parasitic effects.

The LB-PA implementation benefits from less complex T-line device modeling and more straightforward modular design flows. Taking advantage of the differential circuit's symmetry and the two available thick copper layers, the shorted T-line stubs can be rolled up, as shown in Figure 4. This layout results in a compact design and the LB matching network dimensions are comparable to the TB realization. The symmetry points provide good DC bias and supply voltage feed connections. Additional capacitors are inserted between stages to separate gate bias and supply voltage feeds, resulting in additional matching network losses. Another drawback is the necessity of auxiliary components for single-ended-to-differential conversion required for on-wafer measurements. This requires broadband Marchand baluns at the LB-PA input and output, resulting in extra chip area and increasing fabrication cost.

Load-pull simulations determine the optimal PA matching impedance. ***Figure 5*** shows the 140 GHz load-pull simulation results for the TB-PA output stage. The maximum achievable output power of the stage at the optimal load point, $Z_{opt}$, is 8.7 dBm. The output impedance, $Z_{out}$, of the PA stage and the input impedance of the matching balun, $Z_m$, are displayed over frequency with a 140 GHz marker. The matching balun brings the 50 Ω load close to the optimum load point but introduces approximately 1.8 dB loss, reducing the maximum achievable output power.

***Figure 6*** shows the chip micrographs. The total areas, including pads and baluns, are 0.326 $mm^2$ (TB) and 0.34 $mm^2$ (LB).

## BUILDING THE COMPLETE ON-WAFER MEASUREMENT SYSTEM

The core instrument for RF PA validation is often a VNA. This one-box instrument offers many measurement capabilities that are needed to characterize and optimize a PA. The base-

line S-parameters enable the derivation of device parameters like gain, gain compression, amplitude and phase distortion. Pulsed S-parameters, harmonic measurements, noise figure and intermodulation points are additional KPIs that come from an enhanced VNA with an extended feature set. If the DUT is not adequately cooled, pulsed S-parameter measurements may avoid overheating.

PAs are often used beyond their linear range to enhance power efficiency. Here, traditional small-signal S-parameters are not valid. However, a VNA can still determine the corresponding wave quantities, as shown in ***Figure 7***.

External frequency converters commonly extend VNA measurements into sub-THz frequency ranges, reaching 1.1 THz and beyond. The VNA controls the converters and the VNA user interface shows the target frequencies. ***Figure 8*** shows a VNA with external converters. External converters placed near the DUT minimize losses.



## LOAD-PULL

Different impedances are presented to the DUT input/output for comprehensive device characterization and optimization. This replicates the effect of dispersive loads, as an antenna might create. It also unveils the DUT optimization potential and the matching circuitry that optimizes gain, efficiency and other KPIs. This is important since devices behave differently under various impedances. The unpredictable behavior across different conditions requires extensive measurements to

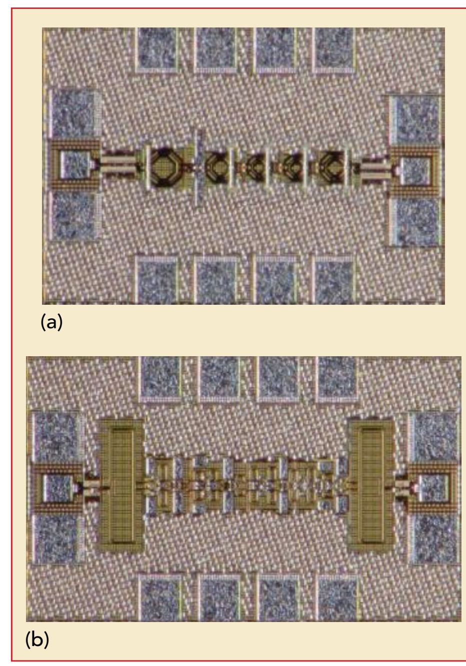


**Fig. 6** TB-PA (a) and LB-PA (b) micrographs.

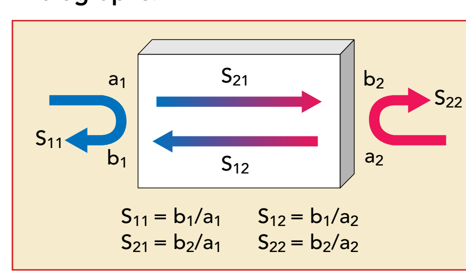


**Fig. 7** Definition of *a* and *b* wave quantities.

**Fig. 8** ZNA VNA with mmWave converters.

create and optimize accurate simulation models. By controlling independent parameters, the load-pull procedure allows DUT performance mapping under different impedances. The optimal performance condition can be established by plotting the DUT performance.

A common approach for creating different impedances is passive load-pull, which uses mechanical tuners to create a varying load. This approach is scalable in frequency and applicable up to 330 GHz. ***Figure 9*** displays a passive load-pull system block diagram.

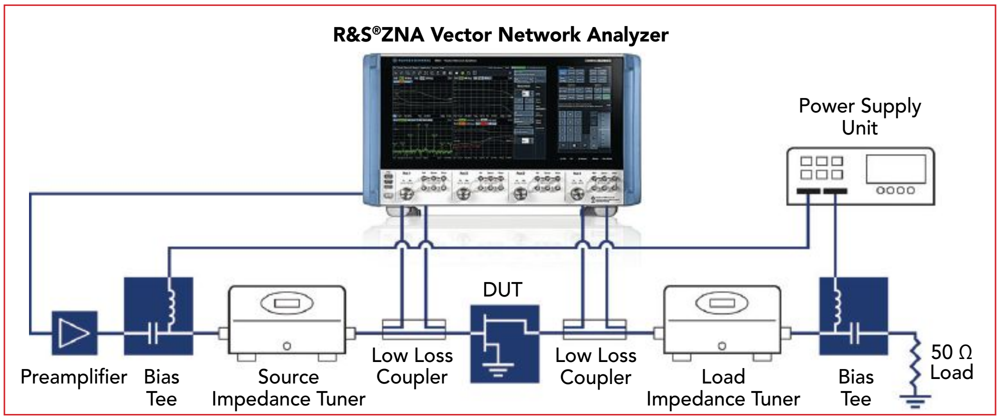


**Fig. 9** **Typical passive load-pull setup.**

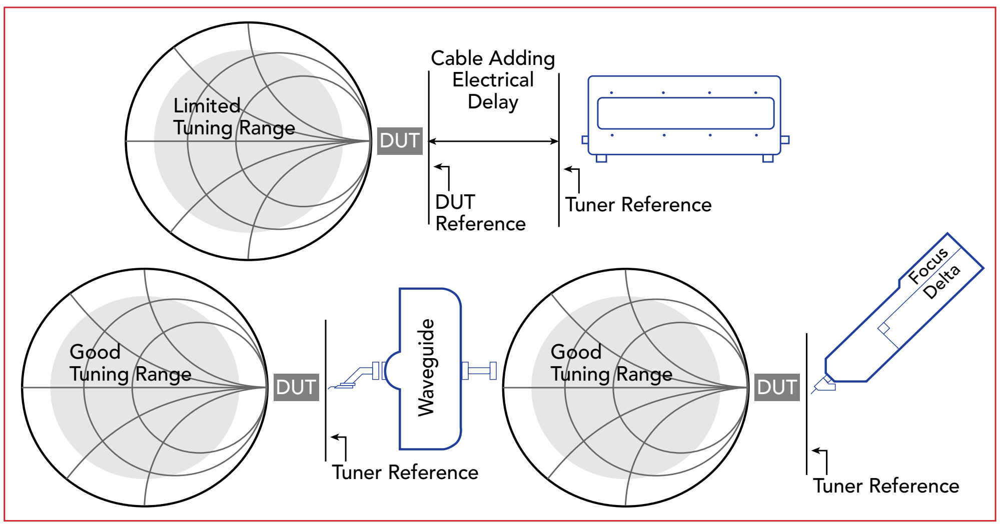


**Fig. 10** **Conventional tuner structure versus Focus Delta tuner with direct RF probe connection.**

Impedance tuners generate a reflection factor that can be controlled over a defined frequency range using the mechanical movement of complex loads within the tuner. In passive load tuning, the returning signal, $a_2$, is always smaller than the transmitted signal, $b_2$, because of transmission losses and tuner reflection. Therefore, the magnitude of the reflection coefficient, $\Gamma$, is always < 1 and the impedance point resides inside the Smith chart. The outer range of the Smith chart is not reachable in a pure passive load-pull system. Reducing loss in the tuner and transmission line between the DUT and the tuner enables a larger accessible Smith chart range, as shown in ***Figure 10***.

Adding frequency converters to D-Band frequencies adds complexity to the setup. To optimize the dynamic range for the receive channels of the forward and reverse waves, *a* and *b*, the tuner separates these signals on the input and output sides of the DUT. Specific down-converter receivers, shown in ***Figure 11***, measure the independent signals.

Measuring the *a* and *b* waves allows the vector load-pull to calculate the real-time tuner impedances presented to the DUT. A standard converter on the DUT's input side provides the test signal. ***Figure 12*** shows the RF and IF signal flow, along with the measurement and

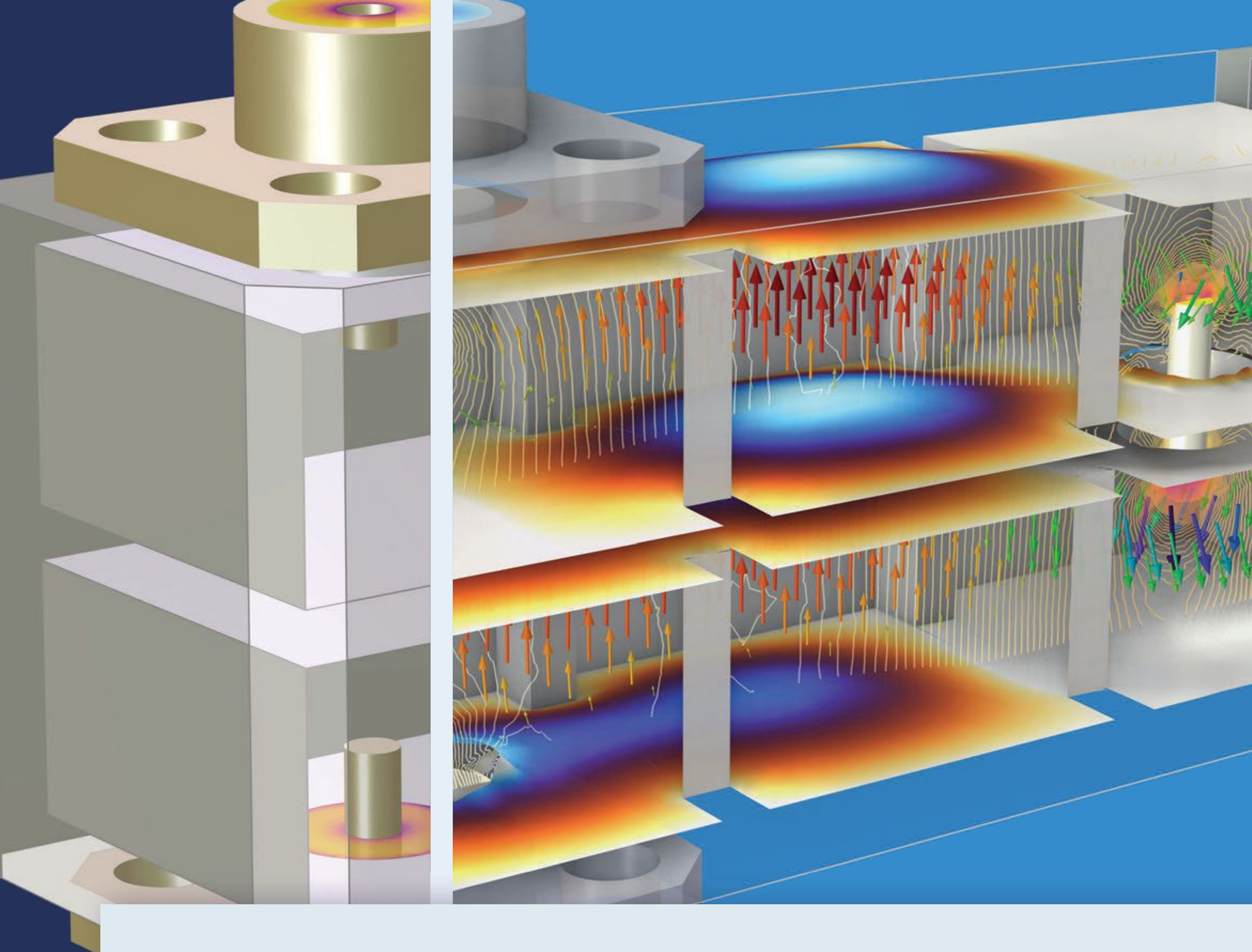

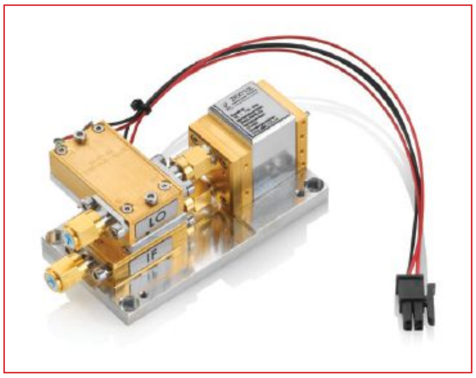


Fig. 11 **R&S ZRX170L mmWave mini receiver modules.**

calibration components. A second converter and power sensor are added for calibration.

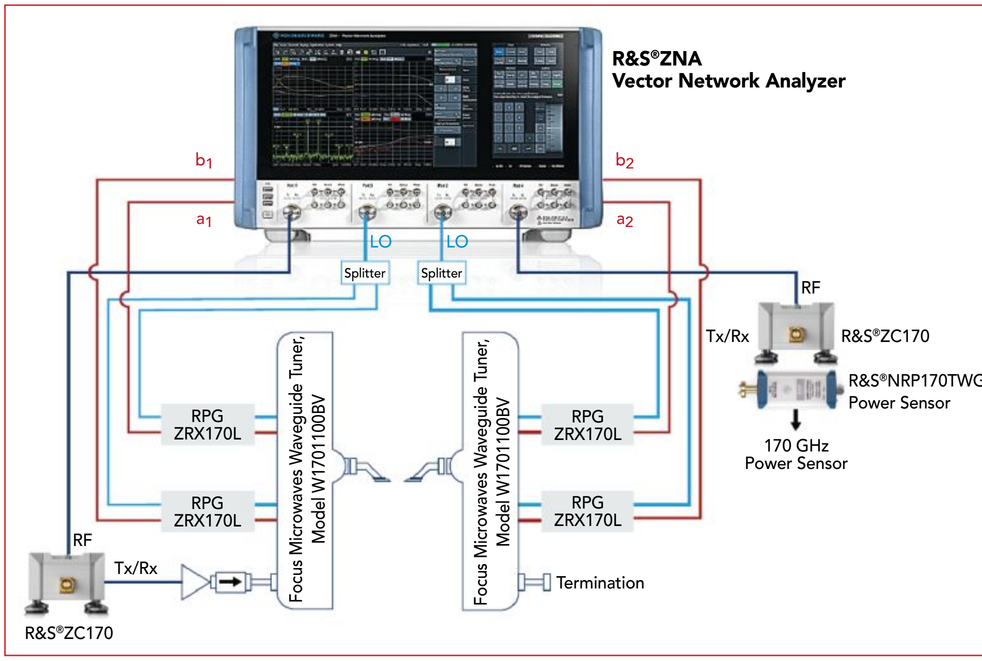


Fig. 12 **Frequency-converted load-pull system.**

## COMPLETE ON-WAFER SETUP

The setup uses a probe station to contact the DUT shown in Figure 6. The challenge is to combine DC and RF probing efficiently. Precaution was taken to have similar landing pads between the two PA variants. Pads often have a combination of DC, digital and RF channels. Based on the layout, one probe needs to support the different channel functions. The MPI TITAN™ Multi-Contact Probe, which supports mixed-signal characterization requirements, shown in ***Figure 13***, handles high-density probing needs, covering pitches down to 50 µm.

As discussed, precise probe positioning is essential to minimize loss between the tuner and DUT. Direct probe connection to the tuner eliminates additional transitions. A waveguide transition is typical in this frequency range to minimize loss while providing a stable connection without phase drift. This transition between the tuner and the mmWave receiver modules or the mmWave converter requires precise positioning. The probe station must support this to enable room for additional amplification blocks or isolators. To address mechanical constraints for this complex setup, MPI Corporation developed a four-axis positioner to support the D-Band tuner plus the measurement system components. The RF connections are on opposite sides of this configuration, while the DC/mixed-signal probes occupy the other opposite sides. MPI's large-area MP4X positioners provide support for the rigid waveguide setup, ensuring mechanical stability and minimizing phase drift during D-Band measurements for repeatable and accurate testing. ***Figure 14*** shows the test system. The screen offers an enlarged view of the DUT from the installed microscope. ***Figure 15*** shows a close-up of the DUT, probes, blue tuners, mmWave receivers and the converters on the sides.

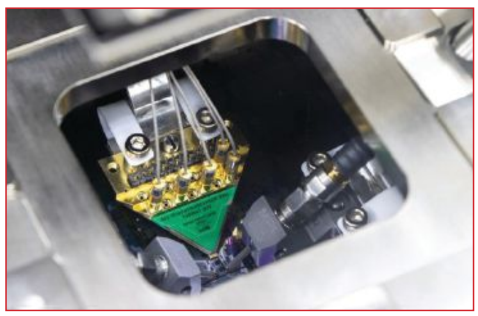

Fig. 13 **Multi-contact probe solution.**

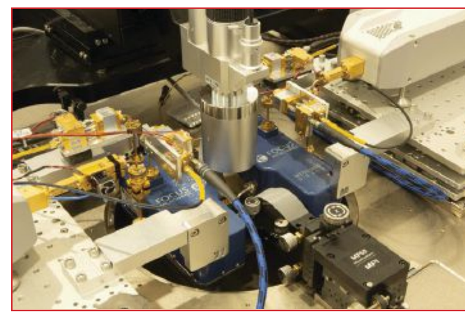

Fig. 15 **Close-up of the on-wafer system.**

Fig. 14 **On-wafer characterization system.**

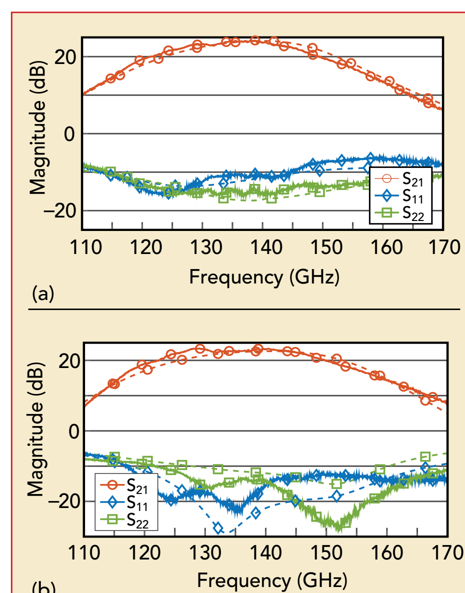


Fig. 16 **Simulated (dashed) and measured (solid) S-parameters without load pull: TB-PA (a) and LB-PA (b).**

## SYSTEM-LEVEL CALIBRATION AND CONTROL

System calibration is important for VNA measurements. There are two steps:

- Calibrate the on-wafer system with the VNA and its converters using MPI calibration solutions and the accompanying software, including test coupons as calibra-


EXODUS ADVANCED COMMUNICATIONS
Unleashing Power,
Enhancing Defense
AMP30021
6-12.0 GHz, 100W Pulse
AMP20071
6.0–18.0 GHz, 200W
AMP20081
80 MHz-1.0 GHz, 400W
AMP20141
0.4-1.0 GHz, 4KW Pulse
AMP60013
X-Band, 5000W CW
LOW NOISE AMPLIFIERS
10 kHz-75 GHz, UP TO 2W
LOW FREQUENCY AMPLIFIERS
10 kHz-2.5 GHz
BROADBAND AMPLIFIERS
10 kHz-8.5 GHz
HIGH FREQUENCY AMPLIFIERS
50 MHz-22 GHz
MILLIMETER AMPLIFIERS
17.5 GHz-50 GHz
PULSE AMPLIFIERS
1 MHz-40 GHz
Power Your Success with Top-Tier RF Modules and Amplifiers
Commercial
Military
EMC
Providing Customers More than 150 Years of
Technical Product and Management Experience
RF & Microwave
Amplifiers
10KHz-75GHz
Amplifiers
CW & Pulse
dBm to KW
www.exoduscomm.com
sales@exoduscomm.com
3674 E. Sunset Road, Suite 100, Las Vegas, Nevada 89120 Tel: 1-702-534-6564

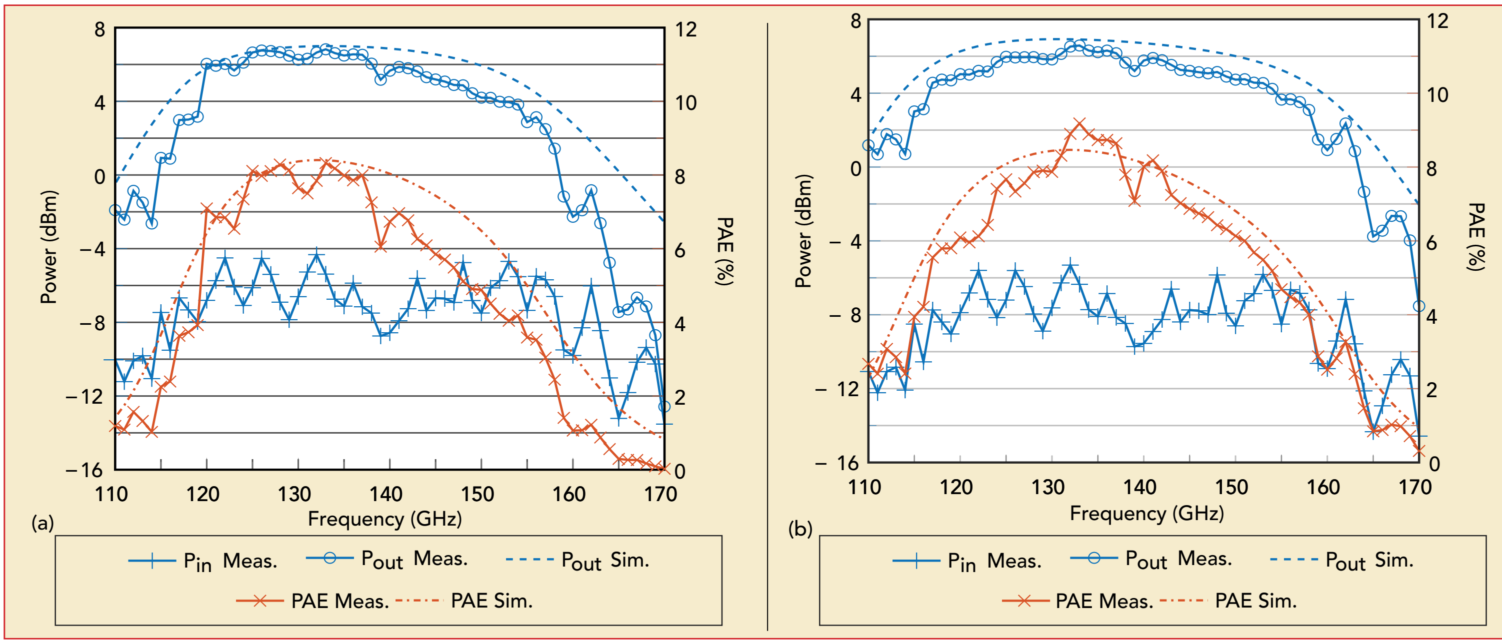


▲ Fig. 17 Simulated (dashed) and measured (solid) $P_{out}$ and PAE without load pull: TB-PA (a) and LB-PA (b).

tion standards

- Calibrate the system load-pull tuners with the Focus Microwaves software.

Once calibration is complete, the Focus Microwaves software acts as the system software. It controls the applied impedance using the tuners and the R&S ZNA to perform the RF measurements for device characterization. The MPI prober ensures stable test conditions in positioning: a cold plate and a controlled, integrated airflow within the probe station cool the DUT.

## D-BAND PA MEASUREMENTS

Engelmann et al.[4] reported validation results for two PAs without load-pull. ***Figure 16*** shows this comparison and S-parameters for TB-PA and LB-PA (including balun and pad losses). Peak small-signal gains of 24.2 and 23.4 dB with 3 dB bandwidths of 23 and 26.2 GHz around the center frequencies of 135.3 and 135.8 GHz were achieved for TB-PA and LB-PA. Both PAs have reverse isolation, S12, < -37 dB over the D-Band frequency range.

***Figure 17*** shows large-signal measurements without load-pull. It shows more significant deviations in saturated output and PAE, particularly for the TB-PA architecture. The PA saturation region deviation is hard to explain when analyzing only small-signal S-parameters since large-signal effects cannot be considered accurately.

As expected, the LB-PA is relatively insensitive to the load impedance, thanks to its output-matching network and broadband Marchand baluns. ***Figure 18*** illustrates the LB-PA $P_{out}$ distribution as a function of the load in linear, 1 dB compression and saturated regimes.

As expected, the TB-PA load-pull measurement shows more sensitivity to load variations in ***Figure 19***. The output power contours shift drastically from the small-signal

to the saturation region. The maximum small-signal output power occurs near the Smith chart's center, indicating excellent 50 Ω small-signal matching. This, however, changes with increasing output power, shown by the constant power contour shift to higher impedances. Output-matching network model inaccuracies, especially at higher frequencies, are the likely cause of the 50 Ω load not transforming to the optimum load point, $Z_{opt}$, for maximum achievable power. Deviations in the load-pull simulations used to determine $Z_{opt}$ are another possibility. However, LB-PA should show similar deviations. The measurement results provide enhanced insights into the PA's large-signal behavior, which simplifies understanding the simulation-to-measurement deviations. The load-pull measurement enables better device modeling and indicates PA load sensitivity. For the PMCW PA Tx module in Figure 2, load-pull data validates whether the impedance variations of the antenna will degrade the PA output power and the overall system performance.

## CONCLUSION

This article addressed the complexity of RF characterization at mmWave and sub-THz frequencies and provided an example of on-wafer D-Band amplifier measurements. Two specific PAs designed for radar sensing applications were investigated using different architectures and output-matching approaches. The example stresses the importance of accounting for load-pull when characterizing active components in the mmWave and sub-THz

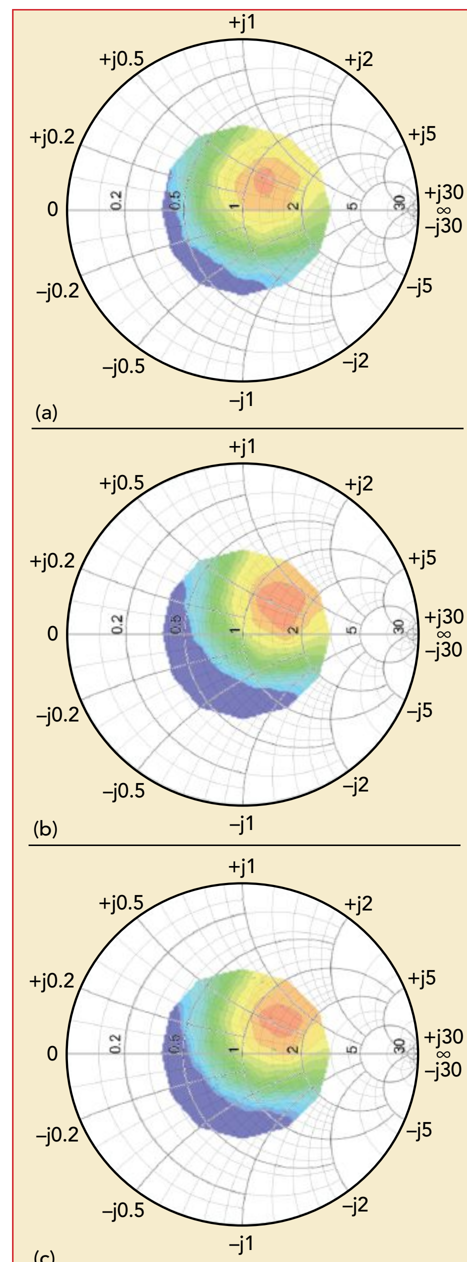

Fig. 18 LB-PA load-sensitivity measurements: (a) small signal; (b) 1 dB compression and (c) saturated.

frequencies, particularly when looking at large-signal parameters. ■

## ACKNOWLEDGMENTS

The authors would like to thank Dr. Sajjad Ahmed at Focus Microwaves and Vince Mallette at MPI Corporation for their excellent collaboration and support for the on-wafer load-pull test system. The authors want to express their gratitude to GlobalFoundries for providing silicon fabrication through the 22FDX® university program. The PA design work was initially funded and supported by the Federal Ministry of Education and Research (BMBF), Germany, through the joint research project REGGAE within the ForMikro research initiative under grant 16E106S1.

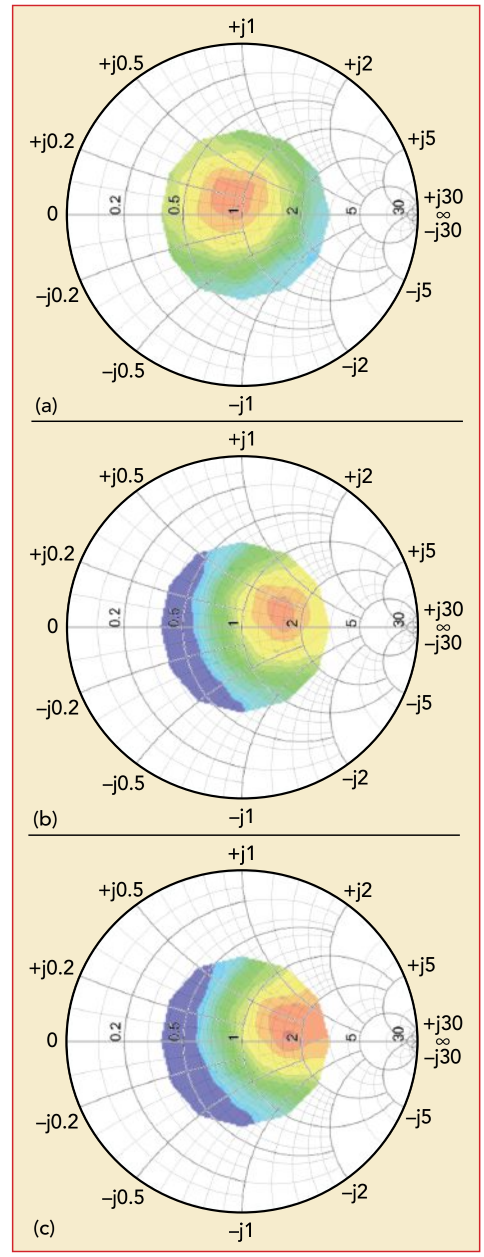


Fig. 19 **TB-PA load-sensitivity measurements: (a) small-signal $P_{out}$; (b) saturated $P_{out}$ and (c) saturated PAE.**

## References


1. D. Simic and P. Reynaert, "A 14.8 dBm 20.3 dB Power Amplifier for D-band Applications in 40 nm CMOS," *IEEE Radio Frequency Integrated Circuits Symposium (RFIC)*, 2018, pp. 232–235.
2. J. Zhang, T. Wu, L. Nie et al., "A 120–150 GHz Power Amplifier in 28-nm CMOS Achieving 21.9-dB Gain and 11.8-dBm Psat for Sub-THz Imaging System," *IEEE Access*, Vol. 9, 2021, pp. 74 752–74 762.
3. M. Cui, Z. Tibenszky, D. Fritsche et al., "An Area Efficient 48 - 62 GHz Stacked Power Amplifier in 22nm FD-SOI," *14th European Microwave Integrated Circuits Conference (EuMIC)*, 2019, pp. 120–123.
4. A. Engelmann, P. Hetterle, F. Probst, R. Weigel and M. Dietz," Design of Two Low DC- Power High-Efficiency D-Band Power Amplifiers in 22 nm FDSOI," *17th European Microwave Integrated Circuits Conference (EuMIC)*, Milan, Italy, 2022, pp. 212–215, doi: 10.23919/EuMIC54520.2022.9923463.
5. F. Probst, A. Engelmann, M. Koch and R. Weigel," A Dual-Channel 15 Gb/s PRBS Generator for a D-Band PMCW Radar Transmitter in 22 nm FDSOI," *IEEE Wireless and Microwave Technology Conference (WAMICON)*, 2023, pp. 129–132, doi: 10.1109/WAMICON57636.2023.10124888.

## L3Harris Adds Electronic Warfare Capabilities to T7 Robot

One of the most efficient ways to innovate technology is to marry two separate capabilities together. The smartphone is a product of this concept, with the initial two technologies — phone and computer — now encompassing hundreds in the palm of your hand.

L3Harris took this concept in an innovative direction recently by attaching an advanced multirole electronic warfare (EW) capability to a T7 robot and demonstrating it at Vanguard 2024, an annual capstone experiment the U.S. Army hosts at Fort Huachuca, Ariz. The combination successfully detected and defeated small uncrewed aircraft systems (sUAS) with the CORVUS-RAVEN system as well as sensed, monitored and decoded electronic signals using the Individual CORVUS Node. CORVUS-RAVEN is a counter-drone system that brings operators passive signal detection capability, enhanced situational awareness and defeat jamming capability. It provides rapid detection and indication of drone threats to inform proportionate defeat.

Vanguard allowed L3Harris and other industry innovators to present emerging technologies and future warfighting concepts to U.S. Army personnel in a relaxed and interactive setting. Recent lessons from Ukraine made this a topical and timely demonstration, driven by an increasing need to improve stand-off and protect mobile personnel from targeted artillery attacks.

The team pulled together the combination of CORVUS-RAVEN on a robot very quickly to meet the requirements of the experiment, coming to fruition in only six weeks.

As the robots can be rapidly repositioned with EW effects turned on and off remotely, their own emitted signals can also be shut down and the robots can be relocated quickly to avoid becoming a target of artillery fire.

T7 and T4 are a strong choice for such deployed EW scenarios, as both robots have aerospace-grade shielding to protect them against electromagnetic interference. This ensures they can carry CORVUS while it is transmitting without being impacted by its signals. Likewise, if CORVUS is actively attempting to detect and sense adversarial signals, the robots' exceedingly low radiated emissions will not hinder its efforts.

The experiment enabled the team to successfully demonstrate the potential of the T7 and T4's deployed capabilities beyond explosive ordnance disposal missions. Using readily available technologies, the concept showed how CORVUS' EW capabilities could be operated through the T7's network, expanding the future roadmap of the robots even further.

*T7 Robot (Source: L3Harris)*

## Detection of GPS Jamming and Spoofing Threats to International Security

Slingshot Aerospace was awarded a contract by the U.S. Space Force's (USSF) Space Systems Command (SSC) to further develop its already operational GPS jamming detection technology by incorporating enhanced geolocation and artificial intelligence (AI) to detect threats around the globe in near real-time and help foreshadow future threats to international security. The technology detects ground-based GPS jamming and spoofing, which can be used by adversaries to reduce combat effectiveness and wreak havoc on commercial industry.

> **Leverage data passively collected by a mesh network of thousands of satellites canvasing the Earth.**

The new program, Positioning, Navigation and Timing-Secure Electronic Navigation Threat Intelligence and Location (PNT-SENTINEL), provides Slingshot new funding to enhance its already operational technology by incorporating AI and predictive analytics to disseminate insights more rapidly for warfighters and support faster, more informed decision-making.

The PNT-SENTINEL contract was awarded as an SBIR Phase 2 contract by SpaceWERX, a space-focused division within the innovation arm of the U.S. Air Force, AFWERX. SSC awarded Slingshot a $1.9 million Phase 1 contract to develop its initial GPS jamming detection capability called Data Exploitation and Enhanced Processing (DEEP) in October 2021. The technology produced as a result of the DEEP contract provides the foundation for PNT-SENTINEL and is currently being used by the USSF to detect GPS jamming and ground-based interference sources as they relate to ongoing conflicts, potential future conflict zones and counterterrorism efforts.

As part of the contract, Slingshot will leverage its AI model called Agatha, which helps identify anomalous spacecraft within large satellite constellations, to further

**For More Information**

Visit mwjournal.com for more defense news.

explore, develop and integrate cutting-edge AI into PNT-SENTINEL.

Slingshot's GPS jamming and spoofing detection and geolocation capabilities leverage data passively collected by a mesh network of thousands of satellites canvasing the Earth. By collecting degradation signals from thousands of satellites that are constantly canvassing the globe, Slingshot can create a near real-time picture of where GPS jamming is taking place on Earth at any given moment.

## HENSOLDT Conducts Research in the Field of Quantum Computing for Radar Resource Management

HENSOLDT has been awarded a contract by the DLR Quantum Computing Initiative (DLR QCI) for the QUA-SAR research project. The research project aims to optimize complex radar remote sensing scenarios. In the research project, HENSOLDT is working together with the Microwaves and Radar Institute of the German Aerospace Center (DLR) and the high-tech start-up Tensor AI Solutions GmbH. The DLR QCI is funded by the German Federal Ministry for Economic Affairs and Climate Protection.

*Electronic Battlefield (Source: HENSOLDT)*

Radar remote sensing uses radio waves to collect data about objects or terrain from a distance. Since conditions on the battlefield change in ever shorter cycles, time is an important factor. Radar systems of the future will be multi-platform and multi-sensor networks that must be operational in highly dynamic environments. The best possible distribution of tasks among sensors and sensor networks is becoming a problem that cannot be solved in real-time with conventional computers. Quantum computers promise to be able to solve this challenge in the future, which would provide a decisive advantage in radar resource management. By participating in QUA-SAR, HENSOLDT is complementing its 'Quantum Sensing and Technologies' technology field, which has existed since the beginning of 2024 and is developing HENSOLDT's technological orientation in the field of quantum technologies.


DC TO 110 GHz

# Cables and Adapters

## System Interconnect and Precision Test

- 375+ models in stock
- Custom assemblies available on request
- Rugged design and construction

### Precision Test Cables

- Options for every environment: armored, phase stable, temperature stable, ultra-flexible, and more.

### Interconnect Cables

- Wide selection of connector options from SMA to 2.92mm
- 0.141, 0.086 and 0.047″ center diameter

### VNA Cables

- Crush and torque resistant
- Competitive pricing

### Adapters:

SMA, BNC, N-Type, 3.5mm, 2.92mm, 2.92mm-NMD, 2.4mm, 2.4mm-NMD, 1.0mm, 1.35mm, 1.85mm, SMP, WR19, WR22, WR28

Mini-Circuits®

## 5G Americas Examines Trust and Security in AI-Powered Wireless Networks

As the adoption of artificial intelligence (AI) in telecommunications accelerates, the importance of ensuring trust and security in cellular wireless networks has never been greater. 5G Americas announced the publication of its latest white paper, "Advances in Trust and Security in Cellular Wireless Networks in the Age of AI." This comprehensive study examines the evolving threat landscape posed by AI-driven technologies and outlines strategic recommendations for securing these systems.

> "As AI adoption grows, so does its potential as an attack vector..."

With AI increasingly integrated into mobile networks, use cases such as anomaly detection, automated threat response and intelligent network management demonstrate its potential to improve performance and security. However, adversarial attacks, intelligent jamming and AI-based intrusions present significant risks, underscoring the importance of secure AI deployment and international collaboration to establish trust in AI-driven telecommunications systems.

Key insights from the white paper include:

- AI-Driven Threats and Mitigation Strategies: The integration of AI into network operations creates new attack surfaces, such as adversarial machine learning and data poisoning. The white paper provides actionable controls and recommendations for safeguarding AI assets and platforms.
- Regulatory and Governance Frameworks: Emerging global standards and regulations, including initiatives by 3GPP, NIST and ISO, are highlighted as essential to developing trustworthy AI systems in telecom.
- Strategic Use Cases for AI in Wireless Networks: From enhancing mobility management to enabling intelligent network planning, AI applications hold transformative potential, provided they are implemented securely and ethically.
- The Role of AI in 6G Development: With the evolution toward AI-native 6G networks, the paper explores how AI can optimize energy efficiency, enable dynamic feature development and support emerging use cases like mixed reality and intelligent IoT.

"AI is revolutionizing wireless networks, enabling unprecedented efficiency, optimization and innovation," said Taylor Hartley, working group leader of the paper and solutions security manager at Ericsson. "However, as AI adoption grows, so does its potential as an attack vector. This white paper serves as a crucial guide for stakeholders aiming to balance innovation with robust security measures."

## Takeaways from IDTechEx's New Automotive Radar Market Report

The automotive industry has been using radar for two and a half decades. During that time, it has transformed from enabling luxury features on the most expensive cars to being used ubiquitously for basic safety features in almost all new cars. IDTechEx's new report "Automotive Radar Market 2025-2045: Robotaxis & Autonomous Cars" covers all things radar, from the established market and tier-one supplier offerings to the most cutting-edge new startups founded in the past couple of years.

The global front radar market is approaching saturation. IDTechEx found that in 2023, 71 percent of new cars were shipped with front radars; in the U.S., with growing regulation on automotive safety requirements, it is 90 percent. As such, the radar market has little room for growth from front radars alone. However, side radars are still fast-growing, with only 40 percent of new vehicles shipped with short-range radar-powered blind spot detection systems.

Blind spot detection applications dominate market demand for short-range radars, but an exciting area of growth is in front short-range radar applications, like junction automatic emergency braking. This requires two short-range radars on the vehicle's front corners, which can see round corners better than the driver and activate the brakes if the car turns into a secondary road where a pedestrian is crossing. Safety rating bodies are already including these features in their arsenal of tests; in the future, these features could be mandated in updated type approval safety requirements that all new cars must follow.

Autonomy and autonomous driving will also be drivers of side radars. Level 2+ is a rapidly growing sector of the market. Cars with this technology enable drivers to remove their hands from the wheel while still watching the road. These typically require a front radar combined with four side radars, offering 360-degree sensing and protection.

New and massively powerful radars are now making their way onto new vehicles. IDTechEx's industry contacts have reported seeing more and more requests for quotations from OEMs for high channel-count systems. IDTechEx expects that high channel-count radars will become commonplace over the next decade.

*Automotive Radar (Source IDTechEx)*

There are two options for radar performance to keep growing. One, change to a higher frequency. This helps by enabling smaller sizes and higher resolutions. Two, use a distributed an-

**For More Information** Visit mwjournal.com for more commercial market news.

tenna. This solves some of the fundamental issues with growing the performance of radars, however, it requires more radar heads, a more complex system and different integration headaches for OEMs. Nonetheless, IDTechEx has seen proposed distributed radar systems with 0.01 degrees of angular resolution using these techniques, which is on par with LiDARs.

## RAN Equipment Market to Remain Uninspiring

According to a newly published forecast report by Dell'Oro Group, market conditions are improving but remain underwhelming for the broader Radio Access Network (RAN) ecosystem as regional 5G coverage imbalances, slower data traffic growth and monetization challenges are weighing on the market. Following the intense 5G acceleration phase from 2017 to 2021, RAN investments tapered off in 2023 and 2024. Conditions are expected to improve slightly over the short term, but the long-term outlook remains subdued.

Additional highlights from the Mobile RAN 5-Year January 2025 Forecast Report:

- Worldwide RAN revenues are projected to grow at a 0 percent CAGR over the next five years, as rapidly declining LTE revenues will offset continued 5G investments.
- Medium-term risks to the baseline are balanced, while the long-term risks are tilted to the downside and characterized by the data growth uncertainty with the existing MBB use case. As the investment focus gradually shifts from coverage to capacity, one of the most significant forecast risks is slowing mobile data traffic growth. Given current network utilization levels and data traffic trends in more advanced markets, there are serious concerns about the timing of capacity upgrades.
- The mix between existing and new use cases has not changed. Private/enterprise RAN is expected to grow at a 20 percent plus CAGR while public RAN investments decline. At the same time, because of the lower starting point, it will take some time for private RAN to move the broader RAN needle.
- 5G-Advanced positions remain unchanged. The technology will play an essential role in the broader 5G journey. However, 5G-Advanced is not expected to fuel another major capex cycle. Instead, operators will gradually transition their spending from 5G toward 5G-Advanced within their confined capex budgets.
- RAN segments that are expected to grow over the next five years include 5G NR, FWA, mmWave, Open RAN, vRAN, private wireless and small cells.

Nxbeam™

# Ka / V / E - Band GaN MMIC Power

## Ka

- NPA2001-DE | 26.5-29.5 GHz | 35 W
- NPA2002-DE | 27.0-30.0 GHz | 35 W
- NPA2003-DE | 27.5-31.0 GHz | 35 W
- NPA2004-DE | 25.0-28.5 GHz | 35 W
- NPA2020-DE | 24.0-25.0 GHz | 8 W
- NPA2030-DE | 27.5-31.0 GHz | 20 W
- NPA2040-DE | 27.5-31.0 GHz | 10 W
- NPA2050-SM | 27.5-31.0 GHz | 8 W

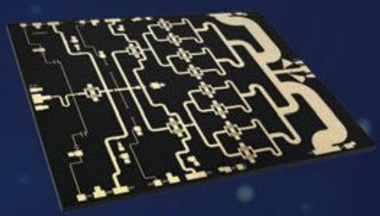

## V

- NPA4000-DE | 47.0-52.0 GHz | 1.5 W
- NPA4010-DE | 47.0-52.0 GHz | 3.5 W

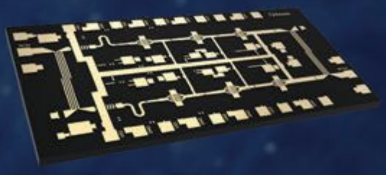

## E

- NPA7000-DE | 65.0-76.0 GHz | 1 W

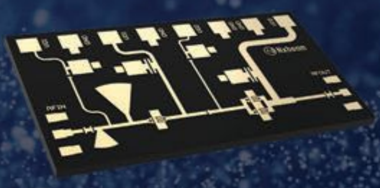

4388 Cerritos Avenue
Los Alamitos, CA 90720

www.nxbeam.com
info@nxbeam.com

Phone: 949-656-2883
info@nxbeam.com

# Around the **Circuit**

Barbara Walsh, Multimedia Staff Editor

## MERGERS & ACQUISITIONS

**Micross Components Inc.**, a portfolio company of Behrman Capital, closed the acquisition of **Integra Technologies**. Integra is an outsourced semiconductor assembly and test (OSAT) post-processing provider focused on high-reliability applications and end markets, headquartered in Wichita, Kan. The acquisition of Integra further positions Micross as a leader in U.S.-based OSAT services and further broadens Micross' portfolio of high-reliability microelectronic services and products. Integra Technologies is a leading U.S.-based provider of comprehensive semiconductor assembly, testing and qualification services. The company specializes in delivering end-to-end solutions that help customers streamline their production processes while ensuring high-quality, cost-effective products.

## COLLABORATIONS

***Microwave Journal***, a leading publication serving the RF and microwave engineering community, and its parent company, **Horizon House Publications Inc.**, announced a strategic partnership with the **IEEE Antennas and Propagation Society (AP-S)** and the **International Union of Radio Science (URSI)** for the 2025 IEEE International Symposium on Antennas and Propagation and North American Radio Science Meeting. This high-profile event will be held in Ottawa, Canada, from 13-18 July 2025 at the Rogers Centre Ottawa. Under this collaboration, *Microwave Journal* and Horizon House will work closely with IEEE AP-S and URSI to manage the sale of exhibit space and sponsorship opportunities for the symposium.

**Quadsat** and **mmt** have partnered to provide Quadsat's electromagnetic emulation services. This news follows the recent launch of Quadsat's global Service Partner Network, designed to give customers worldwide cost-effective and prompt access to Quadsat services. The services range from the characterization of teleport and user terminal antennas, over full satellite network testing to calibration of a wide range of RF measurement devices in the civil and defense domains. mmt specializes in high frequency technology and wireless measurement, especially for wireless communication and antenna technology.

**Infineon Technologies AG** announced the formation of a new business unit to drive the company's growth in the area of sensors by combining the existing sensor and RF businesses into one dedicated organization. The new business unit, Sensor Units & Radio Frequency (SURF), will be part of the power and sensor systems division and include the former automotive and multi-market sense and control businesses. By combining its sensor and RF expertise, Infineon strengthens its competitiveness and go-to-market approach by leveraging cost and R&D synergies, accelerating innovation and adding value to customers.

## ACHIEVEMENTS

**Mobix Labs** has reached a significant milestone with the delivery of its advanced EMI filtered connectors for the **U.S. Navy's** Tomahawk Cruise Missile system. These connectors, integral to the new Block V Tomahawks, help ensure electronic resilience in the face of electromagnetic interference, safeguarding critical missile functions in high-stakes operational environments. As Mobix Labs deepens its footprint in defense technology, this achievement reflects their dedication to advancing military-grade connectivity solutions. The Tomahawk cruise missile, known for its long-range precision and adaptability, has become a mainstay of the U.S. military's defense capabilities, deployed from ships and submarines.

## CONTRACTS

**Raytheon**, an RTX business, was awarded a $529 million contract to supply the **Netherlands** with a Patriot® air and missile defense system fire unit and related equipment. This contract supports the replenishment of a Patriot fire unit donated to Ukraine. The direct commercial sales contract includes a single fire unit consisting of a radar, launchers, command and control stations and other support equipment. Patriot is the only combat-proven ground-based air and missile defense capability in the world able to defend against advanced long-range cruise missiles, tactical ballistic missiles and the full spectrum of air-breathing threats. Patriot is the foundation of air defense for 19 countries, and the system continues to demonstrate its effectiveness against advanced aerial threats and massive complex raid attacks.

The **U.S. Army** has awarded **L3Harris Technologies** full-rate manpack and leader radio production orders under the Handheld, Manpack & Small Form Fit (HMS) program totaling nearly $300 million. These orders continue the proliferation of critical resilient communication solutions for U.S. soldiers and provide seamless interoperability from the tactical edge to the aerial tier in all operational environments, regardless of adversarial electronic warfare attacks. The modern cryptographic compliant L3Harris AN/PRC-158 and AN/PRC-163 radios can switch between Secure But Unclassified – Encrypted and high assurance levels of encryption, enabling interoperability with coalition partners. This capability meets the latest NSA encryption and decryption standards for communications security and transmission security.

In 2024, the **U.S. Navy** awarded **BAE Systems** an $85 million production contract to deliver additional Network Tactical Common Data Link (NTCDL) systems. NTCDL will enable a real-time exchange of voice, data, imagery and full-motion video from a variety of air, surface, subsurface and man-portable sources. Systems under the company's current contract are presently being installed on U.S. Navy aircraft carriers and will be

**For More Information** For up-to-date news briefs, visit mwjournal.com

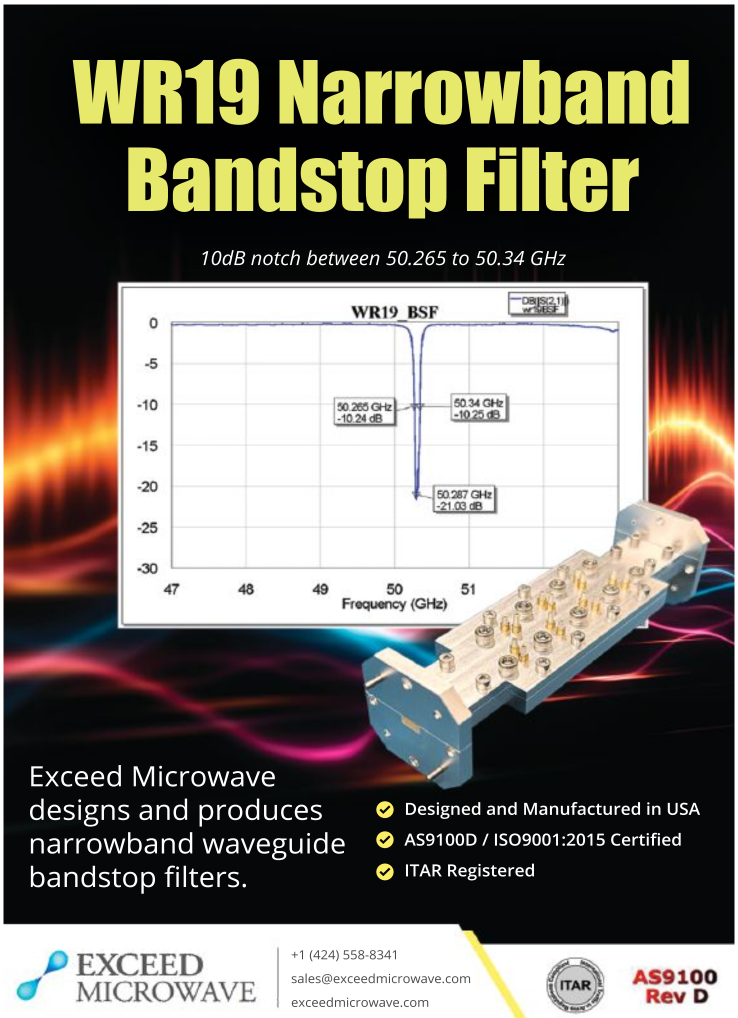





installed on new Constellation-class frigates. NTCDL is a multi-platform solution for all U.S. Navy Common Data Link (CDL) requirements. It is a modular, scalable system designed to increase link capacity and embrace waveform evolution. NTCDL supports multiple, simultaneous, networked operations using currently fielded CDL equipment, as well as next-generation manned and unmanned platforms.

**Sivers Semiconductors** announced that it has been awarded a major chip development program by a leading Tier-1 telecom infrastructure vendor. The $5.4 million program will run from Q1 2025 to Q4 2026 and will support the development of a next-generation, highly integrated beamforming transceiver for various mmWave telecom applications. Sivers' RF-SOI-based SUMMIT beamformer product family leads the industry in key performance metrics of output power, efficiency and noise figure, resulting in longer range, more reliable links, lower cost of ownership and a greener footprint. In addition, Sivers' TRB transceiver product family features state-of-the-art synthesizers with ultra-low phase noise, high performance mixers with superior image rejection and a high level of integration, resulting in a lower bill of materials and time to market.

## PEOPLE

▲ *Matt Markel*

**Epirus** announced the addition of **Dr. Matt Markel**, a renowned expert in radar, autonomy and electronic warfare systems, to the company's executive leadership team as chief technology officer (CTO). With decades of experience at the nexus of technology innovation and national security, Dr. Markel was previously CEO of Spartan Radar, vice president of radar systems at Ghost Autonomy and leader of the radar team at Waymo, formerly the Google Self-Driving Car Project.

## REP APPOINTMENTS

**ATEK Midas**, a designer and supplier of high performance mixed-signal silicon ASICs and RFICs and advanced GaAs and GaN MMICs, announced the appointment of **NWN Inc.** as their exclusive technical representative serving customers in Northern California and Northern Nevada. NWN's experience, product knowledge and reputation make them an exceptional addition to ATEK's network of representatives. NWN specializes in the sale of RF, microwave, mmWave, frequency control and analog components.

**Insight SiP**, a developer of advanced miniature RF modules, has appointed **Hughes Cain & Associates** as its manufacturer's representative for the South-Central U.S., covering Texas, Oklahoma, Louisiana and Arkansas as part of its drive to expand its U.S. business. Hughes Cain has been covering this area since the 1970s and has excellent knowledge of this expanding part of the U.S. electronics market.

INVITED PAPER

# Analysis of the Test and Measurement Equipment Market

Shrikant Mahankar and Kritee Das
*MarketsandMarkets, Pune, India*

According to MarketsandMarkets,[1] the test and measurement (T&M) equipment market is projected to reach $47.01 billion by 2029, increasing from $38.91 billion in 2024, at a compound annual growth rate (CAGR) of 3.9 percent. T&M equipment are instruments and devices used to analyze, evaluate and verify the performance and quality of mechanical and electronic applications. This equipment is used in multiple industries, including automotive, aerospace, defense, IT, telecommunication, education, government, semiconductors, industrial and healthcare.

In MarketsandMarkets' analysis, the T&M equipment market is segmented by product type, service type, vertical and region. The product type segment is further classified as general-purpose test equipment and mechanical test equipment. The service type business segment is sub-segmented as calibration services, repair/aftersales services and others. The vertical type is sub-segmented into automotive and transportation; aerospace and defense; IT and telecommunications; education and government; electronics and semiconductor; and industrial and healthcare. The healthcare industry is likely to witness the fastest growth from 2024 to 2029 due to the increasing demand for patient monitoring and personal emergency reporting services, as well as the demand for advanced medical devices. The Asia-Pacific region is projected to witness the highest growth rate during the forecast period due to rising manufacturing activity in developing nations. Many companies are establishing their production plants and research and development facilities in Asian countries due to favorable government policies.

Stringent government regulations for product safety and environmental protection drive the T&M equipment market.

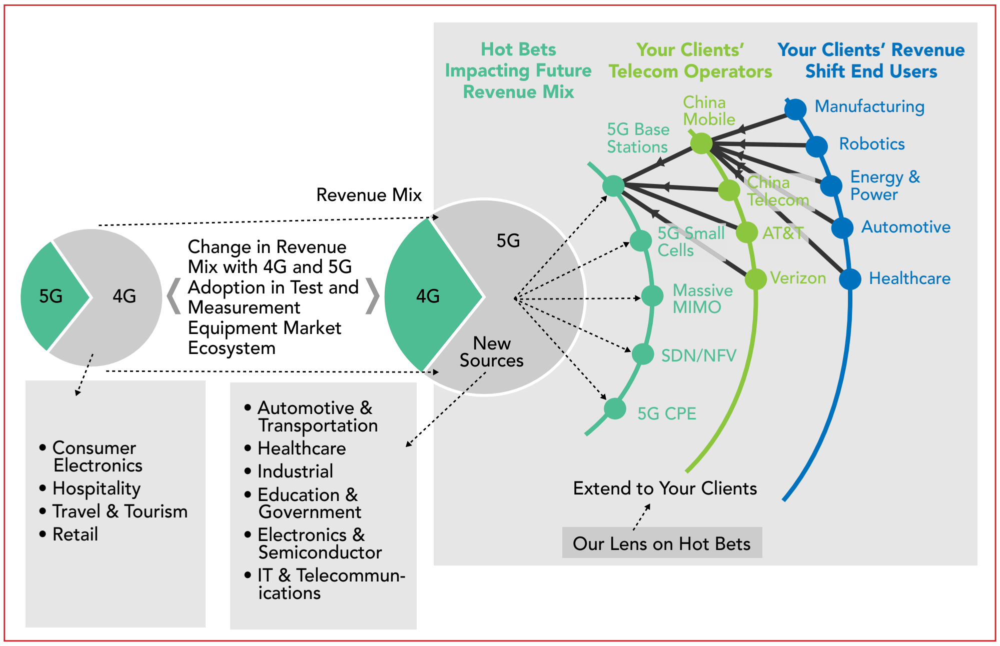


**Fig. 1** **Wireless market segment evolution, applications and ecosystem. *Source:* Secondary research, interviews with experts and MarketsandMarkets analysis.**

Consumer demand for reliable, high-quality products is surging as risks to human life and the consequences of environmental damage increase. Organizations worldwide are focused on implementing government guidelines in their testing services to address product safety and quality concerns. For instance, in the automotive industry, the government has enforced stringent regulatory restraints regarding $CO_2$ emissions from OEMs, creating opportunities for the various market players that offer T&M equipment.

The integration of AI and machine learning (ML) with T&M equipment redefines data analysis, tests and maintenance, which leads to increased effectiveness and efficiency of T&M operations. AI and ML enhance data analysis capabilities by enabling accurate and fast interpretation of complex data sets. Through advanced algorithms, these technologies can identify patterns and anomalies that traditional methods might miss, improving decision-making and providing more precise results. Predictive maintenance powered by AI and ML offers a view of possible equipment failures before they occur, minimizing down time and cutting costs for maintenance.

The integration of Gen AI and AI in T&M equipment has transformed the industry by increasing the efficiency of measurement and testing solutions. Self-healing automation is designed to automatically detect problems in the form of test failure or inconsistency. This allows the AI-powered testing tools to make corrections, reduce errors and make the software testing process more resilient. Defect analysis and scheduling tools can analyze the data gathered, assess the important issues that need attention and schedule the necessary repairs according to their severity, need and priority. These tools also predict possible defects and provide test cases to be executed based on patterns and historical databases.

## NEW REVENUE POCKETS FOR PLAYERS IN THE T&M EQUIPMENT MARKET

The T&M equipment market segments into general-purpose test equipment and mechanical test equipment categories. Of these two business segments, general-purpose test equipment is expected to hold a larger market share. The general-purpose test equipment includes equipment like oscilloscopes, signal generators, multimeters, logic analyzers, spectrum analyzers, BERT solutions, network analyzers, power meters, electronic counters, modular instruments, automated test equipment and power supplies. General-purpose test equipment measures electronic parameters, including voltage, frequency, power, etc. As the demand rises for small, flexible and efficient T&M equipment, companies are focusing on developing equipment that can have multiple functionalities. Advancements in T&M technology have introduced equipment that provides high bandwidth, accuracy and resolution when compared to conventional equipment that has been used for testing. This equipment is used in different applications such as IT and telecommunications, healthcare, automotive and industrial applications.

***Figure 1*** captures the breadth of the applications, architectures and ecosystem that will be important for the wireless segment of the T&M market. In particular, Figure 1 shows the significant drivers for 4G wireless and how 5G will enable new sources for T&M requirements. It also indicates architectures in the outer rings, along with different end users who are participating in those architectures. The final ring gives examples of applications that will be important to the end user and how they translate into an architecture. This straightforward slice shows how broad and interconnected the T&M market will become.

The T&M equipment used in the industrial vertical of the market is essential across various stages of the product lifecycle, including design, manufacturing and maintenance. This includes a wide range of products such as radar systems, solar inverters, industrial motors and drives, wind turbines, HVAC systems and many others. With the rising adoption of renewable energy applications, like wind and solar power, T&M solutions are required to validate performance and compliance. In addition, industry 4.0, including automation and IoT integration, has increased the need for advanced monitoring and predictive maintenance equipment. These factors, combined with increasing investment in infrastructure development and the rising need for quality assurance, present enormous growth prospects for this industry.

## THE T&M EQUIPMENT MARKET ECOSYSTEM

The T&M equipment market ecosystem is broad. It includes all the


Fig. 2 Representative snapshot of the test and measurement ecosystem. *Source:* MarketsandMarkets analysis.

manufacturers, stakeholders and end-user companies of T&M equipment, with driving forces on quality assurance, performance optimization and compliance in a wide variety of applications. In MarketsandMarkets analysis, product manufacturers are further categorized into general-purpose and mechanical test equipment segments. General-purpose test equipment suppliers include companies like Keysight Technologies, Advantest, AMETEK, Anritsu and VIAVI Solutions. The mechanical test equipment manufacturers include companies like Rohde & Schwarz, NI, Fortive, Teledyne Technologies and Astronics Corporation. These companies supply a broad spectrum of end-user companies worldwide, including Lockheed Martin, Northrop Grumman, BAE Systems, Intel Corporation, Qualcomm and Ford Motor Company, among many others. This ecosystem, with a partial snapshot shown in ***Figure 2***, illustrates how T&M solutions act as a foundation for ensuring precision, reliability and innovation across industries.

## CONCLUSION

The T&M equipment market is poised for steady growth. This growth will be driven by technological advancement, stringent regulatory requirements and the integration of AI and ML. Quality and regulatory compliance have become key priority areas for all industries, resulting in increased demand for high-end testing solutions and big opportunities emerging for market players globally. ■

## Reference

1. "Test and Measurement Equipment Market Size, Share & Growth Analysis," *MarketsandMarkets*, August 2024, Web: www.marketsandmarkets.com/Market-Reports/test-measurement-equipment-market-116452716.html.

NEW!

# MI-WAVE

Millimeter Wave Products Inc.

# TARGET GENERATION MODULE

**MI-WAVE's RF Target Generator for Missile Guidance, Electronic Warfare, and Mission-Critical Applications**

| Parameter | Min | Typ | Max | Units |
|---|---|---|---|---|
| IF Input Frequency | 0.1 | - | 3 | GHz |
| RF Output Frequency | 33 | - | 36 | GHz |
| Gain | - | 30 | - | dB |
| Noise Figure | - | 2.2 | - | dB |
| P1dB (Output Power at 1 dB Compression) | - | 30 | - | dBm |
| Attenuation | - | 45 | - | dB |


## KEY CAPABILITIES & FEATURES

### Missile Guidance Systems

- Simulates complex RF targets for seeker calibration and real-time guidance system testing.
- Supports the development of next-generation precision-guided munitions by providing accurate target signal reproduction.

### Electronic Warfare (EW) Testing & Training

- Emulates interference, jamming, and deceptive RF targets for robust EW system validation.
- Enhances operator training by generating realistic mission scenarios.

### Mission-Critical Communication Systems

- Enables testing and validation of secure communication links in extreme RF environments.
- Simulates challenging signal conditions, including multipath fading and signal distortion, for high-reliability communication systems.

## KEY CAPABILITIES & FEATURES

- Real-Time RF Target Simulation – Produces dynamic RF signals with customizable frequency shifts, power levels, and phase variations for highly accurate system validation.
- High-Fidelity Signal Processing – Ensures low phase noise and high signal integrity for reliable and repeatable results, crucial for mission-critical operations.
- Multi-Signal Capability – Simulates multiple independent RF targets with varying frequencies, amplitudes, and phase characteristics.
- Missile Guidance Testing – Provides precise RF target generation to evaluate and calibrate missile seeker performance in real-time scenarios.
- Advanced Attenuation & Gain Control – Offers 45 dB of attenuation and 30 dB of gain for precise control over signal variations.
- Seamless System Integration – Easily integrates with hardware-in-the-loop (HIL) and software-in-the-loop (SIL) testing environments, with remote control options via Ethernet, USB, and GPIB interfaces.

**SEE US AT SATELLITE 2025 BOOTH 2623**

MIWV.COM

2007 Gandy Blvd N Suite 1310
St. Petersburg, FL 33702

Tel: (727) 563-0034
Email: sales@miwv.com

ITAR Compliant · International Traffic in Arms Regulations · Made in the U.S.A. With Pride · 35 Anniversary Years in Business · Certified ISO 9001-2015 Company · Top Defense Manufacturing Service Companies

INVITED PAPER

# Recent Advancements in Terahertz Components Fabrication: A Step Toward Next-Generation Communication Systems

V. Manimala
*Builders Engineering College, Kangayam, India*

N. Gunavathi
*National Institute of Technology, Trichy, India*

The advantages of the THz spectrum (0.1 to 30 THz) make it an attractive option for next-generation communication systems. The spectrum offers highly secure, high-throughput communication with minimal interference. The broader bandwidth available in the THz range significantly enhances the potential for higher data transmission rates compared to traditional RF-based systems.[1] The availability of components in the THz range is more restricted compared to the RF and optical spectral regions. This limitation poses challenges in developing and deploying THz-based systems, as the technology and infrastructure for THz components are still in the early stages of development. A key concern in accepting THz technologies for real-time applications is the cost of the system. The physical size of the THz component decreases with increasing operating frequency. Traditional manufacturing technologies for most microwave components will not be appropriate at THz frequencies. New developments in fabrication technologies are providing a path to meet this requirement. This article discusses some of the more interesting and important recent developments in advanced fabrication techniques suitable for the THz regime.

## MATERIAL SELECTION AND CHARACTERIZATION

Material selection for fabrication is important. Studying the properties of microwave dielectric materials at terahertz frequencies is crucial for precise component design. Accurate characterization of dielectric properties, such as permittivity and loss tangent, helps in designing components with the desired performance characteristics, minimizing signal loss and achieving better overall efficiency in terahertz technology applications.[2]

This area of investigation has garnered interest and is seeing significant activity. For instance, the characterization of photopolymers for their dielectric properties is discussed by Nattapong Duangrit et al.[3] Time-domain spectroscopy techniques have been used to study the dielectric proper-

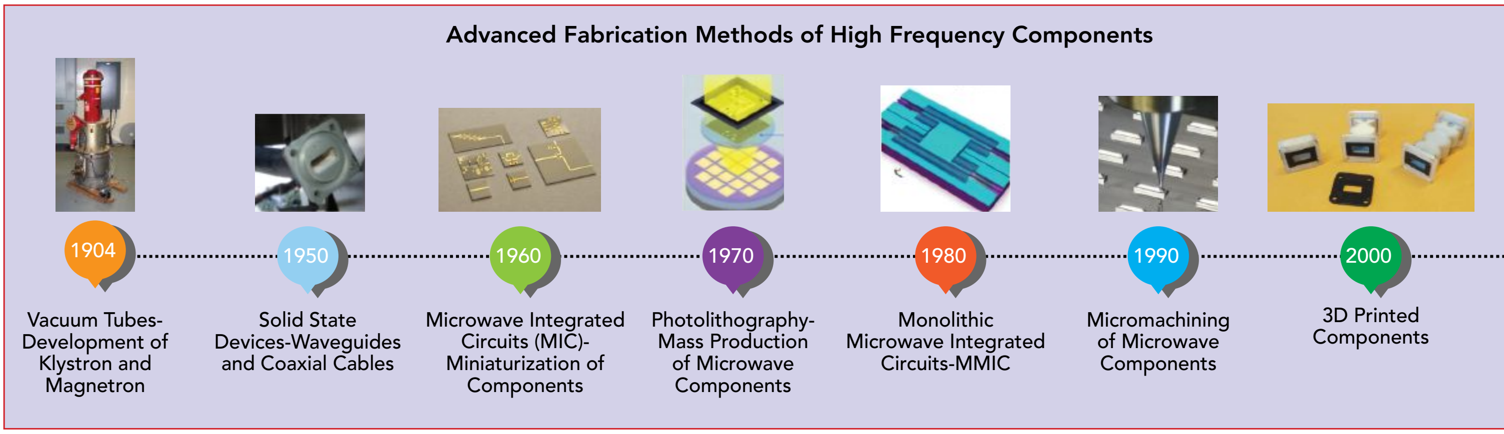


**Fig. 1** **Advances in high frequency component fabrication methods.**

- *2020s:* Automatic Layer Etching
- *2010s:* High-Resolution Lithography
  3D Printing
  Advanced Packaging Techniques
- *2000s:* Epitaxial Growth
  Micromachining
- *1990s:* Wafer Bonding
  Chemical Mechanical Polishing (CMP)
- *1980s:* Physical Vapor Deposition (PVD)
  Deep Reactive Ion Etching (DRIE)
- *1970s:* Ion Implantation
- *1960s:* Chemical Vapor Deposition (CVD)
  Photolithography

**Fig. 2** **Process techniques for high frequency component fabrication.**

ties of polymer samples. Material properties of the most commonly used copper, graphene and carbon nanotube (CNT) and their suitability for THz antenna are studied in a paper by Sasmita Dash et al.[4] Poor radiation efficiency and increased propagation delay are observed for copper-based THz antennas. Conductivity and skin depth of copper tend to be lower at the THz range. CNT has better conductivity and graphene exhibits better performance compared to copper. Miniaturization and reconfigurability are claimed as the advantages of graphene-based antennas. A detailed study on graphene-based antenna geometries at THz frequency has been carried out and reported by Diego Correas-Serrano et al.[5] The conductivity of graphene, which is strongly influenced by its band structure, has been mathematically modeled and analyzed. Dielectrics used in THz frequency metasurfaces are reviewed by Rajour Tanyi Ako et al.[6] The use of dielectrics as substrates and spacers and appropriate fabrication techniques have been studied. Thin film dielectric sheets and liquid-coated and solidified dielectric materials have been studied and proposed for spacers. Thick film or bulk dielectric materials formed by etching or machining techniques have been studied and proposed as solutions.

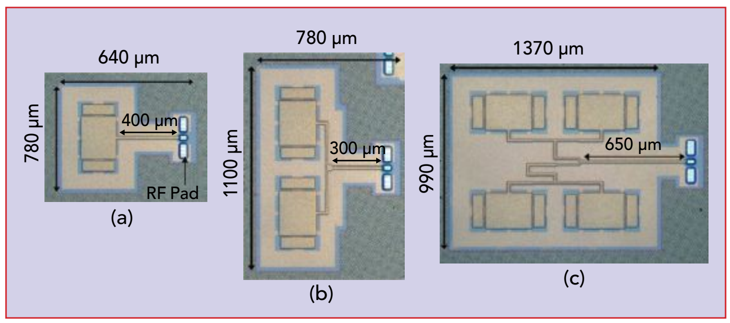


**Fig. 3** **(a) On-chip antenna in 65nm CMOS process.[8] (b) 1 × 2 antenna array on 65 nm CMOS.[8] (c) 2 × 2 antenna array on 65 nm CMOS.[8]**

## ADVANCED FABRICATION METHODS

Traditional fabrication methods require a cleanroom environment, advanced machinery and highly skilled personnel to produce nanoscale components for very high frequency applications. Precise and error-free fabrication techniques are needed to ensure performance in the THz band. Additive manufacturing methods address the limitations of conventional techniques and have been adapted for fabricating a broad range of active and passive components. ***Figure 1*** shows a timeline of some of the important fabrication developments that have gotten the industry to its present state. ***Figure 2*** shows a timeline of some of the processes that support high frequency components and system development.

## CMOS FABRICATION OF THZ COMPONENTS

Reduced gate length in nanometer CMOS transistors, device scaling and the ease of integrating analog and digital components make silicon a viable, low-cost material for THz ICs. In the CMOS process, the antenna is fabricated on a silicon substrate, along with all the other components. This improves the antenna performance by reducing interconnects in on-chip antennas. A prototype test chip for terahertz reconfigurable metamaterial in 180 nm CMOS technology was developed and described by Zihan Ning.[7] Added parasitics resulting from scaling bring additional complications in the design of THz circuits. A 65 nm CMOS process has been used to design a compact broadband antenna array with an operating frequency centered at 300 GHz. This effort has been reported by Changmin Lee and Jinho Jeong.[8] Structures that exhibit improved gain and bandwidth as a result of this study have been fabricated and the antenna is shown in ***Figure 3a***. As reported, a novel ground structure was developed to increase the isolation between elements. This new structure is shown for a 1 × 2 antenna array in ***Figure 3b*** and a 2 × 2 antenna array in ***Figure 3c***.

Metamaterial antennas with substrate-integrated waveguide (SIW) via holes are demonstrated by Mo-

# High Density Without Compromise!

- Test & Measurement
- Broadcast
- Medical

**Learn More**

## High Density Enhances Efficiency with Improved Performance

Step into the next generation of RF performance and high density with the new PX and PRX connector families. Designed as a superior alternative to traditional coax connectors or as an upgrade for existing multi-pin solutions, these advanced connectors offer exceptional performance and scalability, available in configurations ranging from 13 to 53 pins.

| Impedance | Frequency | Housing Contact # | Contact Size | Cable Types |
|---|---|---|---|---|
| 50 Ohm | 100 MHz to 67 GHz | 13, 26, 28, 53 | 16 | RG-178, 316, 405, M17/151(.047") |
| 75 Ohm | 100 MHz to 18 GHz | 13, 23, 48 | 12 | RG-179, SS75086 |

The PHOENIX Company of Chicago™

*Leading Blindmate Microwave Contact Technology*

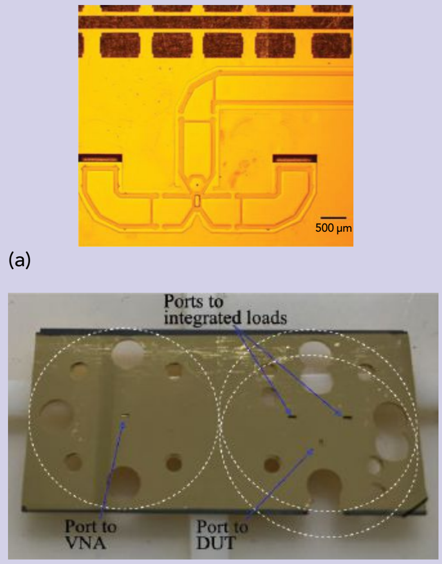


**Fig. 4** **(a) Dual-line antenna array.[15] (b) Silicon-micromachined interposer.[16]**

hammad Alibakhshikenari et al.[9] The antenna described in this paper is fabricated using stacked layers for a compact antenna structure. To reduce surface waves and substrate loss, metallic via holes are formed in the top silicon layer. A standard 0.18 µm CMOS process has been used in a 0.4 THz on-chip antenna design with a slotted radiator.[10] SIW vias connect the top and bottom metal layers and create a back cavity to reduce surface waves. The cavity directs the radiation toward a low-resistivity substrate that improves the broadside radiation. Appropriately designed SIW sidewalls compensate for the effects of the lossy silicon substrate.

## TERAFETS

Antenna-coupled field-effect transistors (TeraFETs) are specialized FETs designed for use in the THz frequency range. These devices combine the high speed electronic properties of FETs with antenna structures, making them capable of detecting, generating and manipulating electromagnetic waves in the THz regime. The modeling and experimental characterization of silicon CMOS detectors for THz radiation using TeraFETs has been extensively studied in the paper from F. Ludwig et al.[11] TeraFET detectors have garnered increasing attention due to their high responsivity, ease of fabrication, ultra-fast response times and significant tunability through adjustments to the gate, doping levels and channel structures.[12]

## SILICON MICROMACHINING

After selecting a suitable material, part of the substrate or a thin film is removed by different etching techniques to obtain micromachined structures. Silicon micromachining uses two main methods: surface micromachining and bulk micromachining. Surface micromachining works on thin films deposited on a silicon wafer to create surface structures. In contrast, bulk micromachining carves features directly from the silicon substrate. Etching is crucial for patterning silicon substrates and includes isotropic and anisotropic types. Isotropic etching, performed wet or dry, creates uniform etching in all directions, leading to rounded features. Anisotropic etching, mainly using dry methods, etches in specific directions, producing sharp-edged features. Both etching techniques are vital for achieving precise and structured results in silicon micromachining. Silicon micromachining has advantages like low fabrication cost, higher tolerance limits, smaller feature sizes and easy integration of components. Micromachined components have reduced surface roughness and insertion loss. Silicon micromachining has been demonstrated as a suitable method for THz frequency components.

A. Madannejad et al.[13] present an innovative silicon-micromachined, low-profile, high gain antenna designed for wideband performance across the entire 500 to 750 GHz waveguide band. The fabrication process is conducted on a silicon-on-insulator (SOI) wafer. A compact silicon-micromachined crossover switch prototype consisting of two hybrid couplers and two SPST switches is demonstrated by A. Karimi et al.[14] The crossover switch prototype is composed of four vertically stacked SOI chips. A silicon-micromachined dual-port, dual-line antenna array with unbalanced feeding is discussed by A. Karimi et al.[15] The fabrication of the antenna array designed in this paper, as shown in ***Figure 4a***, employs advanced silicon micromachining techniques, specifically

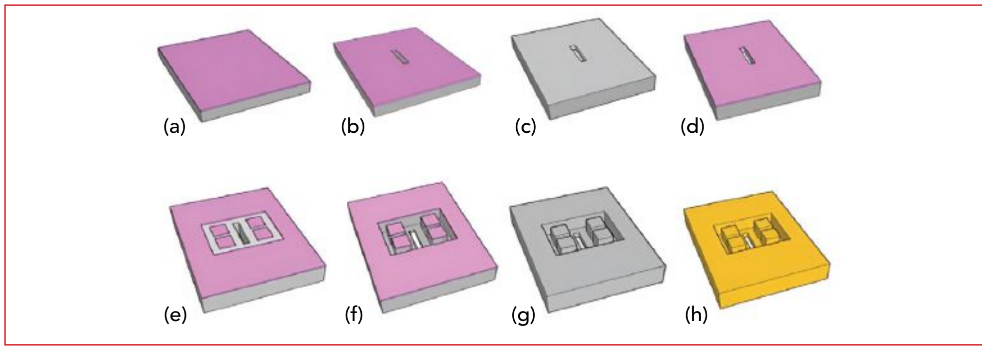


Fig. 5 Fabrication technology for silicon THz antenna feed.[18]

deep reactive ion etching (DRIE) and sidewall metallization. DRIE allows for precise etching of deep, vertical structures in the silicon. At the same time, sidewall metallization ensures uniform conductive coating along the etched features, enhancing the performance and integrity of the antenna array. These techniques enable the creation of complex, high-precision structures required for the antenna's optimal operation in high frequency applications.

***Figure 4b*** shows a silicon-micromachined interposer that has been used in multiport components discussed by Adrian Gomez et al.[16] Silicon-micromachined test interposers offer higher accuracy, lower cost, greater versatility and the ability to integrate loads. These factors make them a crucial tool for advancing the development of sub-THz waveguide components.

Despite the advantages of silicon micromachining, several limitations challenge its application in complex circuit elements and signal chains:

**Scalloped Sidewalls:** The DRIE process can cause scalloping on etched sidewalls, increasing surface roughness and potentially affecting device performance and efficiency.

**Sloped Sidewalls:** Due to varying ion flow and density during deep trench etching, sidewalls may become sloped rather than vertical. Controlling this slope is crucial for maintaining precise dimensions and performance, especially in MEMS systems.

**Aspect Ratio Dependent Etching (ARDE):** ARDE causes variability in sidewall profiles depending on trench aspect ratios, leading to diverse profiles for different device geometries.

**Surface Roughness:** Surface roughness is a critical factor contributing to insertion loss in rectangular waveguides. Minimizing this roughness is essential for low loss, especially at high frequencies.

**IC Integrability:** The fabrication method should be compatible with integrated circuit processes, allowing simultaneous fabrication of active and passive components.

## 3D PRINTING

The advantages of 3D printing have allowed it to replace traditional fabrication methods for THz components. Rapid prototyping and the ability to fabricate design prototypes using a broad range of dielectric and metallic materials are the key advantages of the technique. Low material loss, little hazardous waste generation, the ability to precisely manufacture devices with microscale features, the ease of repeatability and the possibility of fabricating a wide range of components on planar and nonplanar structures using a single tabletop system are other advantages of additive manufacturing. Various 3D-printed antennas used for 5G applications were presented by Rui Xu et al.[17] The impacts and future advancements in antenna fabrication is also investigated.

### 3D-Printed Active and Passive THz Components

In the paper by Shu-Yan Zhu et al.,[18] imprint and dry etching technologies are used to design a Gaussian beam antenna. The paper describes a 100 μm thick silicon substrate etched with a 50 μm × 190 μm slot pattern. The higher aspect ratio demonstrates the advantage of using dry etching technologies. The DRIE process is used to form pillar-shaped photoresist squares. The feed was fabricated by dry etching

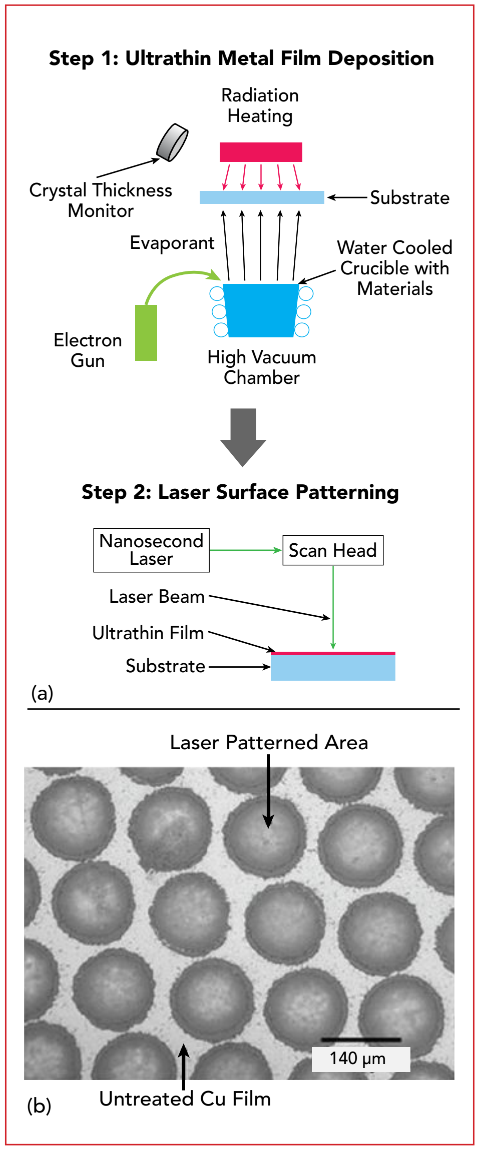


**Fig. 6** (a) Metal film deposition and laser surface patterning.[21] (b) Optical image of metamaterial surface.[21]

and optical lithography in a fabrication process shown in ***Figure 5***.

A two-step 3D printing is used to print a D-Band antenna in the paper from Chao Gu et al.[19] In this example, an antenna prototype is developed that uses metal printing followed by dielectric printing. The structure described in the paper gets 14.2 percent bandwidth and 15.5 dBi gain at 135 GHz, with the gain value resulting from gain enhancement techniques. Broadband propagation characteristics are achieved by using a dielectric ridge waveguide. 3D printing and gold sputtering are combined in the fabrication of topological waveguides in the paper from Muhammad Talal Ali Khan et al.[20] The fabricated metallic waveguide with air channels described in this paper can be used in high speed interconnects.

## LASER-BASED TECHNIQUES

Developments in laser-based manufacturing methods enable the fabrication of ultrathin structures. Transparent conducting surfaces are fabricated on dielectric substrates using laser-based techniques as described by Qinghua Wang et al.[21] Two-step laser-based fabrication is used to achieve ultrathin THz bandpass filtering. The dielectric is coated with a 10 nm thick metal layer and patterns are formed by laser ablation. A nano-pulse laser is used to pattern the metal deposition. Surface resistance and visible transmittance of the fabricated structures are measured using THz time-domain spectroscopy. ***Figure 6a*** shows the thin metal film deposition and laser surface patterning used in this article. ***Figure 6b*** shows an optical image of the laser-based metamaterial surface patterned on an 8 nm thick copper film.

The direct laser writing method is used to fabricate a terahertz metamaterial absorber based on the fractal structure for wideband applications in an article from Hou-Bing Liu et al.[22] From this paper, a negative glue covers the dielectric layer and the patterns are formed on a photoresist using direct laser writing, followed by metal deposition with magnetron sputtering. A laser is used in various processes such as engraving, melting, drilling, cutting, ablation and patterning of THz component fabrication. Direct laser patterning (DLP) is adapted as a suitable maskless method, in the fabrication of various micro apertures and surface patterns in different materials.[23] Changes in design can be easily adapted in femtosecond laser DLP techniques since it uses a maskless printing method.

## CONCLUSION

This article has presented an overview of recent developments in advanced fabrication techniques suitable for the THz regime. THz frequencies hold much promise and they are attracting substantial attention and investment. The availability of well-understood manufacturing techniques opens the opportunity to explore the promise of the THz frequency band for next-generation communication systems. ■

## References

1. M. V and N. Gunavathi, "Experimental Study on THz-FSS Structures using SIW Technology," November 2023, doi: 10.1109/ICRASET59632.2023.10420264.
2. J. Carter et al., "Terahertz Properties of Common Microwave Dielectric Materials," *Journal of Infrared, Millimeter, and Terahertz Waves*, Vol. 44, 2023, pp. 873–884, Web: https://doi.org/10.1007/s10762-023-00940-3.
3. N. Duangrit et al., "Terahertz Dielectric Property Characterization of Photopolymers for Additive Manufacturing," *IEEE Access*, Vol. 7, 2019, pp. 12339–12347, doi: 10.1109/ACCESS.2019.2893196.
4. S. Dash et al., "Material selection for THz antennas," Wiley, 2017, doi: 10.1002/mop.31127.
5. D. Correas-Serrano et al., "Graphene-based Antennas for Terahertz Systems: A Review," *Forum for Electromagnetic Research Methods and Application Technologies (FERMAT)*, April 2017, arXiv:1704.00371.
6. R. T. Ako et al., "Dielectrics for Terahertz Metasurfaces: Material Selection and Fabrication Techniques," *Advanced Optical Materials*, 2019, doi: 10.1002/adom.201900750.
7. Z. Ning et al., "An AI-assisted Terahertz Reconfigurable Metamaterial in Standard 180-nm CMOS," *Optics Communications*, 2024, Web: https://doi.org/10.1016/j.optcom.2024.130934.
8. C. Lee and J. Jeong, "THz CMOS On-Chip Antenna Array Using Defected Ground Structure," *Electronics 2020*, 9, 1137, doi: 10.3390/electronics9071137.
9. M. Alibakhshikenari et al., "Study on on-Chip Antenna Design Based on Metamaterial-Inspired and Substrate-Integrated Waveguide Properties for Millimetre-Wave and THz Integrated-Circuit Applications," *Journal of Infrared, Millimeter, and Terahertz Waves*, Vol. 42, 2021, pp. 17–28, Web: https://doi.org/10.1007/s10762-020-00753-8.
10. R. K. Kushwaha et al., "Design of a SIW on-chip Antenna using 0.18-µm CMOS Process Technology at 0.4 THz," *Optik*, September 2020, Web: https://doi.org/10.1016/j.ijleo.2020.165509.
11. F. Ludwig, J. Holstein, A. Krysl, A. Lisauskas and H. G. Roskos, "Modeling of Antenna-Coupled Si MOSFETs in the Terahertz Frequency Range," *IEEE Transactions on Terahertz Science and Technology*, Vol. 14, No. 3, pp. 414–423, May 2024, doi: 10.1109/TTHZ.2024.3388254.
12. Y. Zhang and M. S. Shur, "TeraFET Terahertz Detectors with Spatially Non-uniform Gate Capacitances," *Appl. Phys. Lett.*, Vol. 119, 161104, 2021, Web: https://doi.org/10.1063/5.0069072.
13. A. Madannejad, M. M. Gohari, U. Shah and J. Oberhammer, "High-Gain Circularly Polarized 500–750 GHz Lens Antenna Enabled by Silicon Micromachining," *IEEE Transactions on Antennas and Propagation*, Vol. 72, No. 5, May 2024, pp. 4077–4085, doi: 10.1109/TAP.2024.3383289.
14. A. Karimi, U. Shah, S. Yu and J. Oberhammer, "A 220–260-GHz Silicon-Micromachined Waveguide MEMS Crossover Switch," *IEEE Transactions on Microwave Theory and Techniques*, doi: 10.1109/TMTT.2024.3373870.
15. A. Karimi, U. Shah, A. Madannejad and J. Oberhammer, "Silicon-Micromachined Subterahertz Frequency Beam-Steered Dual-Port Array Antenna," *IEEE Transactions on Terahertz Science and Technology*, Vol. 14, No. 2, March 2024, pp. 258–268, doi: 10.1109/TTHZ.2023.3344023.
16. A. Gomez et al., "Micromachined Waveguide Interposer for the Characterization of Multi-port Sub-THz Devices," *Journal of Infrared, Millimeter, and Terahertz Waves*, doi: 41. 10.1007/s10762-019-00663-4.
17. R. Xu et al., "A Review of Broadband Low-Cost and High-Gain Low-Terahertz Antennas for Wireless Communications Applications," *IEEE Access*, Vol. 8, 2020, doi: 10.1109/ACCESS.2020.2981393
18. S.-Y. Zhu et al., "Compact High-gain Si-imprinted THz Antenna for Ultra-high Speed Wireless Communications," *IEEE Transactions on Antennas and Propagation*, doi:10.1109/TAP.2020.2986863.
19. C. Gu et al., "A D-band 3D-Printed Antenna," *IEEE Transactions on Terahertz Science and Technology,* doi:10.1109/TTHZ.2020.2986650.
20. M. T. Ali Khan et al., "3D-Printed Terahertz Topological Waveguides," September 2020, Web: https://doi.org/10.1002/admt.202100252.
21. Q. Wang et al., "High Throughput Laser Process of Transparent Conducting Surfaces for Terahertz Bandpass Ultrathin Metamaterials," *Scientific Reports*, Web: https://doi.org/10.1038/s41598-019-38949-1.
22. H.-B. Liu et al., "An Ultra-Wideband Terahertz Metamaterial Absorber Based on the Fractal Structure," *Plasmonics*, Web: https://doi.org/10.1007/s11468-020-01288-3.
23. B. Voisiat et al., "THz Components and Plasmonic Structures Fabricated by Direct Laser Patterning of Metals," *39th International Conference on Infrared, Millimeter, and Terahertz Waves,* 2014, doi: 10.1109/IRMMW-THz.2014.6956327.

INVITED PAPER

# Making Material Measurements with a VNA

Brian Walker
*Copper Mountain Technologies, Indianapolis, Ind.*

Knowing a material's RF properties, such as its complex permittivity and permeability, can be very important. The radome protecting an outdoor radar from the elements must have a known permittivity and thickness to pass radar frequencies with minimal attenuation. How will a thin coating of water on the radome effect performance? The protective cover over the radar embedded in an automobile bumper must be designed to pass the mmWave frequencies emitted and received. How will paint affect the RF transmission through the cover? Antennas are encased in our cellular phones. How do the plastic materials affect the antenna performance? Material measurements with a vector network analyzer (VNA) can measure material properties and answer these important questions.

## HOW IS A VNA USED TO MEASURE MATERIAL PROPERTIES?

Microwave or mmWave signals are applied to a flat material sample with known thickness. Signals incident on the sample should be plane waves applied normal to the sample's surface. This way, RF signals that transit the material pass through the known thickness and not some longer path at an angle. It is sufficient to measure the thickness and the transmission and reflection characteristics of a material to determine its complex permittivity. Permeability may also be determined, but the calculation is greatly simplified if it can be assumed to be unitary.

The VNA is either attached to a pair of antennas for a free-space measurement or to a waveguide with a sample holder. In the free-space method, a pair of horns may be used to send and receive the signal and dielectric lenses are positioned to focus the beams onto the specimen. In ***Figure 1***, the sample is held by a fixture in the center between the antennas of a system offered by Compass Technology Group and at a position where the focused beams are most planar. Calibration is performed using a shorting plate as the reflect and an empty sample holder as the through. Time domain gating is used around the sample position in bandpass mode to eliminate stray reflections and multipath. The sample is then inserted and S-parameter measurements are made.

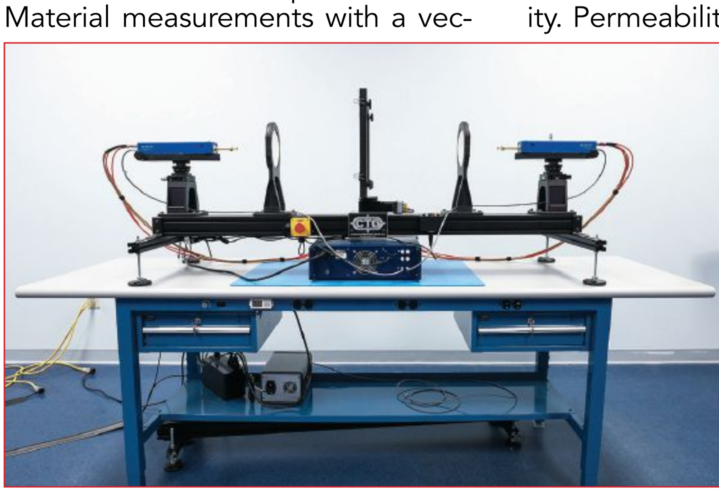

**Fig. 1** **Free-space measurement test setup. *Source:* Compass Technology Group.**

A material might also be measured by inserting it in a waveguide path. The MCK measurement system from SwissTo12, shown in ***Figure 2***, is configured in this manner. Two corrugated horn antennas operating over a given waveguide bandwidth are placed end to end

**Fig. 2** **SwissTo12 MCK measurement system.**

# RF Field Measurements

## World's First Handheld Spectrum Analyzer with 150 MHz Analysis Bandwidth

From the company that introduced the world's first handheld spectrum analyzers, Anritsu now launches another first: **150 MHz analysis bandwidth to 54 GHz in a field portable instrument**.

Validate the quality and integrity of your radars, transmitters, EW systems, or satellite ground stations. Measure signal quality, identify interfering signals, and measure radar pulses—all in a single instrument.

- **Real-time Spectrum Analysis Highlights Modulation Bandwidth and Signal-in-Signal or Short Burst Interference**
- **IQ Capture and Streaming with IQ Signal Master™ MX280005A Software Provides Unmatched Insights**

Anritsu Field Master Pro™ MS2090A and MS2720xA Remote Spectrum Monitors give you greater understanding and analysis capabilities of your RF environment.


## The New Enhanced Site Master™ MS208xA

In 1995, Anritsu launched the world's first field portable cable and antenna analyzer in response to the explosion in installations of base stations to support the global mobile phone industry. Anritsu has continuously enhanced and developed the Site Master to meet the requirements of a wide range of cellular, LMR, broadcast, EW, radar and defense systems.

The new MS2085A and MS2089A Site Master offers the best ever accuracy, reliability, and functionality.

- **New ReadyCal for Quick and Error-Free Measurement Setup**
- **Faster Sweeps for Greater Response and Shorter Measurement Cycle Times**

Coupled with a fully featured spectrum analyzer, the new Site Master contains all of the capabilities that field engineers require in a single robust and reliable instrument.

Anritsu
Advancing beyond

Discover how you can achieve measurement confidence with Anritsu.
Learn more at **www.anritsu.com/test-measurement**

and a material under test (MUT) is placed between them. These systems measure the S-parameters, reflection and transmission through the MUT and a mathematical inversion converts these measurements to a complex permittivity.

SPEAG's Dielectric Assessment Kit (DAK) product line, based on the open coaxial probe method, provides high-precision dielectric parameter measurements, including permittivity, conductivity and loss tangent, over a wide frequency range from 4 MHz to 67 GHz. The advanced hardware technology and user-friendly software of DAK instruments are designed for accurate, precise and non-destructive measurements, making them ideal for use in telecommunications, material science, bioelectromagnetics, biomedical research and industries like automotive, electronics and food.

The DAK System (DAKS) is the first system capable of measuring thin-layer materials and small liquid volumes, as well as DAK single probes. DAKS is a low-cost, portable and easy-to-use dielectric assessment system kit that combines the DAK technology, shown in ***Figure 3***, with the miniature portable R60 and R140B vector reflectometers from Copper Mountain Technologies. The direct and rigid connection of the probe to the reflectometer allows the probe to be moved to the MUT after calibration, greatly simplifying measurements in the lab. The DAK product line includes the DAK-TL2, shown in ***Figure 4***.

## HOW IS THE PERMITTIVITY INVERSION COMPUTATION DONE?

The computation is an inversion because the material's complex permittivity determines the transmission and reflection of the RF waves. The inversion must solve for the unique permittivity that causes the measured reflections. Uniqueness is an important consideration. In any inversion problem, multiple parameter values could create the same outcome, so seeding the problem with a best-guess solution is usually necessary.

How is complex permittivity calculated from the S-parameters? First, the transmission and reflection properties at the interfaces and within the material are modeled when illuminated by a plane wave. As detailed by Dr. Schultz[1]

**Fig. 3** **SPEAG DAK measurement system.**

**Fig. 4** **SPEAG DAK-TL2 measurement system.**

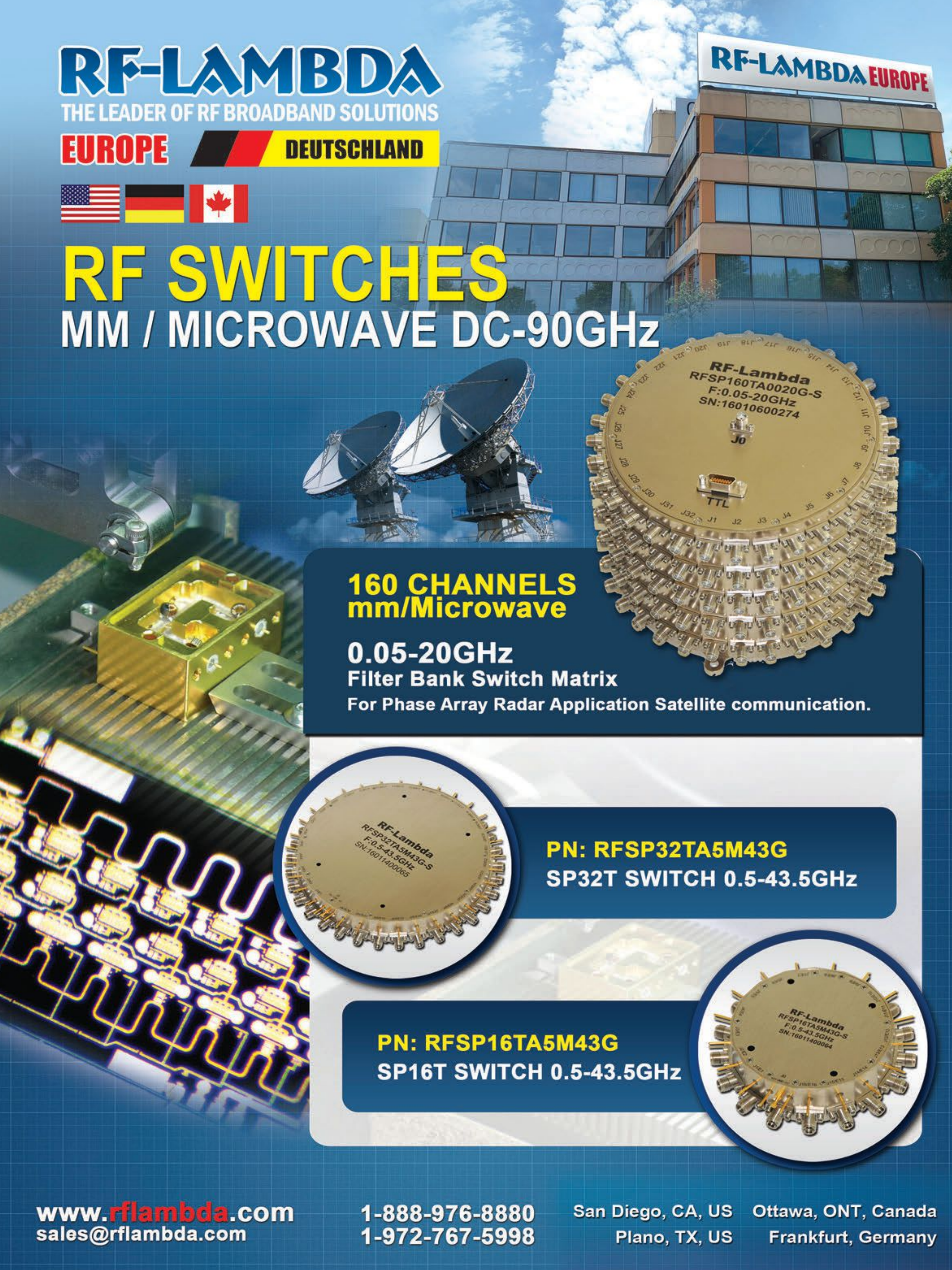
RF-LAMBDA
THE LEADER OF RF BROADBAND SOLUTIONS
EUROPE
DEUTSCHLAND
RF-LAMBDA EUROPE
RF SWITCHES
MM / MICROWAVE DC-90GHz
RF-Lambda
RFSP160TA0020G-S
F:0.05-20GHz
SN:16010600274
160 CHANNELS
mm/Microwave
0.05-20GHz
Filter Bank Switch Matrix
For Phase Array Radar Application Satellite communication.
PN: RFSP32TA5M43G
SP32T SWITCH 0.5-43.5GHz
PN: RFSP16TA5M43G
SP16T SWITCH 0.5-43.5GHz
www.rflambda.com
sales@rflambda.com
1-888-976-8880
1-972-767-5998
San Diego, CA, US
Plano, TX, US
Ottawa, ONT, Canada
Frankfurt, Germany

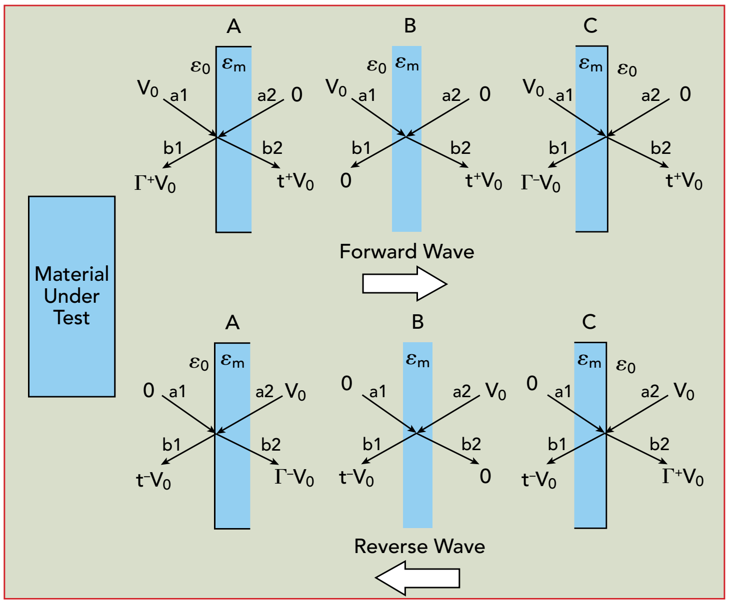


▲ **Fig. 5** **Modeled material zones.**

and shown in ***Figure 5***, the MUT can be divided into three zones: Zone A is an infinitely thin left-hand surface to model signal reflection, Zone B is a central section to model signal transmission and Zone C is another infinitely thin surface to model a second reflection with a 180-degree phase shift compared to the first reflection. Reflections occur whenever a wave passes from a medium with one dielectric constant to another, $\varepsilon_0$ to $\varepsilon_m$ and $\varepsilon_m$ back to $\varepsilon_0$, in this case.

In this analysis, $\varepsilon_0$, the permittivity of air, is 8.854 pF/m or may be normalized to 1.0. The material permittivity, $\varepsilon_m$, will also be normalized by this value. For non-magnetic materials, the permeability, $\mu_m$, can be set to 1.0.

S-parameter matrices can be built for the three zones, but transfer parameters are more useful since they can be multiplied to obtain the composite result for the entire slab of material.

Transfer parameters relate the a and b used in Figure 4 by ***Equation 1***:

$$\begin{vmatrix} b_1 \\ a_1 \end{vmatrix} = \begin{vmatrix} T_{11} & T_{12} \\ T_{21} & T_{22} \end{vmatrix} \begin{vmatrix} a_2 \\ b_2 \end{vmatrix} \qquad (1)$$

Filling in the values for $a_1$, $a_2$, $b_1$ and $b_2$ from the forward and reverse case of Zone A in Figure 5 and noting that $\Gamma\text{-} = -\Gamma\text{+}$, ***Equation 2*** can be used to solve for the four transfer parameters:

$$\begin{vmatrix} T_{11} & T_{12} \\ T_{21} & T_{22} \end{vmatrix}_A = \begin{vmatrix} t^- + \dfrac{\Gamma^{+2}}{t^+} & \dfrac{\Gamma^+}{t^+} \\ \dfrac{\Gamma^+}{t^+} & \dfrac{1}{t^+} \end{vmatrix} \qquad (2)$$

The tangent voltages of the plane wave must be the same on each side of the interface for both forward and reverse waves. Substituting $\Gamma\text{-} = -\Gamma\text{+}$ and equating the results in ***Equation 3***:

$$1 + \Gamma^+ = t^+ \text{ and } 1 - \Gamma^+ = t^- \qquad (3)$$

Eliminating the transmission parameters $t^+$ and $t^-$, the transfer matrix for Zone A can be written in terms of $\Gamma$+ alone. Dropping the "+" and doing the substitution yields ***Equation 4***:

$$\begin{vmatrix} T_{11} & T_{12} \\ T_{21} & T_{22} \end{vmatrix}_A = \frac{1}{1+\Gamma} \begin{vmatrix} 1 & \Gamma \\ \Gamma & 1 \end{vmatrix} \qquad (4)$$

The reflection at the interface is a known function of the normalized permittivity and permeability and it

is given by ***Equation 5***:

$$\Gamma = \frac{\sqrt{\frac{\mu_m}{\varepsilon_m}} - 1}{\sqrt{\frac{\mu_m}{\varepsilon_m}} + 1} \text{ or } \frac{1 - \sqrt{\varepsilon_m}}{1 + \sqrt{\varepsilon_m}} \quad (5)$$

for $\mu_m = 1$

Note that if $\varepsilon_m = 1$ and $\mu_m = 1$, then $\Gamma = 0$, or no reflection for an air-to-air interface.

From the forward and reverse wave cases for Zone B, the transfer matrix can be determined as in ***Equation 6***:

$$\begin{vmatrix} T_{11} & T_{12} \\ T_{21} & T_{22} \end{vmatrix}_B = \begin{vmatrix} t & 0 \\ 0 & \frac{1}{t} \end{vmatrix} \quad (6)$$

The propagation velocity of a wave is a function of the permittivity and permeability. For free space, $\frac{1}{\sqrt{\mu_0 \varepsilon_0}} = c$, which is the speed of light. Using normalized $\varepsilon_m$ and $\mu_m$, the wave speed in the MUT is given by ***Equation 7***:

$$v_m = \frac{c}{\sqrt{\mu_m \varepsilon_m}} \; m/s \quad (7)$$

The "*t*" in Equation 6 may be expressed in terms of the permittivity and permeability as given by ***Equation 8***:

$$t = e^{-jk_m d} \quad (8)$$

Where: Material wave number, $k_m = \frac{2\pi f}{v_m}$ rad/m

and *d* is the thickness of the material in meters.

Finally, substituting $-\Gamma$ for $\Gamma$ into Equation 4 gives the transfer parameters for Zone C as shown in ***Equation 9***:

$$\begin{vmatrix} T_{11} & T_{12} \\ T_{21} & T_{22} \end{vmatrix}_C = \frac{1}{1-\Gamma} \begin{vmatrix} 1 & -\Gamma \\ -\Gamma & 1 \end{vmatrix} \quad (9)$$

Multiplying all three matrices gives the expression in ***Equation 10***:

$$T_m = \frac{1}{1-\Gamma^2} \begin{vmatrix} 1 & \Gamma \\ \Gamma & 1 \end{vmatrix} * \begin{vmatrix} t & 0 \\ 0 & \frac{1}{t} \end{vmatrix} * \begin{vmatrix} 1 & -\Gamma \\ -\Gamma & 1 \end{vmatrix} = \frac{1}{t(1-\Gamma^2)} \begin{vmatrix} t^2 - \Gamma^2 & \Gamma(1-t^2) \\ \Gamma(t^2-1) & 1-\Gamma^2 t^2 \end{vmatrix} \quad (10)$$

Finally, converting the transfer parameters to S-parameters using the standard conversion formula gives the expression in ***Equation 11***:

$$S_m = \frac{1}{1-\Gamma^2 t^2} \begin{vmatrix} \Gamma(1-t^2) & t(1-\Gamma^2) \\ t(1-\Gamma^2) & \Gamma(1-t^2) \end{vmatrix} \quad (11)$$

With these equations, the S-parameters, in terms of $\varepsilon_m$ and $\mu_m$, have been determined as measured from one surface of the MUT to the other. The Nicolson-Ross-Weir (NRW) algorithm[2,3] or an iterative solver can determine the permittivity and permeability that fits the measured data. In the free-space methods, the NRW method is not recommended and a four-parameter method is preferred since it eliminates the need to precisely position the sample under test.

For a non-magnetic sample, it is sufficient to measure $S_{11}$ and $S_{21}$, guess at the permittivity, $\varepsilon_m$, calculate $\Gamma$ and *t* and then use an iterative method to improve the guess and minimize the errors in ***Equation 12*** and ***Equation 13***:

$$S_{21} = \frac{t(1-\Gamma^2)}{1-\Gamma^2 t^2} \quad (12)$$

$$S_{11} = \frac{\Gamma(1-t^2)}{1-\Gamma^2 t^2} \quad (13)$$

As a check, note that $S_{21} = t$ if there is no reflection, $\Gamma$. Also, $S_{11} = \Gamma$ if there is no transmission, $t$. After a potential solution is found, it is a good idea to plot the calculated versus measured values of $S_{11}$ and $S_{21}$ to assess the accuracy of the solution.

The primary issue with this method is that for materials with a low loss tangent, the imaginary part of $\varepsilon_m$ is small. Changing the value of this quantity has only a tiny effect on the complex value of $S_{21}$. Most optimizer strategies will struggle with this problem. Compass Technologies, SwissTo12 and SPEAG have all overcome this issue with their software.

The equations detailed in this article provide a helpful background for an engineer who needs to perform material measurements. Integration experts at Compass Technologies, SwissTo12 and SPEAG provide measurement systems and software to perform these measurements and calculate permittivity. For a nominal fee, they can also make batch measurements for those who do not wish to procure a dedicated system.

## PRACTICAL CONSIDERATIONS

Sometimes troublesome resonances may occur at frequencies where the sample thickness is an integer multiple of half wavelengths and measurements may contain singularities. This occurs when using both reflection and transmission inversions on non-magnetic specimens. A video demonstrating the focused-beam measurement technique is available on the Copper Mountain Technologies website.[4]

Several practical considerations may prove helpful:

- If TRL calibration is performed, it is helpful to normalize the $S_{21}$ response while viewing it in the Smith Chart format. To do this, place a marker in the middle of the frequency band. Move one of the antennas until a 90-degree phase shift is attained for the "line" standard. For the "through" standard, move the antenna back until the phase is zero once again.
- Time domain gating, a standard feature of all Copper Mountain Technologies VNAs except the "M" series, should be applied to the area occupied by the MUT to eliminate multipath reflections from other surfaces in the lab.
- Different material measurements require different solutions. Lower frequency measurements might be performed with a focused-beam system from Compass Technologies. Liquid materials would best be measured with a system from SPEAG. mmWave measurements could be made with the MCK system from SwissTo12 or a table-top free-space measurement system from Compass.
- The waveguide measurement fixture from SwissTo12 can measure plain, coated or multilayer solids, liquids and powders.

## CONCLUSION

There are many ways to make material measurements. Copper Mountain Technologies has a wealth of experience with metrology-grade VNAs covering frequencies from 1.5 to 330 GHz. The best solution may also require fixturing and other areas of expertise in addition to the measurement techniques. To account for the impact that RF material properties, such as their complex permittivity and permeability, may have on a design and minimize their effects, it is often helpful to enlist a partner with expertise in these areas. ■


### References

1. J. W. Schultz, "Focused Beam Methods," 2012, First ed., pp. 44–48.
2. W. B. Weir, "Automatic Measurement of Complex Dielectric Constant and Permeability at Microwave Frequencies," *Proceedings of the IEEE*, Vol. 62, No. 1, January 1974, pp. 33–36, doi: 10.1109/PROC.1974.9382.
3. A. N. Vicente, G. M. Dip and C. Junqueira, "The step-by-step Development of the NRW Method," *SBMO/IEEE MTT-S International Microwave and Optoelectronics Conference*, 2011, Web: https://doi.org/10.1109/IMOC.2011.6169318.
4. "Free Space Material Characterization at Millimeter Wave: Using Frequency Extenders with CTG's Focused Beam System," Copper Mountain Technologies, Web: coppermountaintech.com/webinar/free-space-material-characterization-at-millimeter-wave-using-frequency-extenders-with-ctgs-focused-beam-system.

Microwave Journal

SPECIAL**FOCUS**

# CABLES & CONNECTORS

# CABLES & CONNECTORS

## SPECIALFOCUS
TABLE OF CONTENTS

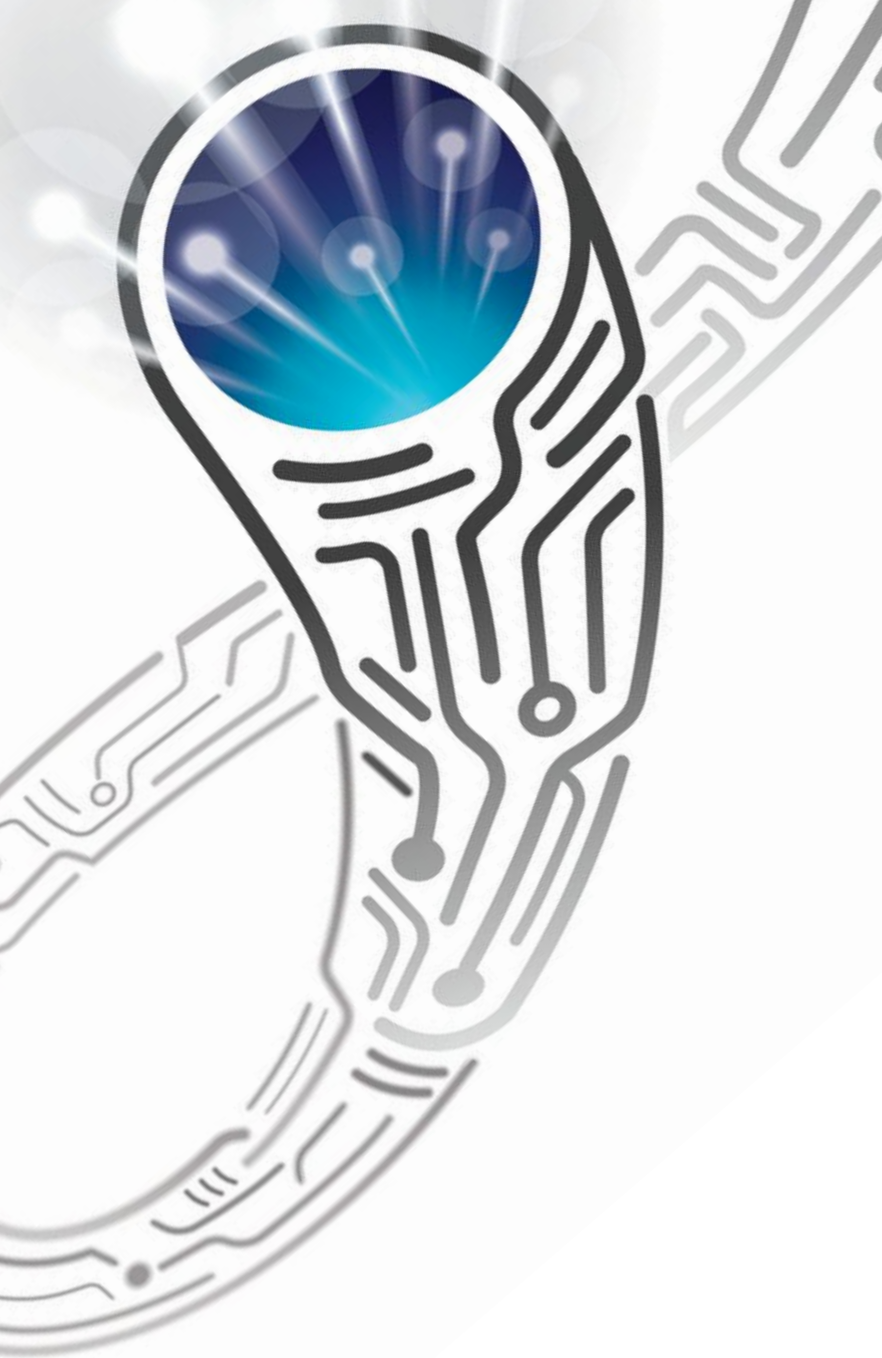


### Cover Feature

**78** **Evolution of Interconnects in Benchtop RF Test**
*Jim Alexander, Dan Birch and David Beraun, Samtec*

### Special Report

**86** **Supporting Commercial Vehicle Production Through Modular Innovation**
*Robert Weirauch, HUBER+SUHNER*

### Product Features

**94** **Proprietary Connector Design Enhances Quality and Phase Stability**
*Junkosha*

**96** **High-Density Connection Enhances PXIe Test & Measurement**
*The Phoenix Company of Chicago, Inc.*

**100** **Selecting the Right RF Cable Assembly**
*Smiths Interconnect*

### Tech Brief

**104** **Durable RF Cable Assemblies**
*Swift Bridge Technologies*

### Departments

**105** **New Products**



STAFF

**Group Director:** Carl Sheffres
**Associate Publisher:** Michael Hallman
**Media Director:** Patrick Hindle
**Brand & Content Director**: Jennifer DiMarco
**Technical Editor:** Eric Higham
**Associate Technical Editor:** Cliff Drubin
**Editorial & Media Specialist:** Kelley Roche
**Associate Editor:** Kaitlyn Joyner

**Multimedia Staff Editor:** Barbara Walsh
**Electronic Marketing Manager:** Chris Stanfa
**Senior Digital Content Specialist:** Lauren Tully
**Digital Content Specialist:** Vincent Carrabino
**Director of Production & Distribution:** Edward Kiessling
**Art Director:** Janice Levenson
**Graphic Designer:** Ann Pierce

**EUROPE**
**Office Manager:** Nina Plesu

**CORPORATE STAFF**
**CEO:** William M. Bazzy
**President:** Ivar Bazzy
**Vice President:** Jared Bazzy

# Evolution of Interconnects in Benchtop RF Test

Jim Alexander, Dan Birch and David Beraun
*Samtec, New Albany, Ind.*

In addition to test instrumentation, such as a vector network analyzer (VNA), the test fixture for the device under test (DUT) is a critical element of RF benchtop evaluation. The DUT can range in complexity from a single chip or component to an entire printed circuit board (PCB) subsystem. When assessing the performance of a DUT, the ideal scenario is to have the test equipment directly connected to the ports of the DUT. However, this approach is typically not feasible due to practical considerations. Therefore, a test fixture is used between the DUT and the test equipment.

The test fixture usually consists of a combination of connectors, cables and PCBs. One of the main goals for the test fixture is to make it as electrically transparent as possible. This means the fixture should not affect the measurement results across the full bandwidth of the measurement being made. Further analysis on de-embedding test fixtures and considerations is given by S. Sankararaman et al.[1]

This article reviews how some types of interconnects (cables and connectors) in benchtop RF tests have evolved in response to changing test needs in the context of the important technical challenges for modern test fixtures.

## TECHNICAL CHALLENGES

VNAs are commonly used in RF benchtop tests. These powerful and versatile tools have evolved dramatically since the introduction of commercially available VNAs in the 1970s. At that time, these devices were made up of multiple bays of test racks of various instruments. Since their inception, VNAs have developed into systems with fast sampling rates, FFT-based spectrum analysis, wide bandwidths and deep memory to support the analysis of complex wideband signals. The relatively recent addition of a direct digital synthesis allows newer VNAs to expand from narrowband analysis to nearly unlimited bandwidth possibilities.[2]

Fortunately, the technological advances in VNAs have also dramatically increased the speed of measurements. For example, full-band frequency sweeps in the 1970s could easily take more than one hour. Today, VNAs can complete a frequency sweep in a fraction of a second. This speed change enhanced the role of the VNA and enabled real-time measurement capability, often incorporating environmental stimuli such as temperature changes and vibration. It is important to note that these stimuli not only affect the performance of the DUT, but also the test fixturing.

As microwave devices and systems continue to proliferate, new frequency bands, such as 32 GHz and 43.5 GHz, become important for applications like 5G wireless and K-Band satellite communications. The VNA cables that support benchtop RF testing are commonly optimized for minimal loss and phase stability over time, flexure and temperature. An example of a VNA and its associated cables is shown in ***Figure 1***. With applications in new bands, there are opportunities to optimize new cable and/or connector variants. For example, a cable design optimized for 32 GHz can provide a lower loss solution than a cable that was optimized for 40 GHz.

In addition, today's test fixtures require interconnects, both cables and connectors, to support higher physical channel counts than ever before and provide higher density in a reduced space. They must operate with high linearity, meaning no suckouts or non-linear phase changes in the band and demonstrate repeatability after mating/unmating the interconnects. This is especially true in the initial system bring-up. Satisfying all these interconnect needs in cables and connectors has been challenging for interconnect suppliers.

## CABLE AND CONNECTOR EVOLUTION

In the early days of RF benchtop testing, choosing a cable or con-

**Fig. 1** Samtec Nitrowave™ cables in a test application using Keysight P502A USB VNAs.


**Fig. 2** **Samtec REF-228591 evaluation kit with multiple compression-mount connectors.**

nector was often an afterthought. Designers frequently used whatever was available. Today, connecting to the PCB can be accomplished with a variety of different interconnects, each with its advantages and disadvantages for handling complex signals.

### SMA Connectors

Since the 1960s, sub-miniature version A (SMA) connectors have served RF and microwave applications. Today, they are used in applications up to 27 GHz. Traditionally, SMAs were soldered onto the board using through-hole technology. Later, surface-mount versions became popular and edge-mount SMAs were used for the highest frequency applications. Older connectors, especially through-hole designs, are well suited for use in rugged conditions that see heavy use. However, these connectors may require extensive skill and/or expensive tooling to get optimal results. SMA connectors can still be an excellent choice due to their wide availability and notable ruggedness as long as their bandwidth supports the DUT's upper-frequency limit.

### Compression-Mount Connectors

Existing in some form or another since the 1960s, compression RF connectors have gained favor recently since they can more readily support higher frequencies. This has a lot to do with the solder joints, more specifically, eliminating them.

At lower frequencies, solder joints have proven to be a reliable method of attaching interconnects. However, as frequencies and data rates have increased, the inevitable variations in attributes like the size and shape of solder joints translate into variations in electrical performance.[3] With solderless connectors, the electrical contact is established between the two contacts by screwing the connector to the PCB. Over the years, push-on compression-mount connectors have been adapted to use threads to provide more consistent performance and ensure secure attachment.

Compression-mount connectors provide several advantages. These include improved signal integrity compared to soldered connectors, faster assembly and the ability to remove and reuse, which can be very helpful in a test fixture for RF benchtop testing.[4] For instance, Samtec test fixture cards are optimized for breakout performance, allowing users to swap out their compression-mount connectors quickly, depending on the test setup. ***Figure 2*** shows an example of the Samtec REF-228591 evaluation kit containing 1.35 mm, 1.85 mm, 2.40 mm and 2.92 mm compression-mount connectors.

Unlike soldered connectors, compression-mount connectors access the PCB signal layers through micro-vias. This avoids the need for large through-holes and blind vias. In terms of performance, this can translate into excellent impedance, which improves high speed transmission.[4]

## THE IMPORTANCE OF ALIGNMENT

Small compression-mount connectors are well suited for use in test, prototype and diagnostic applications. This is due, in large part, to their performance and ease-of-use advantages. One concern with these types of connectors is the risk of misalignment. Unfortunately, it can be challenging to detect this misalignment.[5,6]

Interconnects are needed at all signal inputs and outputs. At higher frequencies, even slight misalignments of a connector are sufficient to cause failure.[7] Fortunately, the industry has addressed connector misalignment by adding visual indicators to aid in the proper alignment of small compression-mount connectors, as shown in ***Figure 3***. These alignment marks can significantly speed up assembly and alignment while improving yield. These alignment features work with fiducials on the PCB to ensure proper placement and contact of the compression-mount connectors. Ganged connectors are also available with alignment features to help avoid misalignment.

**Fig. 3** **Alignment features indicated with arrows.**

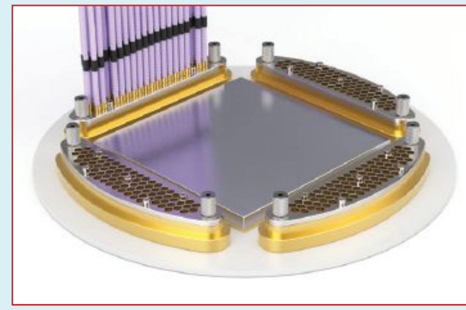

**Fig. 4** **A ganged compression connector simplifies test fixture board design.**

## GANGED SOLDERLESS INTERCONNECTS

As the need for connectors in a test fixture increases, the design can become bulky and space-constrained. A solution to this challenge has been the regular use of ganged solderless connectors in RF benchtop testing. A ganged connector enables more channels. In addition, ganged solderless compression systems can improve the speed of swapping out connectors, reliability and real estate issues.

***Figure 4*** shows an example of a Samtec Bulls Eye® high performance test assembly with ganged solderless connectors and cables. Our research shows that a configura-

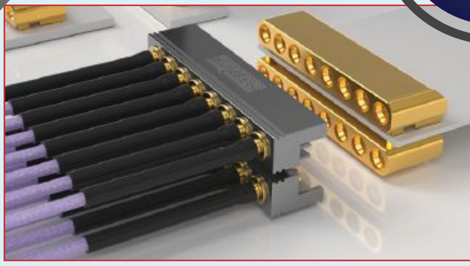

▲ Fig. 5 Belly-to-belly ganged connector configuration.

tion like the one shown in Figure 4 can have good performance because cable losses are lower than PCB losses. Further minimizing loss, ganged connectors increase connection density and they can be placed closer to the DUT.

The benefits of ganged connector solutions can be leveraged even more by changing the plane in which the cables approach the fixture. This becomes particularly important when the test fixture has z-height restrictions. In these applications, bringing the cables in parallel to the PCB is advantageous. There can also be density improvements from unique solutions that enable connectors to be mated on both sides of the PCB, also known as "belly-to-belly," as shown in ***Figure 5*** for Samtec's Magnum RF® GPPC-RA-SM product with a 3.94 mm (.155 in.) profile.

## PERFORMANCE ANALYSIS

To demonstrate the advantages of the ganged connector configuration, two ganged cable connectors and a circuit trace of the same length are analyzed. The goal of this analysis was to understand the insertion loss (IL) and return loss performance for a test fixture over a wide frequency range. ***Figure 6*** shows a comparison of loss for a circuit trace and two ganged cable connectors. One of the ganged connectors uses 0.047 in. diameter low loss cables and the other uses 0.086 in. diameter low loss cables. The results indicate that ganged cable connectors minimize fixture IL substantially, especially

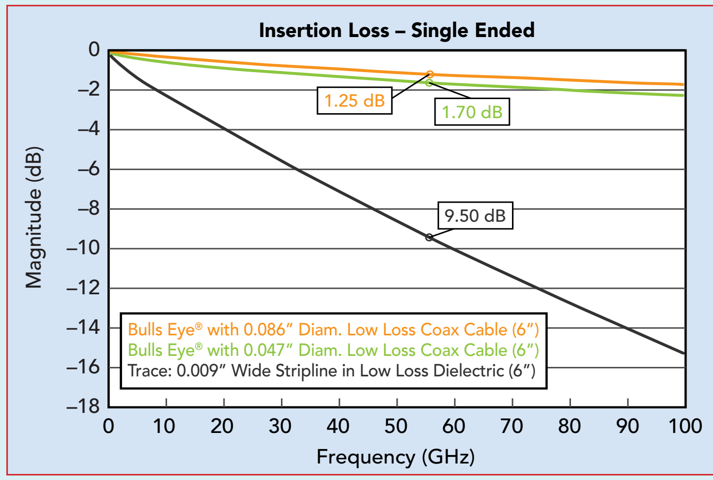


▲ Fig. 6 Insertion loss comparison for ganged cable connectors and a stripline trace.

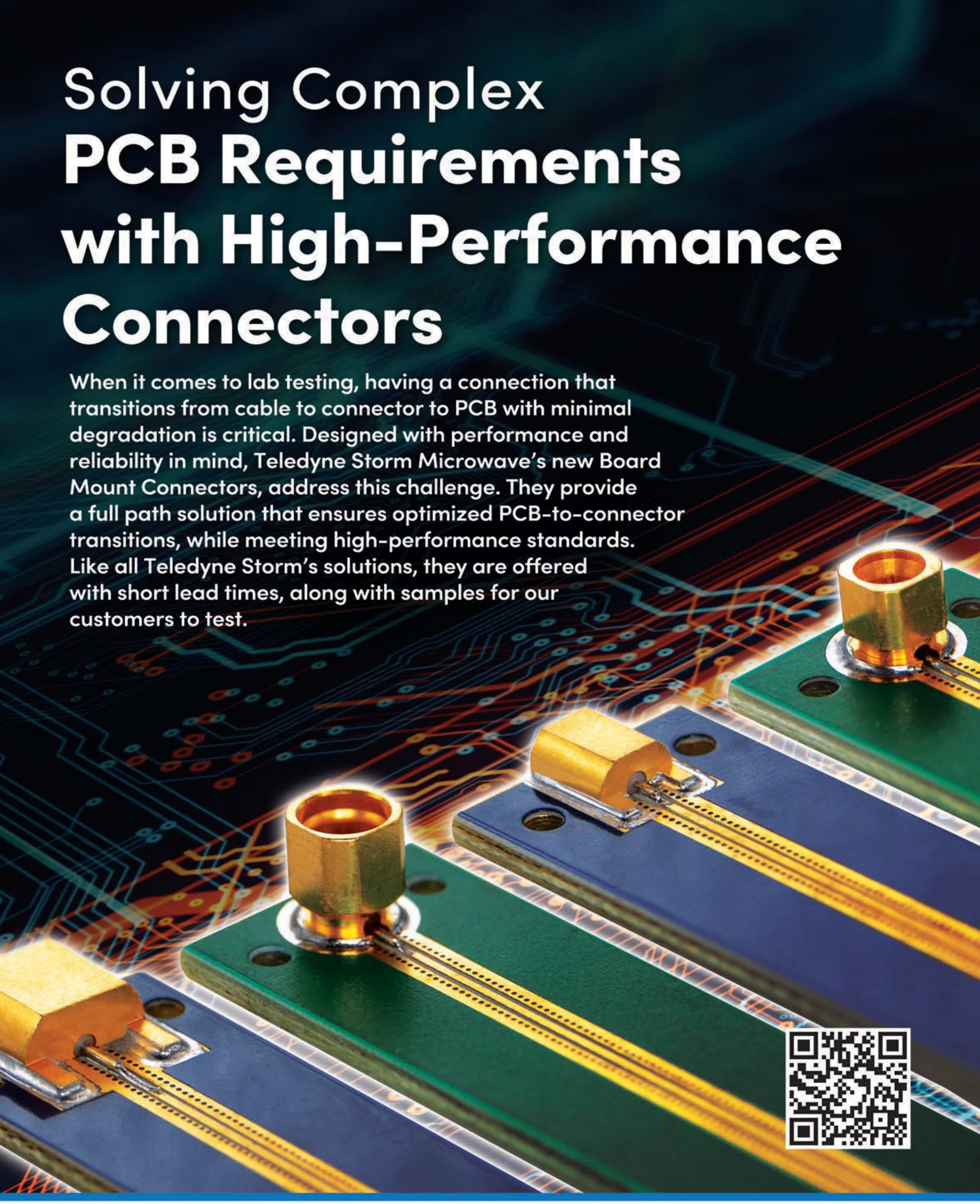
Solving Complex
PCB Requirements
with High-Performance
Connectors
When it comes to lab testing, having a connection that transitions from cable to connector to PCB with minimal degradation is critical. Designed with performance and reliability in mind, Teledyne Storm Microwave's new Board Mount Connectors, address this challenge. They provide a full path solution that ensures optimized PCB-to-connector transitions, while meeting high-performance standards. Like all Teledyne Storm's solutions, they are offered with short lead times, along with samples for our customers to test.

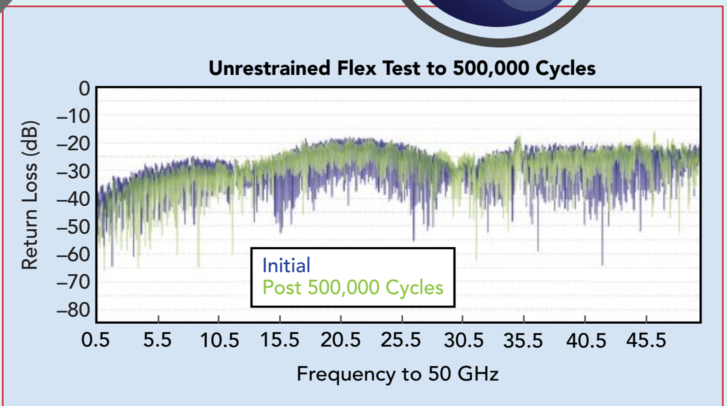


**Fig. 7 Phase stability before and after 500,000 cycles of flexure.**

as frequency increases, when compared to a low loss dielectric stripline trace of the same 6 in. length as the cables. These results give test fixture designers confidence when using ganged compression-mount connectors.

When using a VNA, interconnect phase and amplitude stability are key considerations for optimal performance. For cables in particular, stability over flexure is critically important, as different test points are accessed on the fixture. For consistent measurements, switching to a low loss, high performance microwave cable works very well in dynamic applications. ***Figure 7*** shows cable return loss performance to 50 GHz for a Samtec Nitrowave LL043 Series cable before and after 500,000 flexure cycles. In this case, the cable, which is well suited for use in RF benchtop testing applications, incorporates an interlayer in its construction. This architecture is a major contributor to the overall performance stability.

## IMPORTANCE OF CABLES

The cables used in the analysis are high performance microwave cables. As the connectors described in this article have evolved in RF benchtop testing, the associated cables have also evolved. Standard microwave cable types, like the RG142 50 Ω cable, are available from many different suppliers. Additionally, VNA suppliers, such as Rohde & Schwarz, also supply cables for test applications.[8]

Some designs require high performance, multichannel cables and there is also a growing need for flexible cables for benchtop testing and other applications. Products like the W. L. Gore & Associates PHASEFLEX® Microwave/RF Test Assemblies[9] and Samtec's Nitrowave cables[10] provide excellent mechanical durability and electrical performance over flexure. This is important because when a test fixture is calibrated, the cable is typically in one static position. However, after calibration, the cable may be moved to different test


Mini-Circuits

points on the device. In this case, stability becomes important to maintain a calibrated signal.

## LOOKING AHEAD

Throughout the evolution of RF benchtop testing, interconnect suppliers and instrumentation vendors have made their products easier to use. This evolution has provided more consistent performance and supported expanding frequency ranges. Interconnect suppliers are expected to continue adapting to the changes made by test equipment manufacturers. The need for greater channel counts and higher density will continue to drive the need for ganged connector solutions at lower pitch and higher bandwidth.

Additionally, the opportunity to upgrade existing technology will become increasingly important. An example of this is 1 mm connectors, which have traditionally been rated to a maximum frequency of 110 GHz. New applications have spurred the need to upgrade designs and push these connectors and cables to operate at 125 GHz or even higher frequencies. Undoubtedly, times have changed and great attention is now being placed on interconnect technology. As new technological challenges emerge, manufacturers will continue to advance the state-of-the-art in interconnects. ■

## References

1. S. Sankararaman, S. Tucker, I. Novak and G. Blando, "Realistic Use Cases for Edge, Angled, and Vertical Launch Connectors up to 100GHz," *DesignCon 2024*.
2. J. P. Dunsmore and J. -P. Teyssier, "The Evolution of Vector Network Analyzers to Provide Precision Vector Spectrum Analysis for 6G Applications: VNA Evolves for 6G EVM Signals," *IEEE Microwave Magazine*, Vol. 25, No. 12, Dec. 2024, pp. 77–90, doi: 10.1109/MMM.2024.3438711.
3. "Webinar: Impact of Solder Reflow on High Bandwidth Connectors, Samtec gEEk® spEEk," *Samtec*, Web: https://www.samtec.com/support/videos/webinar-impacts-of-solder-reflow-on-high-bandwidth-rf-connectors-781934976/.
4. "What are Solderless Compression Mount Connectors?," *everything RF*, https://www.everythingrf.com/community/what-are-solderless-compression-mount-connectors.
5. "Mechanical Consideration for Compression Mount RF Connectors," Samtec gEEk® spEEk, December 2022.
6. Jean-Jacque DeLisle, "How to Reliably Align Compression Connectors for Millimeter Wave Applications," *Microwave Journal*, Vol. 66, No. 3, March 2023, pp. 70-80.
7. M. Griesi, Z. Speraw, E. Loy and S. Wronowski, "Millimeter Wave Design: Optimizing Performance in RF Compression Mount Connectors," *Samtec*, Web: https://suddendocs.samtec.com/notesandwhitepapers/samtec-millimeter-wave-design.pdf.
8. VNA accessories, Rohde & Schwarz.
9. "Data Sheet: GORE® PHASEFLEX® Microwave/RF Test Assemblies," *Gore*.
10. High-Performance RF Microwave Cable Assemblies, *Samtec*, Web: https://www.samtec.com/rf/cables/high-performance-microwave/.

# Supporting Commercial Vehicle Production Through Modular Innovation

Robert Weirauch
*HUBER+SUHNER, Herisau, Switzerland*

The electrification of commercial vehicle fleets continues to take place at a rapid pace. This is certainly true in China and Europe, where politics is forcing change. The zero-emission city bus market in Europe alone grew by 45 percent within the first six months of 2024, according to ACEA.[1] At the same time, over 42 percent of city buses are now zero emission, which is close to three times more than the 15 percent on the streets only five years ago.[1]

Simultaneously, the sales of electric trucks remain on the rise, too, with the market set to be worth approximately $20.25 billion by 2032.[2] This reflects steady growth spotted over several years. For example, the ICCT reported that light- and medium-duty electric truck sales in Europe increased by 200 percent in 2023 as users continue to steadily pivot away from internal combustion engine vehicles.[3]

The growing popularity of commercial electric vehicles (EVs) has followed the rollout of several ambitious "green" policies and regulations across the globe. One prominent example of this is the European Commission's recent climate target, which recommended a reduction of the European Union's net greenhouse gas emissions by 90 percent by 2040.[4] This target is intended to help the region reach climate neutrality by 2050 and the use of electric trucks and buses can play a pivotal role in achieving this.

## THE CHALLENGES TO OVERCOME

Bus and truck manufacturers are increasing their efforts to deliver EVs to the mass market for all vehicle segments. This is especially true for those involving heavy-duty, long-haul operations. As might be expected, this has resulted in higher production volumes, which will only continue to increase as these vehicle types grow in popularity.

This has placed growing pressure on manufacturers to meet ever-increasing customer demands. This is not only true in terms of expected delivery lead times but also pertains to performance. Not only must manufacturers find a way to reduce the overall assembly manufacturing times and optimize the cable

# Stability™ CABLES DELIVER THE MEASUREMENT STABILITY YOU NEED!

## Stability Wafer™
Maury Microwave

Light-weight and stable to improve your on-wafer measurements.

## Stability VNA™
Maury Microwave

Stable, repeatable, flexible and durable for the most precise VNA measurements.

## Stability plus™
Maury Microwave

**Armored** and stable to minimize uncertainties in your critical mw & RF measurements.

**Low Profile** and optimized for high density applications.

## Stability flex™
Maury Microwave

Extremely flexible and easy to use on your test benches.

## Stability TVAC™
Maury Microwave

Guaranteed performance for your critical thermal vacuum chamber measurements.

Maury Microwave

**STORE.MAURYMW.com**

assembly process to get vehicles on the roads faster, but they must also find innovative methods of obtaining the maximum performance levels out of cables and connectors.

In the age of electrification, electromagnetic compatibility issues must be overcome. These occur when key electrical systems, components and equipment interfere with one another, preventing them from working together simultaneously. Therefore, new ways of connecting cable screens must become a reality.

Usually, vehicle manufacturers are focused primarily on the direct costs of the solutions. As a result, not enough attention has been paid to indirect production costs such as assembly, test and production equipment or even reworks. Recently, a number of manufacturers have realized this challenge and have started to turn toward modular solutions as the best approach to EV production.

## THE MODULAR ERA FOR CONNECTIVITY

HUBER+SUHNER has been developing high-voltage solutions since the start of this new age of electrification. In the beginning, many pressing issues had to be overcome. First and foremost, manufacturers must ensure that all cables and connectors deliver their maximum performance. These issues raise other questions. What is the best way to avoid any electromagnetic compatibility issues? How can the process time and effort during assembly be reduced? For HUBER+SUHNER, the adoption of a modular approach answers all these questions.

## THE LATEST GENERATION OF HIGH-VOLTAGE CABLE ASSEMBLIES

Modular cable assemblies have become crucial to modern production practices. Because modular manufacturing requires production from pre-assembled parts, these ready-to-install assemblies are helping to reduce production times. This is due, in large part, to OEM manufacturers no longer needing the extensive knowledge and experience with increasingly complex harnesses.

Solutions like the HUBER+SUHNER RADOX® modular automotive cable assembly (mCAY) now come with end-of-line testing proof. This means that manufacturers can install one of these assemblies immediately into their commercial EVs. ***Figure 1*** shows an example of where high-voltage cable assemblies are used in commercial vehicles.

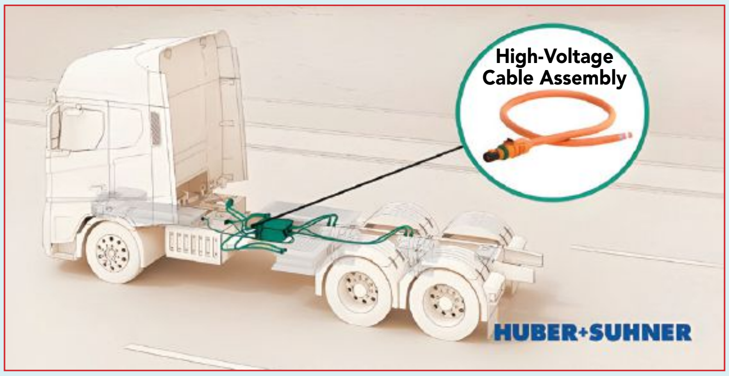


Fig. 1 **High-voltage cable assembly and RADOX HV cables in an application.**

## EVOLVING PARTNERSHIPS, NOT JUST TECHNOLOGIES

As modular technologies have become a reality, they have changed the way HUBER+SUHNER operates within the market. This is evidenced by the transition from a cable-only supplier to a complete solutions provider in this high-voltage field. This change in positioning helps suppliers and it also gives OEM manufacturers access to new solutions, like the RADOX technology. The result is innovative EVs and high-quality final products.

## MAKING OPTIMAL CONNECTIONS WITHIN VEHICLES

One significant benefit of the mCAY solution is the implementation and use of electromagnetic pulse technology (EMPT). The investment to build in-house assembly capabilities using EMPT has been substantial, but it has been recognized and adopted through its market acceptance. EMPT, which applies short, high-power electric currents to join and form conductive materials, has allowed companies that use the technology, like HUBER+SUHNER, to move beyond traditional crimp technology, which poses some technical limitations under current loads.

The EMPT process does not introduce significant heat into connection points. This means that the materials used retain full strength and are perfectly suitable for harsh environments. This also helps ensure that these materials and connection points deliver high-quality electrical performance over their lifetimes. The latest connectors on the market, combined with RADOX high-voltage cables, form a reliable cable assembly that acts as the connecting core for high-power applications.

## A COMPLETE SOLUTION FOR COMMERCIAL EVS

A modular approach is not a one-size-fits-all approach to vehicle production. Many manufacturers want to use solutions with some level of personalization. Product personalization is essential for delivering tailored customer experiences to different user segments, including "off-the-road" or other industries. Suppliers in this segment of the industry, like HUBER+SUHNER, have been supporting customers with tailored designs to ensure that solutions meet their needs. The goal of this modular, customized approach is to become a one-stop shop for commercial EV systems.

## SUPPORTING INTENSIVE VEHICLE APPLICATIONS WITH RADOX TECHNOLOGY

RADOX cable technology was first introduced to the automotive market several years ago. Standing for "radiation X-linked," RADOX makes use of the cross-linking process. In this process, the cables are exposed to controlled electron beams that penetrate the polymer structure. This creates crosslinks that improve the material's properties

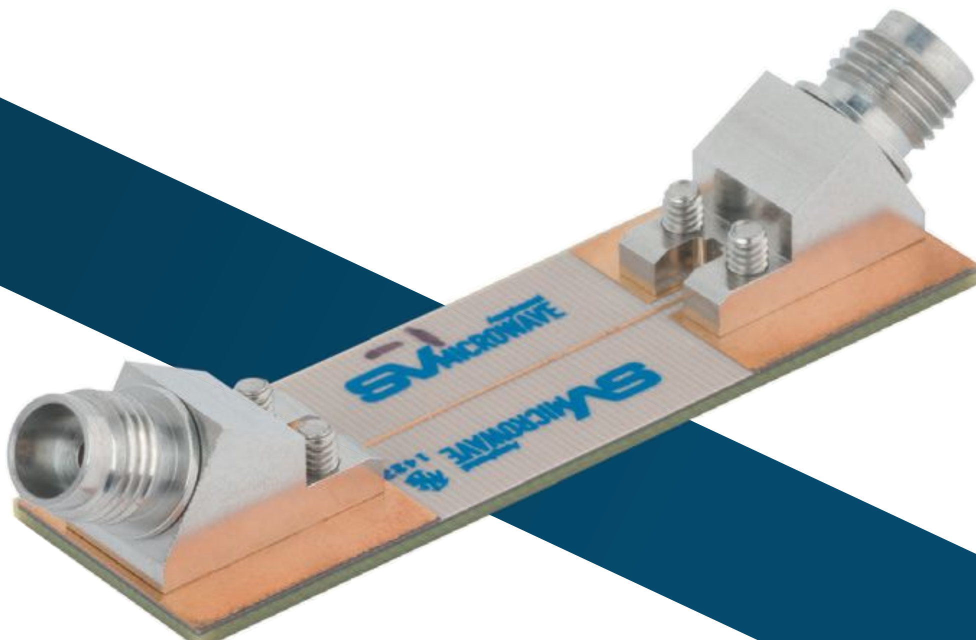

without affecting its overall composition. This enables notable improvements in the thermal, mechanical and chemical properties of the cable insulation material, making them a suitable solution for heavy-duty vehicle applications.

RADOX materials are designed to withstand extreme heat, especially temperatures that cause overheating and degradation or may even lead to components melting. At the same time, these materials can also work optimally in extremely cold conditions that may lead insulation to become brittle, frozen or fall off entirely. They can also handle moisture and humidity, which typically can result in short-circuiting and corrosion.

Vehicles may encounter chemicals while in use. This exposure can quickly affect the insulation performance and the likelihood of electrical overloads that cause system failures. The RADOX materials have also been shown to be effective in overcoming these challenges.

In addition, screened RADOX high-voltage cables can carry high AC loads, ensuring powertrain systems work effectively throughout the vehicle's lifetime. The RADOX cables have a robust design; they will meet the flame resistance standards of ECE R118 and are Accord Dangereux Routier (ADR)-compliant. ADR is the European treaty regarding the transport of dangerous goods. Additionally, the RADOX process enables high UV and resistance to weathering for applications directly exposed to different environmental conditions.

## DISTRIBUTING HIGH-VOLTAGE EFFICIENTLY

Based on well-defined interfaces and internal architectures, components of the HUBER+SUHNER modular high-voltage distribution unit (mHVDU) can be tailored to customer specifications with short lead times. This is helping OEMs bring new EVs to the market much faster while maintaining a high level of quality with what is essentially an off-the-shelf solution. The modular systems and components are tested and validated against various global automotive regulations and standards.

The mHVDU incorporates the modular concept to achieve greater flexibility and scalability than traditional power distribution solutions, including input, output and fuse applications. This unit also plays a vital role as part of a complete system solution. The mHVDU is compatible with other key elements of the HUBER+SUHNER high-voltage portfolio, including the RADOX cables and the EV-C connection system. It is also highly adaptable, as the design uses standardized components that are commonly available in the market. ***Figure 2*** shows an illustration of how the mHVDU and RADOX cables can be used in a variety of commercial vehicle applications.

Recognizing that the mHVDU will be exposed to the same harsh environments and conditions as the RADOX cables, the unit has been designed to withstand major temperature fluctuations, vibrations and other mechanical loads. This was done to provide a reliable solution that ensures the best performance in heavy-duty applications. Pairing the mHVDU with high-voltage cables and connection systems has led to significant improvements in powering and distributing energy across various systems.

## CONNECTIONS WITH GREATER RESISTANCE TO SHOCK AND VIBRATION

To make high-voltage connection systems capable of withstanding vibration and shock during actual vehicle use; it is necessary to ensure superior reliability and enhance the solution's vibration resistance. HUBER+SUHNER has developed the EV-C 2 high-voltage connection system to mitigate these concerns and meet the demanding conditions that may disrupt the performance of heavy-duty EVs. This enhanced connection system is designed for ambient temperatures between -40°C to 140°C. The whole system is classified in accordance with the defined voltage ranges of voltage class B. This includes the HV circuits that use AC or three-phase current components, such as the electric drive system. EV-C 2 also offers an insulation resistance of greater than 200 MΩ when measured at 1000 VDC, in accordance with DIN EN 60512-3-1. When plugged in, the connection system fulfills IP6K9K and IP6K7 protection ratings.

The EV-C 2 has a precoated thread to increase tightness and mechanical resistance. It also has an improved sealing concept for a stronger, more rugged design. The EV-C 2 product line was launched

**Fig. 3 RADOX high-voltage cable used in RADOX® EV-C 2 connection system.**

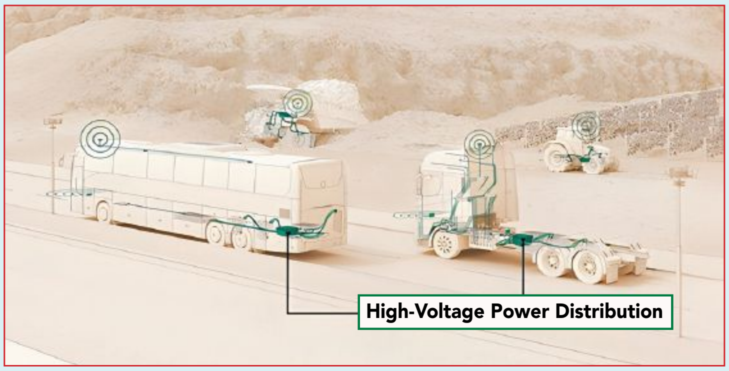


**Fig. 2 The use of the mHVDU and RADOX cables.**

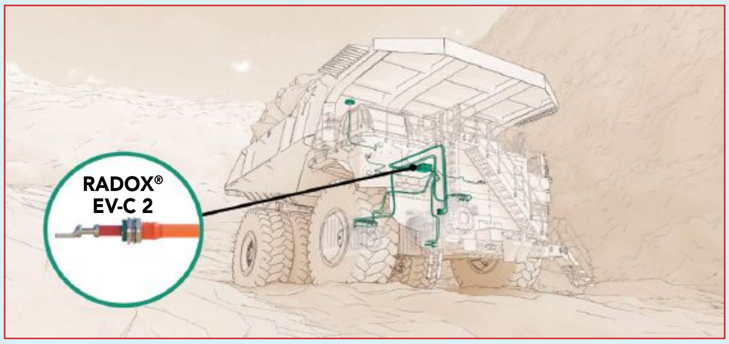


**Fig. 4 RADOX® EV-C 2 connection system application illustration.**

molex

# RF Connectivity Solutions That Redefine Adaptability

**Radio frequency (RF) transmission is essential for efficient wireless communication in today's ultra-connected world. Trust our extensive expertise and comprehensive portfolio of customized and off-the-shelf RF connectivity solutions for reliable performance across industry applications.**

### Precision Test Connectors
### Frequencies 1 GHz up to 110 GHz

- Superior signal integrity and reliability
- Supportive of 1.0mm, 1.85mm, 2.4mm and 2.92mm sizes
- Optimized SMA two-hole flange connections

### High-Frequency Adapters

- 1 GHz up to 110 GHz

### Cardinal Test Cable Assemblies

- High frequencies reaching up to 110 GHz
- Durable for extended use
- Excellent phase and amplitude stability
- Low VSWR for superior performance

Explore Our
RF Connectivity
Solutions Here

*creating connections for life*

in March 2024. When it was launched, care was taken to ensure that selected materials would enable manufacturers to use a connection system that complies with the latest directives laid out in the "Restriction of Hazardous Substances in Electrical and Electronic Equipment RoHS 3" (EU 2015/863) directive. To simplify the installation process for this modular approach that is proving effective in vehicle production, a shorter thread runout has been implemented for thin-wall applications. The EV-C 2 connection system with RADOX cables is shown in ***Figure 3*** and a typical application is illustrated in ***Figure 4***.

## CONNECTIVITY: TODAY AND BEYOND

As the use of fuel cells and electric commercial vehicles continues to grow, it is becoming essential that the automotive industry evolves to ensure reliable high-voltage connections over the lifetime of the vehicle and connection system. Through the development of RADOX® and modular technologies, HUBER+SUHNER continues to drive this evolution within the commercial vehicle segment, focusing on energy flow and its distribution. In this segment, flexibility is crucial. Solutions need to be customizable to address specific individual project needs as well as broader market needs. That is why suppliers like HUBER+SUHNER are moving beyond single-function commodity components to supply complete solutions for the end users, teaming with customers from the design phase to the finished product. In today's market, this is the best way to support the ongoing transition into modular systems that will enable alternative powertrains. ■

## References

1. "Zero emission bus registrations +45% in Europe in H1 2024, says ACEA: Germany and Spain grew, France decreased," *Sustainable Bus*, July 30, 2024, Web: sustainable-bus.com/news/acea-zero-emission-bus-registrations-2024-half-europe.
2. "Global Electric Truck Market Size, Share & Trends Analysis Report, by Propulsion (BEV, PHEV & FCEV), Type (Light-Duty Trucks, Medium-Duty Trucks & Heavy-Duty Trucks), Range, Battery Type, Battery Capacity, Level of Automation, End User, By Region (North America, Europe, APAC, and Others), and Segment Forecasts, 2024 – 2032," *Factview Research*, January 2024, Web: factviewresearch.com/report/global-electric-truck-market.
3. S. Ananda, E. Mulholland and A. Musa, "Race to Zero European Heavy-Duty Vehicle Market Development Quarterly (January–December 2023)," *International Council on Clean Transportation*, March 19, 2024, Web: theicct.org/publication/race-to-zero-eu-hdv-market-development-q4-2023-mar24.
4. "2040 climate target," *European Commission*, Web: climate.ec.europa.eu/eu-action/climate-strategies-targets/2040-climate-target_en.

# Proprietary Connector Design Enhances Quality and Phase Stability

Junkosha
*Irvine, Calif.*

As wireless communication technologies continue to advance, demands on test and measurement applications are evolving rapidly. Cable and connector innovations now play a pivotal role in maintaining the precision and reliability required for modern testing environments. Looking ahead, the integration of artificial intelligence (AI) into test and measurement processes is set to drive significant advancements, enabling smarter and more efficient systems. Additionally, the ongoing expansion of 5G and IoT is expected to generate new testing challenges, requiring cutting-edge solutions to ensure higher carrier frequency and data rates. With the evolution of these technologies, sophisticated testing will become increasingly essential to validate and sustain the reliability of these interconnected systems.

The rapid rollout of 5G has transformed the landscape for test and measurement equipment. The higher mmWave frequencies central to 5G deliver faster data speeds and introduce challenges such as increased sensitivity to flexure and mechanical stress. This could affect system development and device performance characterization phases, where precision and repeatability are critical. It may also include the commissioning of the complete system and ongoing monitoring within a production test environment. To address these complexities, test setups must rely on robust, high-precision cabling and interconnects.

At the higher mmWave frequencies, "phase and amplitude performance that endures" is a statement that the cabling and interconnects must fulfill, particularly in the test and measurement environment. At these frequencies, interconnects are very small, meaning that connector design can be a challenge. In addition, the transmission signal becomes more sensitive to cable bending and temperature changes, resulting in an environment that requires phase-stable cables. Key to these test setups are high performance interconnects that establish dependable connections across a range of devices and components. The choice of connectors is influenced by the specific instrument, its application requirements and the electrical and mechanical performance characteristics. This emphasizes the importance of tailored interconnect solutions in modern test environments.

Junkosha, a pioneer in high performance interconnect solutions, has once again demonstrated its commitment to meeting the industry's rigorous demands with the recent launch of its proprietary connector designs. Integrated into its microwave/mmWave coaxial cable assemblies, these new connectors are engineered to meet the rigorous demands of next-generation high speed, high-capacity communications systems. ***Figure 1*** shows examples of these assemblies designed for wide temperature ranges while being slim and durable.

Accuracy is crucial, especially at mmWave wavelengths where instances of flexure and mechanical stress can affect the accuracy of results. Junkosha's integrated approach to cable and connector design addresses these challenges, enabling reliable and repeatable measurements under demanding conditions. Junkosha's branded connectors mark a significant expansion of the company's capabilities. Featuring 80 unique types, each adorned with the "J mark" emblem symbolizing Junkosha's quality promise, these connectors are engineered to complement the

**Fig. 1** **Junkosha cable assemblies with connectors with J-mark.**

Fig. 2 **MXW7 series of cables.**

Junkosha microwave/mmWave coaxial cable assemblies. Designed with a safety-lock mechanism for enhanced durability and a multi-lock system for ease of use, the connectors ensure robust signal integrity and operational reliability in high frequency environments.

Advancements in 5G leverage higher mmWave frequencies where cabling and interconnect solutions must be robust to withstand the rigor they are subjected to in any given scenario. Junkosha's innovations are poised to play a pivotal role in enabling the high speed, high-capacity networks of the future. The Junkosha Microwave/mmWave Coaxial Cable Assembly MWX7 Series, known for the lowest phase and amplitude deviation and best linearity over temperature and flexure, is already an industry benchmark. Coupled with the addition of proprietary connectors, these assemblies promise consistent performance in testing and calibration. Developed with EPTFE tape-wrapped dielectric technology, the MWX7 Series delivers consistent phase and amplitude stability in response to temperature and mechanical fluctuations. Furthermore, the cables offer reduced phase and amplitude drift from mechanical fluctuations, supporting repeatable results. As a result, Junkosha provides some of the industry's best phase and amplitude stability across its MWX7 Series of RF cables. This ensures reliable, repeatable results for applications ranging from aerospace and defense to autonomous vehicle development. ***Figure 2*** shows examples of the MWX7 phase-stable cable assemblies with various cable diameters and terminating connectors.

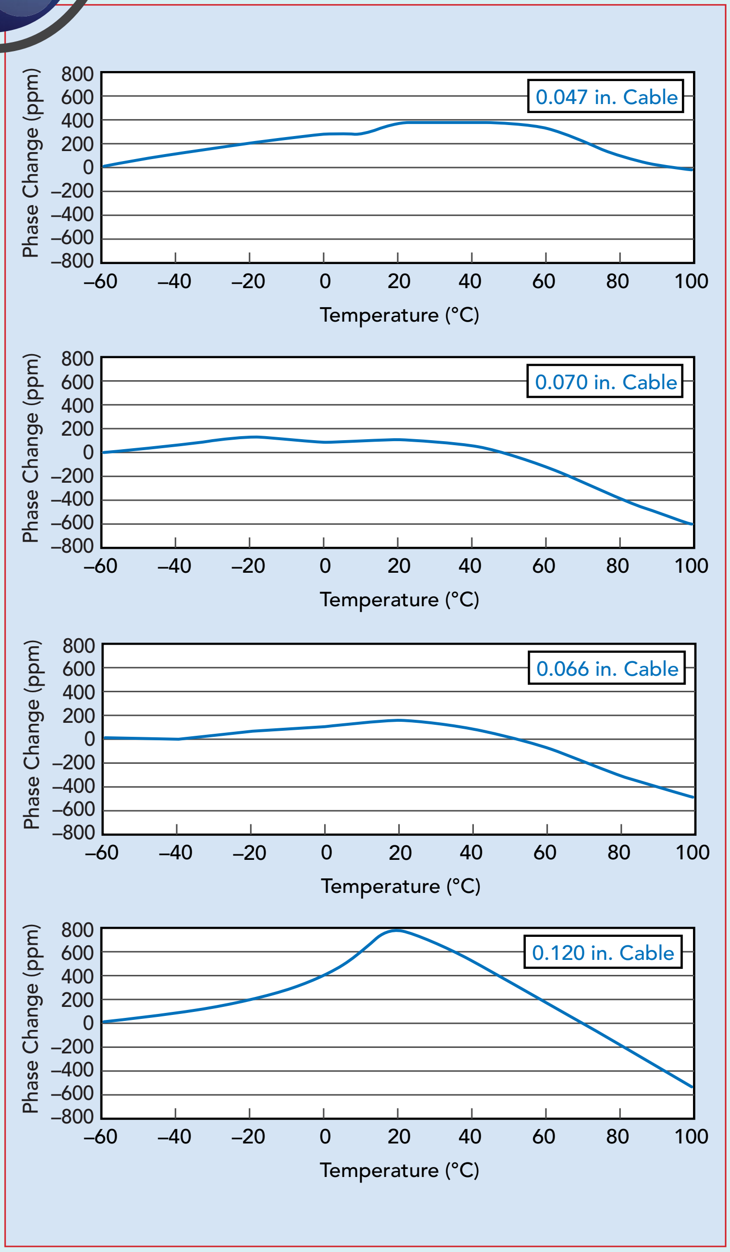


Fig. 3 **Phase stability versus temperature at 18.5 GHz.**

The demand for mmWave frequencies continues to grow every year, driven by diverse applications ranging from space and defense to emerging commercial markets such as autonomous vehicles. Achieving reliable system performance at higher mmWave frequencies requires interconnect solutions that deliver consistent phase stability. This is particularly critical in test and measurement environments, where precise and repeatable performance is essential to validate and optimize system designs. ***Figure 3*** shows phase stability performance versus temperature for several diameters of the MXW7 series of cables, measured at 18.5 GHz.

Leveraging its expertise in fluoropolymer processing and high performance cable manufacturing, Junkosha's move into connector design reflects a strategic response to the escalating demands from the microwave and mmWave markets, driven by 5G, AI and data center growth. All of these require advanced interconnect solutions capable of supporting high speed and data-heavy workloads. By offering both high performance cables and precision-engineered connectors, the company is positioned to address the diverse needs of industries navigating the transition to higher frequencies and data-intensive applications.

As 5G continues to drive innovation, Junkosha's integrated interconnect solutions provide customers with more options. They address diverse industry requirements with a combination of high performance cables and precision-engineered connectors to meet the challenges of tomorrow's sophisticated systems. Through continuous product development and customer collaboration, Junkosha remains at the forefront of enabling innovation for the connected world of the future.

**Junkosha**
**Irvine, Calif.**
**www.junkosha.com/en**

# High-Density Connection Enhances PXIe Test & Measurement

The Phoenix Company of Chicago, Inc.
*Naugatuck, Conn.*

The tremendous growth of manufacturing automation and the increasing complexity of products in all industries continue to create a strong demand for modular test solutions. One of the most popular choices for advanced test and measurement is the PXIe platform. This platform uses a variety of instrument modules from DC to mmWave to create flexible, high performance solutions for validation and production testing.

These modules include instruments such as switches, multiplexers and vector and signal analyzers often using up to 20 SMA connectors on the module panel, or in the case of multiplexer modules, over 50 SMB connectors. Demand across the frequency spectrum for higher performing PXIe modules is creating the need for connector performance beyond what these traditional connectors can provide. The Phoenix Company's series of instrumentation connectors provides the next generation of mechanical and electrical performance, augmenting high density with superior performance.

## INSTRUMENT MODULES

The PXI chassis is the foundation of the test system and has a fixed number of slots to accept test modules. Most modules have a single slot width but may increase to double or triple slot widths depending on functionality or the required space for connectors. Modules using many RF connectors such as the SMB, often require a double slot width to mount all connectors, wasting valuable chassis space. Existing multipin connectors can fit a single-slot module; however, limited connector performance may reduce bandwidth specifications.

## CONTACT DESIGN AND PERFORMANCE

The Phoenix Company developed a new family of multipin connectors, shown in ***Figure 1***, to improve single-slot efficiency. This was accomplished with a high density of size-16 PkZ® microwave contacts that also achieve electrical performance beyond that of the existing SMB or multipin connectors. The heart of this connector system is the PkZ microwave contact designed to overcome tolerance gaps found in modular mating applications. Mating up to 53 microwave contacts at one time requires careful control of design and manufacturing tolerances to avoid exceeding the mating limits of the connector system. The PkZ provides a forgiving solution

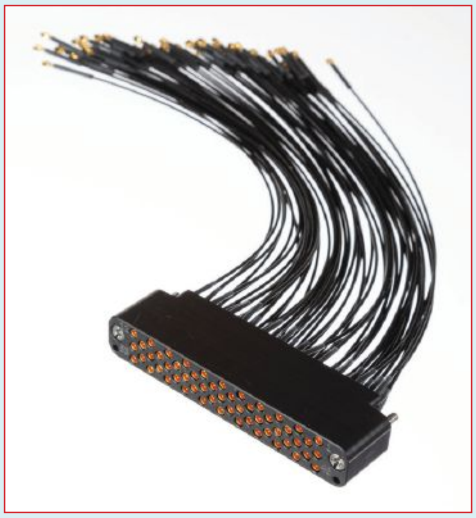

Fig. 1 **53-pin panel mount receptacle.**

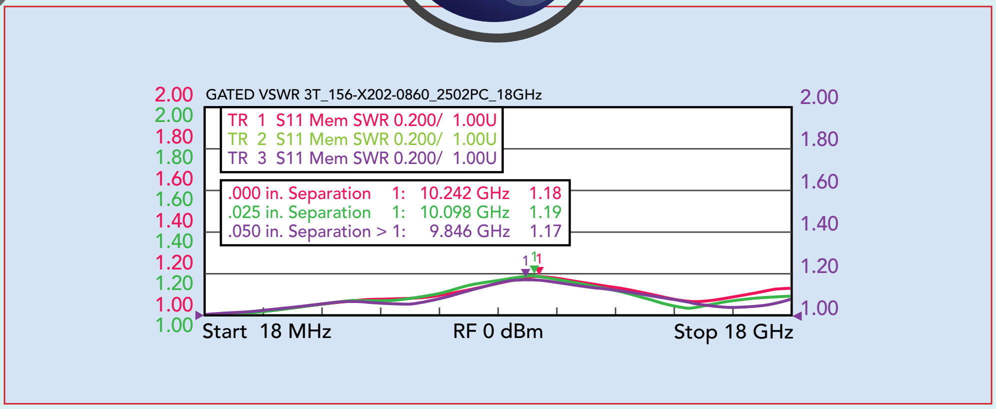


Fig. 2 **Gated VSWR at three mating conditions.**

through an air dielectric and careful control over internal conductor ratios to perform well even when not fully mated.

***Figure 2*** shows the gated VSWR performance to 18 GHz of a mated pair of size-16 PkZ contacts. The chart demonstrates the unique ability of the PkZ contact to provide constant impedance over mating gap conditions. The plot shows three traces representing the contacts at different mating conditions: full mating, a 0.025 in. separation and a 0.050 in. separation. As seen, there is no material performance difference over this mating range. This is important because tolerance stack-up always occurs. Eliminating this mechanical consideration from the electrical performance allows the PkZ to operate to higher frequencies in a high-density platform and sets it apart from legacy multipin connectors.

Fig. 3 **53-pin plug housing.**

## HOUSINGS

As mentioned, one of the most important design goals of a connector system is limiting tolerances in areas critical to microwave performance. Reliably mating large quantities of microwave contacts involves careful consideration of the following mechanical features in a multipin housing:

- Radial contact stability
- Contact retention
- Axial mating tolerance
- Insertion forces
- De-mating forces
- Cable type, termination and cable management.

Addressing each of these objectives requires unique design features in the contacts and the housings to achieve a robust design with the precision to operate into the mmWave region. The PkZ contacts snap into the housing and have a specific design feature in length and diameter that limits the radial float. The plug and receptacle housings have corresponding features to provide optimal contact stability. Contact retention in the housing is specified at a minimum of 10 lbs. per contact. Each contact design features a solder termination to the cable shield to achieve superior electrical and mechanical performance.

PkZ contact radial stability in the plug housing is further enhanced with guide pins and a cable guide plate that isolates the cable's bend radius from the PkZ contact. This eliminates the need for a traditional backshell and clamp, which may deform the cable and affect microwave performance. Housings are available in 13-, 26-, 28- and 53-pin sizes, all in single-slot widths. Insertion and de-mating forces become significant at this level. They are addressed through integrated jackscrew hardware shown in ***Figure 3***, which not only draws the mating halves together but also manages the separation in a controlled manner to avoid damage.

### 50 Ω and 75 Ω Cable Versatility

The PkZ contact accommodates standard 50 Ω RG cable groups and 1.37 mm cable for improved flexibility in applications like routing cables inside a single-slot module. For higher frequencies, contacts are available for RG-405 cables to 50 GHz and M17/151 0.047 in. cables to 67 GHz. 75 Ω contacts are available in a size-12 format with performance to 18 GHz. ***Figure 4*** shows gated performance for a mated pair of the 75 Ω PkZ series on Harbour Industries SS75086 cable to 18 GHz.

This family of multipin connectors and microwave contacts from the Phoenix Company incorporates specific features designed to offer the PXI test market a new choice for high frequency performance in a high-density package.

**The Phoenix Company of Chicago, Inc.**
**Naugatuck, Conn.**
**phoenixofchicago.com**

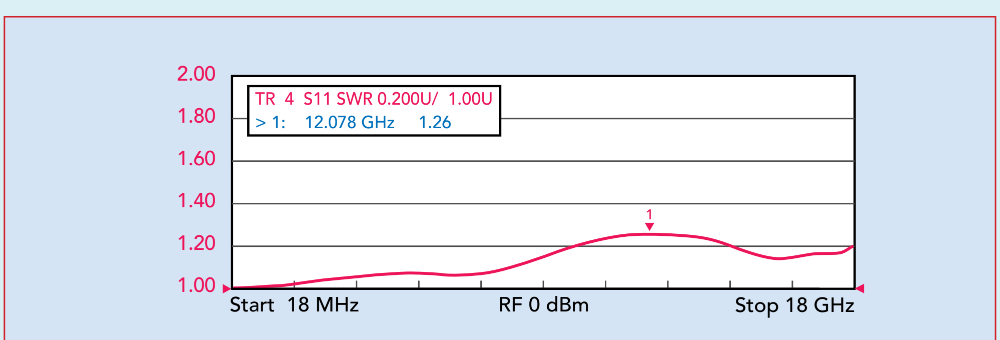


Fig. 4 **Gated performance of the 75 Ω PkZ series.**

# Selecting the Right RF Cable Assembly

Smiths Interconnect
*Stuart, Fla.*

RF cabling is utilized in many mission-critical radar, communication and navigation system applications that may be ground-, sea- or space-based. To ensure that the correct RF cable assembly is chosen for your application, a number of factors need to be considered. The SpaceNXT™ QT RF cable assemblies equipped with the new Mini-Lock connectors from Smiths Interconnect provide superior solutions that address all these important considerations.

## EXCELLENT PERFORMANCE

Performance is often the first thing users think about when assessing the needs of the application. When considering performance, many aspects should be included. SpaceNXT QT/Mini-Lock cable assemblies can operate up to 110 GHz with very low insertion loss and VSWR values. This makes these assemblies ideal for a wide variety of applications. The patent-pending technology that Smiths Interconnect uses avoids common electrical bead resonance and other RF issues found at very high frequencies. These RF cable assemblies provide excellent performance in harsh environments with an operating temperature range of -65°C to 165°C. They are made with low loss fluoropolymer dielectric and constructed with materials that meet the outgassing requirements of NASA/ESA when tested per ASTM E595. Phased matched pairs and sets are available with a standard tolerance of ± 1 degree per GHz or ±2.8 picoseconds. ***Figure 1*** shows the input VSWR response of a cable assembly from 11 MHz to 110 GHz. As the graph in Figure 1 shows, the VSWR stays below 1.2:1 to around 80 GHz, maintaining values below 1.4:1 until just below 110 GHz.

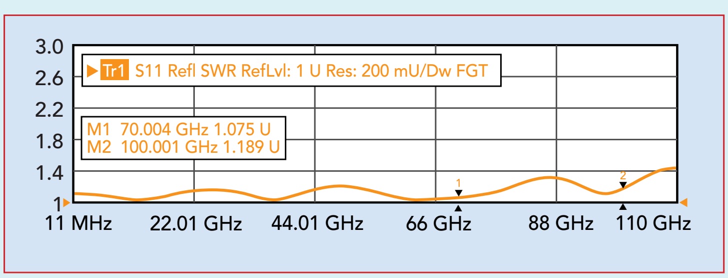


Fig. 1 **Typical VSWR versus frequency for SpaceNXT QT cable.**

Fig. 2 Mini-Lock mating connectors.

Fig. 3 Mini-Lock connector with quick-lock mechanism.

## THE ULTIMATE RELIABILITY

In mission-critical applications, RF cable assemblies must be properly connected, remain connected when mated and be capable of withstanding multiple matings and dematings without degradation. SpaceNXT™ QT/Mini-Lock cable assemblies have an audible click when properly installed. The connectors have a pull strength of more than 50 lbs., meaning the cable would likely break before the connection would be lost. In addition, they have been qualified to meet MIL-STD-202G, Method 204 (vibration standards) and MIL-STD-202G, Method 213, Condition I (shock standards). They incorporate an ethylene tetrafluoroethylene (ETFE) material for maximum radiation resistance. Should an application require multiple connections, the Mini-Lock connectors can be mated and demated more than 100 times without degradation. In addition, the dependability of the connectors and cable assemblies is backed with reliability data and lot traceability. An example of a mating connector and a cable assembly is shown in ***Figure 2***. The connection mechanism of the high frequency Mini-Lock connector can be seen in action in an instructional video.[1]

## EASE OF INTEGRATION

In addition to excellent performance and ultimate reliability, an RF cable assembly needs to be easy to integrate. The Mini-Lock connector has a quick-lock mechanism for blind-mate connections with low insertion force, enabling faster integration with reduced labor costs. Since there is no coupling nut, there is no requirement for a torque wrench. This makes the small, lightweight connectors ideal for use in tight spaces or high-density applications. ***Figure 3*** shows an end view of the Mini-Lock connector with the quick-lock mechanism and the connector mounted to the cable.

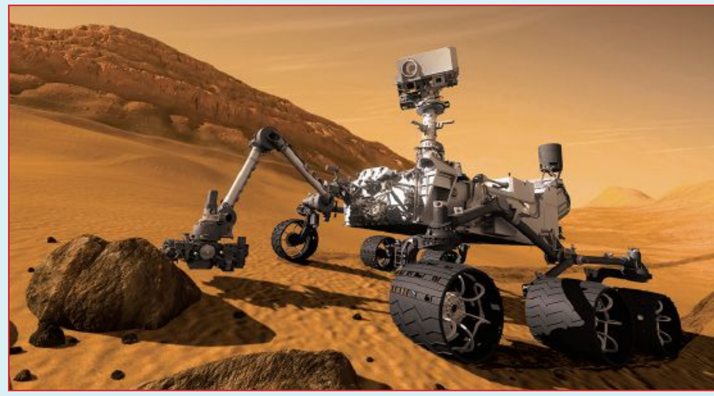

Fig. 4 Mars Rover.

## PROVEN SUPPLIER

The final consideration when determining the best solution for an application is the pedigree of the supplier. Products from Smiths Interconnect have been trusted for use in hundreds of defense, commercial and scientific programs on land, at sea and in space. An example of an actual application is the Mars Rover Program shown in ***Figure 4***. RF cable assemblies continue to be involved in many mission-critical GEO/MEO/LEO satellite systems, radar systems, electronic warfare, uncrewed vehicles and many other demanding applications. With long-standing relationships with the world's leading companies and organizations, Smiths Interconnect's capabilities have been used from application concept to deployment/launch and have included design reviews, qualification testing, special process documentation, lot traceability and custom packaging. To ensure success, only select RF cable assemblies that provide excellent performance, have the ultimate reliability, are easy to integrate and are readily available from proven suppliers should be considered for your future applications. Smiths Interconnect SpaceNXT™ QT/Mini-Lock cable assemblies are the ideal solution trusted by industry leaders around the world.

Smiths Interconnect is a leading provider of high-reliability connectivity products and solutions serving segments of aerospace and defense, medical, semiconductor test and industrial markets. It designs and manufactures technically differentiated electronic components, microwave, optical and RF products and sub-systems that connect, protect and control critical applications.

## References

1. "High Frequency Mini-Lock Connector," Smiths Interconnect, Web: youtube.com/watch?v=IxFDNCk_nr4.

**Smiths Interconnect**
**Stuart, Fla.**
**smithsinterconnect.com**


TIMES
MICROWAVE SYSTEMS
AN AMPHENOL COMPANY
InstaBend®
High Performance Microwave Assemblies
InstaBend® 047
InstaBend® 086
InstaBend® 141
Available through verified distribution partners

# Durable RF Cable Assemblies

Swift Bridge Technologies' DuraWave PS test port extension cable assemblies are engineered to deliver exceptional durability and performance in the most demanding environments. Designed for both indoor and outdoor use, these assemblies provide excellent phase and amplitude stability while withstanding physical and environmental challenges. Built to endure, DuraWave PS assemblies feature internal ruggedization that protects against crushing, torque and kinking, ensuring consistent performance with an extended service life. The connector body and interfaces incorporate seals to prevent fluid, dust and dirt ingress at connections to the test equipment and the DUT. The abrasion-resistant, flame-retardant polyurethane jacket adds an extra layer of protection, allowing these assemblies to maintain their integrity even in harsh conditions.

Despite their rugged nature, these cable assemblies are flexible, accommodating a 2 in. minimum bend radius without compromising electrical performance. This flexibility makes them easy to route through tight or hard-to-reach spaces, further enhancing their practicality. Available in standard and custom lengths up to 25 ft., DuraWave PS assemblies can be tailored to suit a wide range of applications.

Designed to meet or exceed OEM cable performance, configurations with N-Type connectors support frequency ranges from DC to 6 GHz with a maximum return loss of -25 dB. Configurations to 18 GHz have a maximum return loss of -20 dB. For higher frequency applications, options include 2.92 mm and 2.4 mm connectors, both of which support frequencies to 43.5 GHz with a maximum return loss of -18 dB.

DuraWave PS cable assemblies are used in RF and microwave testing, industrial and manufacturing environments and telecommunications applications. They provide a reliable, cost-effective solution for general-purpose test applications. Combining precision performance with robust durability, these assemblies are built to deliver repeatable, high-accuracy measurements over a long service life.

**Swift Bridge Technologies**
**Portland, Ore.**
**www.swiftbridgetechnologies.com**

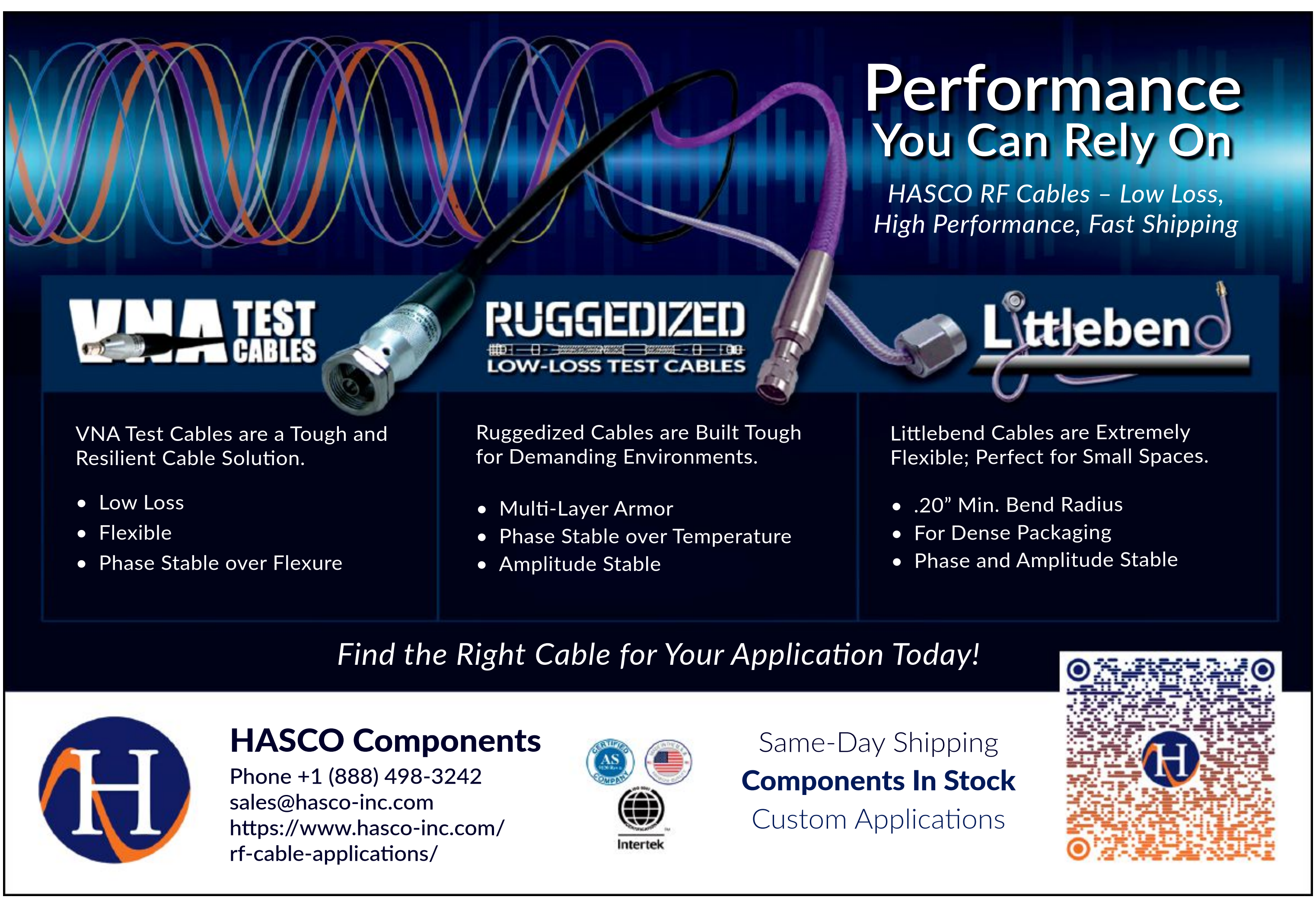

### PT CABLES


Anoison challenges the perception that top-quality test cables are always expensive and bulky. What is essential when choosing test cables? Low insertion loss, high phase stability, good RF shielding, proper connector selection, durability and flexibility. Why are high-quality test cables necessary? Accurate measurements, calibration impact and repeatability. The Anoison PT family of test cables achieves these requirements with equal to or better specifications, less bulk and weight and at a significantly lower price than you are used to.

**Anoison**
**www.anoison.com**

### 1.0 MM TEST CABLE ASSEMBLIES

VENDORVIEW

Fairview Microwave launched its new 1.0 mm test cable assemblies, designed for high performance test setups requiring superior durability and signal integrity. Made with an armored, ultra-low loss, phase-stable coax cable, these assemblies are available in 1.0 mm male-to-male and 1.0 mm male-to-female configurations. They support frequencies up to 110 GHz. In addition, they provide exceptional phase stability, low insertion loss and rugged crush resistance.

**Fairview Microwave**
**www.fairviewmicrowave.com**

### HLL228R SERIES CABLE

VENDORVIEW

The HASCO HLL228R Series cable is a ruggedized, low loss, phase-stable cable that are designed for demanding environments where durability and signal integrity are critical. The low loss LL228 cable operates from DC to 50 GHz. These cables feature enhanced shielding and robust construction to withstand harsh conditions, including extreme temperatures, moisture and physical stress. Their low loss design minimizes signal degradation, while phase stability ensures consistent performance over time, especially in high frequency applications.

**Hasco**
**www.hasco-inc.com**

### ARMORED & STABLE CABLE ASSEMBLIES

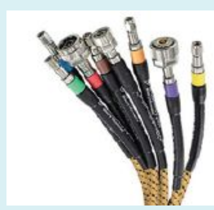

Setting the standard for high performance ruggedized cable assemblies, the Maury Microwave StabilityPlus™ Series is your interconnect choice for reliable and repeatable measurements, providing amplitude and phase stability with flexure, superior flexibility, ease-of-use, durability and a compact form factor. Color-coded connectors significantly reduce the potential for connection errors, offering clear indications of compatibility and intermatability. Discover how StabilityPlus can enhance your test setup today.

**Maury Microwave**
**www.maurymw.com**

### ELBOW RIGHT-ANGLE MMWAVE CABLE ASSEMBLY

VENDORVIEW

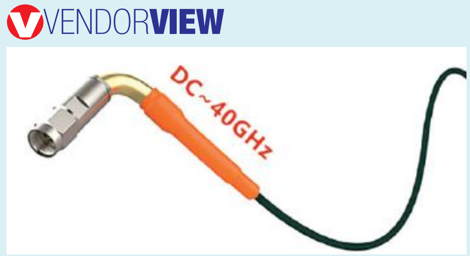


The 40 GHz high performance elbow right-angle mmWave cable assembly, launched by MIcable, features a 90-degree elbow 2.92 mm right-angle connector paired with the C29F low loss phase-stable cable (with a 2.54 mm diameter). It offers the same exceptional electrical performance as straight assemblies while providing superior mechanical reliability compared to conventional right-angle assemblies. This product is suitable for production line and laboratory testing, as well as various equipment and system connections.

**MIcable Inc.**
**www.micable.cn**

### FLEXIBLE CABLE

VENDORVIEW

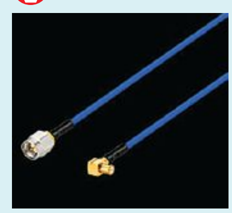

Mini-Circuits' model FL086-12SMMCR+ is a 12-in. length of Hand-Flex™ semiflexible coaxial cable for system and test applications from DC to 6 GHz. Insertion loss is typically 0.7 dB while return loss is typically 27 dB, both at 6 GHz. It includes a right-angle MCX male connector, SMA male connector and insulated outer jacket. With a minimum bend radius of 6 mm without tools, the cable assembly is hand-formable to almost any shape to replace worn 0.086 in. diameter semirigid cables.

**Mini-Circuits**
**www.minicircuits.com**

### INSTRUMENTAL CABLE

VENDORVIEW

Mini-Circuits' model VNAX-2FT-EMERF+ is a test cable with low loss across its 2 ft. length. Insertion loss is typically 2.4 dB to 40 GHz and typically 3.7 dB to 67 GHz while return loss is typically 34 dB to 40 GHz and 26 dB to 67 GHz. Terminated with stainless-steel 1.85 mm connectors, female at one end and male at the other, the RoHS-compliant cable has stable amplitude and phase with flexure and connects as much as 17 W at 67 GHz.

**Mini-Circuits**
**www.minicircuits.com**

## MMCX POWER OVER COAX RF CONNECTOR

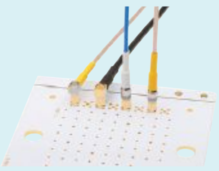

The MMCX Power over Coax (PoC) RF Connector, merging power and data over a single coaxial cable. With a frequency range of DC to 6 GHz, it delivers superior performance for modern applications while ensuring backward compatibility with existing systems. This innovative connector reduces complexity and boosts efficiency, making it ideal for compact, high performance solutions. Elevate your connectivity with this cutting-edge technology, tailored for today's digital demands.

**Molex**
**www.molex.com**



## DESIGN, MODEL AND SIMULATE COPPER CABLES


OptEM Cable Designer is a software tool that gives engineers the ability to design, model and simulate copper cables that meet compliance requirements and certification. Engineers can investigate cable behavior, test material effects and calculate cable mass and cost – all prior to prototyping and measurement – allowing companies to reduce prototype iterations and manufacturing cost. The software takes advantage of the latest technologies to give engineers a powerful design environment for cable development and costing.

**OptEM Engineering**
**www.optem.com**

## SMPX INTERCONNECTS

VENDORVIEW

Rosenberger's new SMPX interconnects are a key component to accelerate the development of 224G system architectures and enable future technologies. This 54 mm pitch, multiport solution has over 24 standard configurations available (customization available as needed). With high frequency up to 110 GHz, solderless compression mounting to PCB, over 10k mate cycles and more, these products are the perfect high performance sub-miniature push-on solution. Available now from RFMW.

**RFMW**
**www.rfmw.com**

## VECTOR NETWORK ANALYZER

VENDORVIEW

The Rohde & Schwarz vector network analyzer series provides precise, fast and versatile solutions for RF and microwave measurements. With a frequency range up to 1.1 THz and multiport options up to 48 ports, these high performance analyzers are ideal for analyzing passive and active components like filters, amplifiers, mixers and multiport modules. Offering excellent RF characteristics and a range of analysis functions, Rohde & Schwarz network analyzers empower users to assess crucial parameters efficiently.

**Rohde & Schwarz**
**www.rohde-schwarz.com/us**

## MULTIPORT SMPM SOLUTIONS

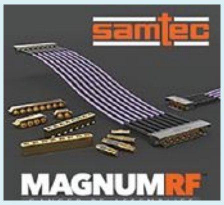


Magnum RF® is Samtec's newest line of ganged multiport connectors. Magnum RF® delivers an SMPM interface into a tightly packaged solution, offers 40 percent greater density, decreased processing time and better positional alignment versus single channel options. Cable-to-board and board-to-board mated sets are available.

**Samtec**
**www.samtec.com**

## MINI-LOCK CONNECTORS

SMPM Mini-Lock connectors can be selected for use with Smiths Interconnect's high frequency cable assemblies. The innovative, patent pending design approach has allowed for high frequency operation up to 110 GHz. It is compact, light-


## ISM RF & MW ENERGY

# 2.4 GHz Building Blocks

Flexible, Scalable Capabilities up to 6 kW

LEARN MORE

### Signal Generator/Controller

ISC-2425-25+

**Key Features:**

- 30 to +25 dBm (0.1 dB steps)
- Frequency from 2.4 to 2.5 GHz (1 kHz steps)
- Closed loop and feed forward RF power control modes
- User-friendly GUI and full API

### 300W SSPA

ZHL-2425-250X+

**Key Features:**

- 300W output power
- Supports CW & pulsed signals
- 42 dB gain
- 60% efficiency
- Built-in monitoring and protection

### 4-Way Splitter with Phase & Amplitude Control

SPL-2G42G50W4+

**Key Features:**

- 2.4 to 2.5 GHz
- Drive up to 4 amplifier stages from 1 ISC-2425-25+ controller
- Precise control of amplitude and phase on each path

Coming soon

### High Power 4-Way Combiner

COM-2G42G51K0+

**Key Features:**

- 1.2 kW power handling (sum port)
- 0.1 dB insertion loss
- 0.15 dB amplitude unbalance
- 1° phase unbalance
- 4x N-Type to 7/16 DIN

Mini-Circuits

weight, offers superior RF performance and high reliability testing for demanding applications. Mini-Lock connectors are suitable for harsh mechanical stress environments such as radars, satellites, space flight, military, UAV and UGV applications.
**Smiths Interconnect**
**www.smithsinterconnect.com**

## 0.8 MM VERTICAL LAUNCH CONNECTOR


In the relentless and ever-demanding world of high frequency interconnect products, the realm beyond 110 GHz stands out. Currently, the 0.8 mm connector reigns supreme at 145 GHz. Over five years ago, Southwest Microwave pioneered the 1.0 mm vertical launch connector. Building on that milestone, they are now developing a new 0.8 mm vertical launch connector for micro-strip. Although all elements are still in the preliminary prototyping phase, the outlook is promising and progress is moving swiftly.
**Southwest Microwave**
**www.southwestmicrowave.com**

## COMPRESSION MOUNT CONNECTORS

30-degree solderless PCB compression-mount connectors let you achieve edge launch-like performance anywhere on the board. Features include brand-new body orientation angled 30 degrees away from the PCB, improved electrical performance over standard surface-mount connectors, solderless design for fast installation and DC up to 65 GHz.
**SV Microwave**
**www.svmicrowave.com**

## RUGGEDIZED, PHASE AND MAGNITUDE STABLE RF CABLES

DuraWave™ PS43 was developed by Swift Bridge Technologies to exceed OEM performance through 43.5 GHz. These ruggedized, phase and magnitude stable RF cables are well-suited for on-site field testing, manufacturing environments and the testing laboratory. Insertion losses at 43.5 GHz are typically 30 to 40 percent lower than the OEM's test port cables with VSWR < 1.25 (< -18 dB S11 and S22). These assemblies are available on DigiKey with precision 2.92 mm and 2.4 mm connectors in various gender combinations.
**Swift Bridge Technologies**
**www.swiftbridgetechnologies.com**

## BOARD-MOUNT CONNECTORS

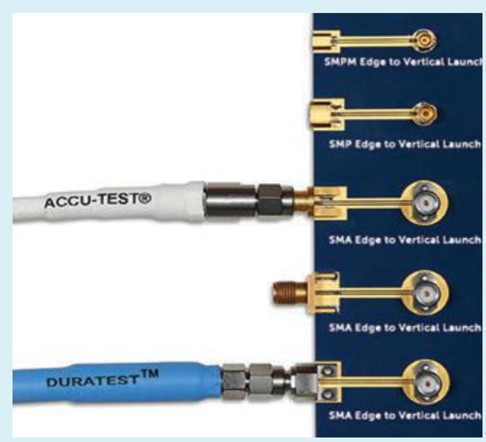


Teledyne's new board-mount connectors are designed with performance and reliability in mind. When it comes to lab testing, it is crucial to have a connection that transitions from cable to connector to PCB with minimal degradation. Teledyne Storm's full path solution allows customers peace of mind that everything mates together properly and meets high performance standards. All solutions are offered with short lead times and provide test samples.
**Teledyne Storm Microwave**
**www.teledynestorm.com**

# Sapphire Oscillators Deliver Next-Generation Phase Noise Performance

Saetta Labs
*Boulder, Colo.*

Saetta Labs is shipping their new SL1 series sapphire loaded cavity oscillators (SLCO), the next generation ultra-low phase noise microwave oscillator technology. These sapphire oscillators outperform all other microwave oscillators in terms of phase noise. Models are available at 7.00 GHz, 8.00 GHz, 10.00 GHz and 10.24 GHz. The SL1-8.00 GHz oscillator exhibits a phase noise of -154 dBc/Hz at 10 kHz and -170 dBc/Hz at 100 kHz. ***Figure 1*** shows the phase noise performance of the SL1-8.00 oscillator.

## INTEGRATED TECHNOLOGY

Saetta Labs' sapphire oscillators are a single, fundamental mode, pure microwave oscillator that replaces three or four traditional oscillators and their integrated hardware while achieving an order of magnitude higher performance. Prior to the sapphire oscillator, the best microwave reference was created by multiplying a high frequency quartz OCXO, cleaning up with a SAW filter or oscillator then phase locking a dielectric resonator oscillator (DRO). This combined performance is the limit of what is achievable with traditional technology. Saetta's sapphire oscillator replaces all three oscillators while significantly outperforming them.

The SL1 series oscillators have all the internal circuitry necessary to phase lock (discipline) to a 10 MHz reference. Without a 10 MHz reference, the SLCO is frequency stabilized to an internal reference, is voltage tunable and can be externally phase locked. Electronic tuning is ±1 ppm for a 0 to 1 V tune voltage and output power is 12 dBm.

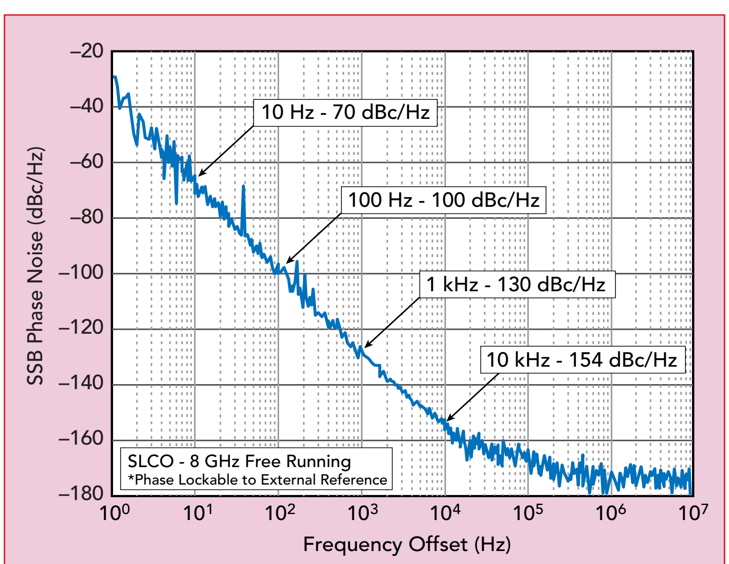


**Fig. 1** **SSB noise versus frequency offset for 8 GHz SLCO.**

## SAPPHIRE OSCILLATOR TECHNOLOGY

Sapphire oscillators are a completely different breed of microwave oscillator, relying on a whispering gallery mode instead of an electromechanical (quartz/SAW) or TE/TM mode (DRO) approach. The whispering gallery in sapphire is a dielectric resonant mode more common in optical systems. The resonance is maintained within the sapphire by near-perfect internal reflection between the dielectric boundary between the sapphire and a vacuum. The metal walls do not contain the fields, eliminating the loss of the metal wall boundary in traditional TE or TM mode resonators. Saetta's sapphire resonator technology has loaded Qs in excess of 100,000, which enables the lowest phase noise oscillators available and operate fundamentally at X-Band.

Saetta's technology extends into the amplifier and bias. Biasing their amplifiers through their proprietary ultra-low-noise architecture reduces the 1/f noise that contributes to the phase noise of the oscillator. All low noise circuitry is double- or triple-regulated.

Thermal stabilization is where Saetta has made the sapphire oscillator commercially possible. Using a proprietary ultra-high-resolution thermoelectric temperature control, they have stabilized the sapphire oscillator for room and extended temperature use (0°C to +40°C), holding to within ±100 ppb, typical, without the need for an external reference. When using an external reference, the oscillator stability matches that of the reference through phase locking.

## ADVANCED RADAR SYSTEMS

The phase noise of the oscillator in any radar system sets the funda-

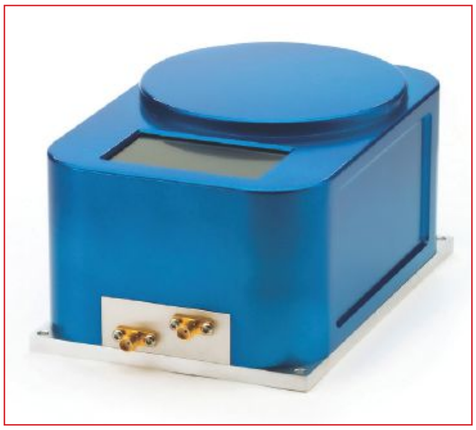

Fig. 2 Saetta Labs X-Band SLCO.

mental limits achievable in terms of range and resolution, regardless of how good the hardware is after the oscillator. Recent releases of digital-to-analog converters (DACs) and analog-to-digital converters can now drive array elements directly and achieve a 10logN reduction in noise with a converter on each N-element. The latest converter technology is achieving extremely low phase noise floors and 1/f, pushing the limits of achievable phase noise and significantly outperforming traditional oscillator technology.

Take a 10 GHz X-Band radar as an example. Flight targets may range from approximately subsonic to hypersonic or, for simplicity's sake, 1x to 5x the speed of sound. At sea level, this is a Doppler shift of 20 to 100 kHz. A multiplied crystal has a flat phase noise response in this range at approximately -135 dBc/Hz for a top-tier system. Compare that to the SL1-10.00 GHz sapphire oscillator with a phase noise of -150 dBc/Hz at 10 kHz and -170 dBc/Hz at 100 kHz. For the past two decades, quartz-based oscillators have only improved the phase noise by 5 to 10 dB. Sapphire oscillators from Saetta Labs improve upon the current state-of-the-art by 15 to 35 dB while eliminating reference design time with multiple loops.

## QUANTUM COMPUTING

Synthesizer design for quantum computing has evolved from using traditional synthesizers to modulating each qubit directly with a microwave DAC to manipulate phase, frequency and amplitude. The new DACs have lower phase noise than even the best traditional quartz/SAW-based systems. The sapphire oscillator has significantly lower noise and can improve the phase noise of the qubit DAC drivers.

## THE NEXT GENERATION

Saetta Labs was founded to bring the next generation phase noise levels of sapphire oscillators to real-world applications in a compact module. Their oscillators vary in size based on frequency. A 10 GHz oscillator is 102 (W) × 147 (L) × 76 mm (H). With a broad array of uses, from laboratory standards to deployable radar systems, our sapphire oscillators are available to extend the state-of-the-art in low phase noise systems. All Saetta Labs SLCOs are manufactured and tested in Boulder, Colo., using U.S. suppliers. ***Figure 2*** shows an example of the highly integrated SLCO X-Band oscillator.

**Saetta Labs**
**Boulder, Colo.**
**saettalabs.com**

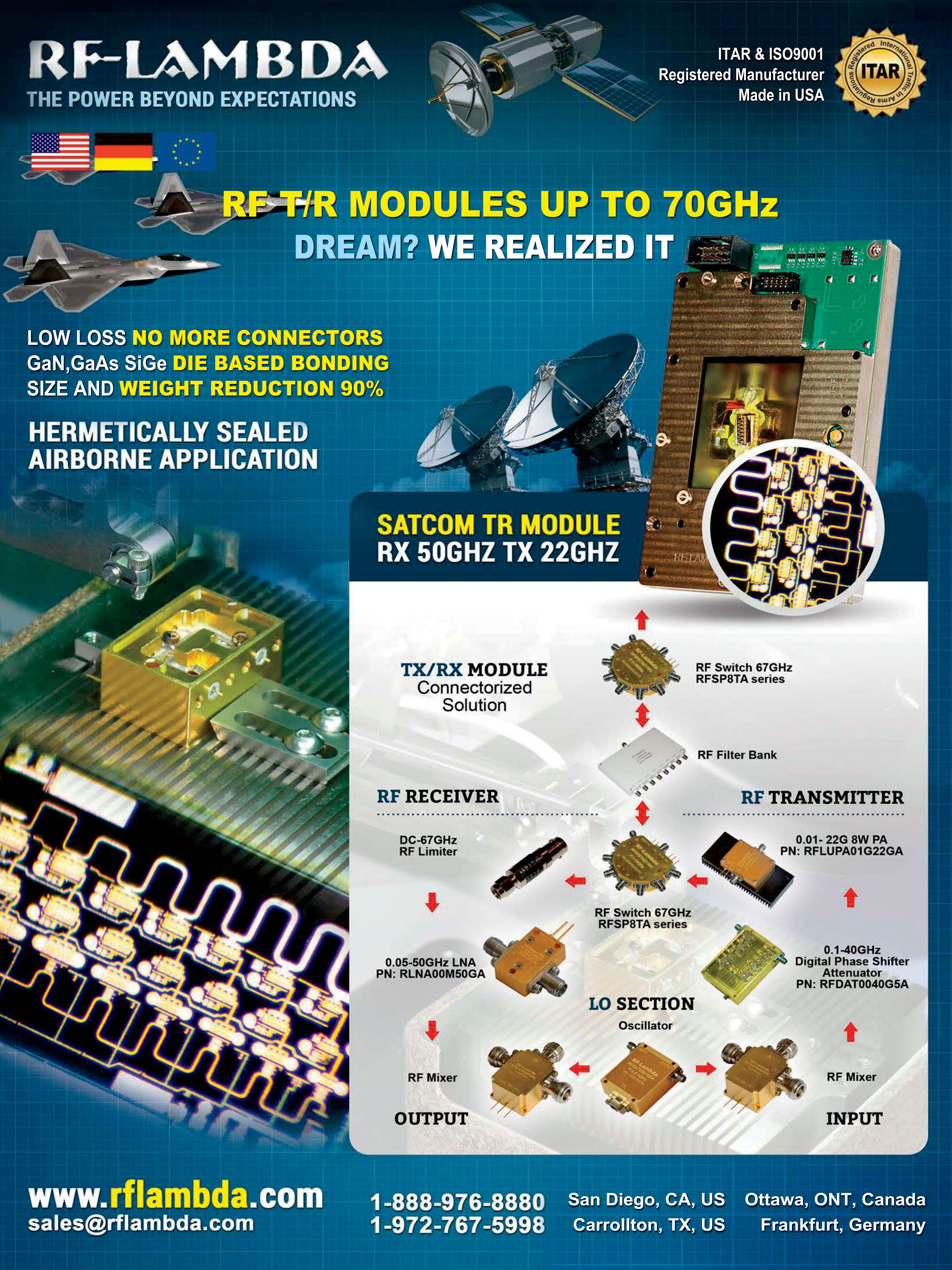

RF-LAMBDA
THE POWER BEYOND EXPECTATIONS
ITAR & ISO9001
Registered Manufacturer
Made in USA
ITAR
Registered International Traffic in Arms Regulations
RF T/R MODULES UP TO 70GHz
DREAM? WE REALIZED IT
LOW LOSS NO MORE CONNECTORS
GaN,GaAs SiGe DIE BASED BONDING
SIZE AND WEIGHT REDUCTION 90%
HERMETICALLY SEALED
AIRBORNE APPLICATION
SATCOM TR MODULE
RX 50GHZ TX 22GHZ
TX/RX MODULE
Connectorized
Solution
RF Switch 67GHz
RFSP8TA series
RF Filter Bank
RF RECEIVER
RF TRANSMITTER
DC-67GHz
RF Limiter
0.01- 22G 8W PA
PN: RFLUPA01G22GA
RF Switch 67GHz
RFSP8TA series
0.05-50GHz LNA
PN: RLNA00M50GA
0.1-40GHz
Digital Phase Shifter
Attenuator
PN: RFDAT0040G5A
LO SECTION
Oscillator
RF Mixer
RF Mixer
OUTPUT
INPUT
www.rflambda.com
sales@rflambda.com
1-888-976-8880
1-972-767-5998
San Diego, CA, US
Carrollton, TX, US
Ottawa, ONT, Canada
Frankfurt, Germany

# Unlocking High Frequency Data Acquisition With a 12-bit Digitizer

Teledyne SP Devices
*Linköping, Sweden*

**TABLE 1**

TYPICAL ADQ35-WB PERFORMANCE

| Parameter | Condition | Typical | Max. | Unit |
|---|---|---|---|---|
| **Basic parameters** | | | | |
| Bandwidth lower | -3 dB | 120 | 500 | kHz |
| Bandwidth upper | -3 dB | 7 | | GHz |
| Usable bandwidth | | 9 | | GHz |
| Input range | | 1.4 | | $V_{pp}$ |
| Input impedance | AC | 50 | | W |
| Input impedance | DC | 10 | | kW |
| Coupling | | AC | | |
| Connector type | | SMA | | |
| **Dynamic performance dual-channel mode at 5 GSPS** | | | | |
| Crosstalk | < 5 GHz | -60 | | dBFS |
| Noise power density | 0 to 2.5 GHz | -149 | | dBFS/Hz |
| SNR | Up to 2 GHz | 53.5 | | dBc |
| SFDR | Up to 2 GHz | 58 | | dBc |
| IM3 | 1.6 GHz, -7 dBFS | -70 | | dBc |
| IM3 | 5.9 GHz, -7 dBFS | -47 | | dBc |
| ENOB relative full-scale | 100 MHz, -1 dBFS | 8.8 | | bits |
| ENOB relative full-scale | 2 GHz, -1 dBFS | 8.5 | | bits |

Precision and performance are paramount in high frequency data acquisition. The ADQ35-WB 12-bit digitizer from Teledyne SP Devices stands out as a versatile and powerful solution designed to meet the demanding needs of various applications, from radar systems to scientific instruments. The ADQ35-WB is a high performance data acquisition module that offers dual-channel and single-channel configurations. With a sampling rate of up to 10 GSPS in single-channel mode and 5 GSPS per channel in dual-channel mode, it provides exceptional flexibility for different use cases. ***Table 1*** shows some of the typical performance characteristics, along with the dynamic performance in dual-channel mode at 5 GSPS per channel.

One of its standout features is the 9 GHz of usable analog bandwidth, which makes this device ideal for capturing high frequency signals with great accuracy. Equipped with 12-bit vertical resolution, the

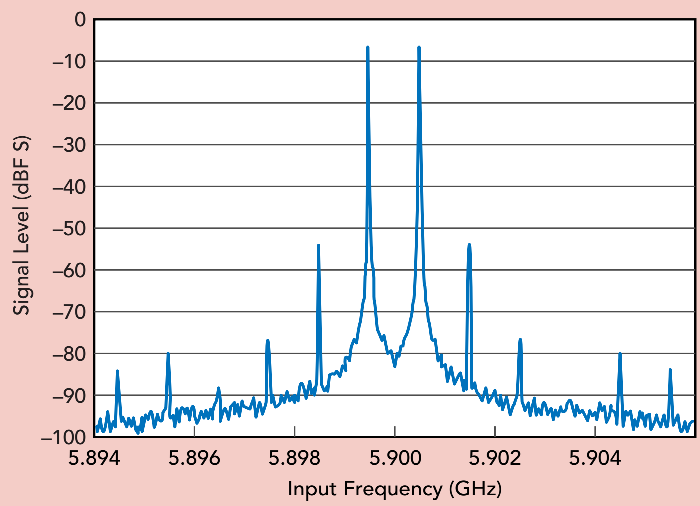


▲ Fig. 1 **FFT typical two-tone performance at 5.9 GHz.**

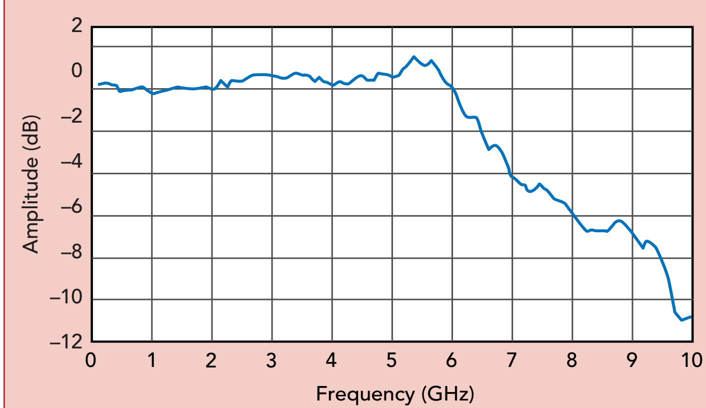


▲ Fig. 2 **Frequency response on a linear scale.**

ADQ35-WB ensures high precision in data acquisition, allowing for detailed and accurate signal representation. This level of resolution is crucial for applications that require fine-grain data analysis and interpretation. ***Figure 1*** shows typical two-tone fast Fourier transform (FFT) performance at 5.9 GHz. Additionally, the digitizer comes with 8 GB of onboard memory, providing ample storage for large datasets and enabling efficient data processing. The digitizer also supports peer-to-peer streaming at speeds of up to 14 Gbyte/s, facilitating rapid data transfer to GPUs, CPUs or SSDs. This high speed streaming capability ensures that data can be processed and analyzed without bottlenecks, making the ADQ35-WB suitable for time-sensitive applications.

At the heart of the ADQ35-WB is the open onboard AMD Kintex UltraScale KU115 field-programmable gate array (FPGA). This powerful FPGA offers extensive resources for custom real-time digital signal processing (DSP), allowing users to implement tailored algorithms and processing techniques directly on the hardware. This capability is particularly beneficial for applications that require real-time data analysis and decision-making.

One of the challenges in high frequency data acquisition is dealing with analog imperfections such as temperature-dependent baseline drift and noise. The ADQ35-WB addresses these issues through advanced error correction and performance enhancement techniques. By addressing analog imperfections and providing extensive customization options, the ADQ35-WB ensures that you can capture and analyze data with the highest level of accuracy. By leveraging FPGA-based real-time DSP, the digitizer can correct for baseline drift and improve the signal-to-noise ratio, resulting in cleaner and more accurate data. With these techniques, the ADQ35-WB can achieve the frequency response shown in ***Figure 2***, where 0 dB is the nominal input voltage range of 1.4 $V_{pp}$.

The ADQ35-WB is designed for easy integration into existing systems. Its PCIe form factor ensures compatibility with standard PC interfaces, while the included Digitizer Studio software provides a user-friendly platform for control and configuration. This software simplifies the setup process and allows users to configure the digitizer to meet their specific needs quickly. Its ease of integration and user-friendly software further enhance its appeal, making it a valuable addition to any data acquisition system.

Teledyne SP Devices offers several firmware options to enhance the functionality of the ADQ35-WB. The default data acquisition firmware (FWDAQ) is always included, providing a solid foundation for standard data acquisition tasks. For more specialized needs, optional firmware such as waveform averaging (FWATD) and pulse detection (FWPD) can be added. Additionally, the DEVDAQ FPGA development kit allows users to create custom firmware tailored to their specific requirements.

The ADQ35-WB is designed to excel in a wide range of applications. In radar systems, its high sampling rate and bandwidth enable precise detection and analysis of fast-moving targets. For scientific instruments, the digitizer's high-resolution and real-time processing capabilities are essential for capturing and analyzing complex signals. Other applications include scanning acoustic microscopy, LiDAR, particle physics and time-of-flight mass spectrometry.

In summary, the ADQ35-WB 12-bit digitizer from Teledyne SP Devices is a powerful and versatile tool for high frequency data acquisition. Its combination of high sampling rates, wide analog bandwidth and advanced DSP capabilities makes it ideal for a variety of applications. Whether you are working in radar, scientific research or any other field that requires precise and reliable data acquisition, the ADQ35-WB offers the performance and flexibility you need to achieve your goals. Explore the capabilities of the ADQ35-WB and unlock new possibilities in your high frequency data acquisition projects.

**Teledyne SP Devices, Linköping, Sweden**
**www.spdevices.com/en-us**

# Using Uncertainty Quantification to Predict Reliability in High Frequency Device Design

COMSOL
*Burlington, Mass.*

Designing high frequency devices requires a thorough understanding of theoretical precision and how prototyping or manufacturing tolerances affect performance. Real-world factors, such as variations in fabrication processes and material properties, result in discrepancies between ideal simulations and actual performance that must be addressed. By predicting how tolerances influence performance, uncertainty quantification (UQ) enables engineers to optimize designs for more reliable, consistent outcomes.

**Fig. 1** **Microstrip patch antenna mockup models.**

The COMSOL Multiphysics® software offers functionality for UQ studies and electromagnetics modeling. The latest release, version 6.3, introduces many updates for electromagnetics and important additions to UQ functionality for microwave components. This update was introduced in the RF Module, an add-on to the software that allows a user to examine how different input parameters impact device S-parameter performance.

## THE CHALLENGE: FROM SIMULATION TO REAL-WORLD PERFORMANCE

***Figure 1*** shows a batch of 100 microstrip patch antennas fabricated from a simulation model that estimates an ideal $S_{11}$ of -20 dB.

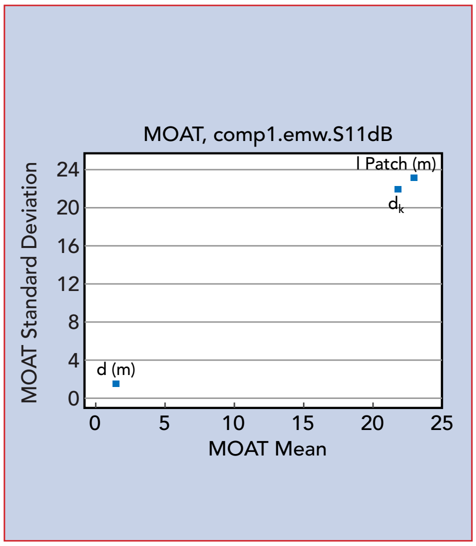


Fig. 2 **MOAT screening results.**

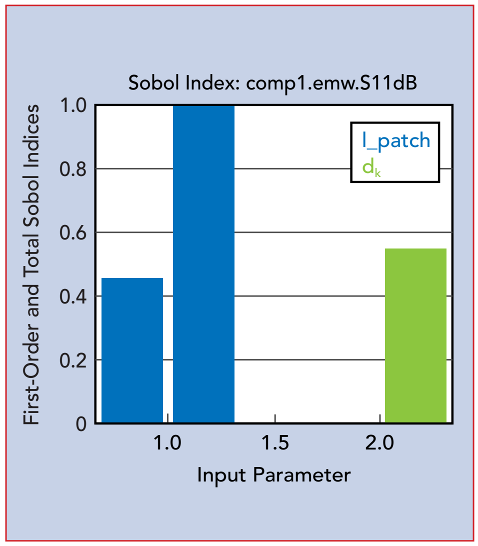


Fig. 3 **Sobol indices for a sensitivity analysis.**

Considering manufacturing and material variations, how many of these antennas will meet a design target of $S_{11} \leq -10$ dB?

In real-world manufacturing, variations in critical parameters, like the patch dimensions, substrate thickness and dielectric constant, are inevitable. These variations create antenna performance deviations. For example, small patch length changes may shift the resonant frequency, while inconsistent thickness or dielectric properties can cause impedance mismatching. Without accommodating these factors, even well-designed antennas may not achieve the intended performance.

UQ systematically analyzes how design parameter variations affect system performance and estimates how many antennas will meet the specified performance criteria. The standard process involves a screening study, a sensitivity analysis, uncertainty propagation and a reliability analysis. COMSOL Multiphysics® offers an intuitive workflow for performing these analyses.

## MORRIS ONE-AT-A-TIME (MOAT) SCREENING

The goal of a screening study is to perform a qualitative analysis to identify input parameters with the greatest influence on performance indicators or quantity of interest (QoI), $S_{11}$ in this case. The MOAT method computes the mean and standard deviation. They are the average QoI effect of varying a parameter and assessing the variability in that parameter's effect, indicating potential interactions with other parameters.

Typical parameters and ranges in printed antenna simulations include:

- Substrate thickness, *d*, can vary by approximately ±7 percent from 0.060 in. (~1.524 mm), based on manufacturer data. Setting σ to 3.5 percent of *d* captures about 95 percent of the variations within ±2σ.
- Patch length (*l_patch*) has a nominal value of 52 mm and the tolerance depends on the fabrication method. Non-high-precision PCB etching can reduce the tolerance to 0.127 mm, whereas milling with loose anchoring can yield a tolerance of ±2σ ≈ 0.520 mm.
- Dielectric constant, $d_k$, is often 3.38 ± 0.05. For stricter coverage (e.g., ±3σ), $\sigma = 0.005 \times d_k \approx 0.0169$, resulting in ±0.0507 around the nominal value.

Filtering out less important parameters can make subsequent UQ analyses more efficient. ***Figure 2*** shows results with *l_patch*, $d_k$ and *d*. The screening analysis indicates that substrate thickness is less influential than the other parameters.

## SENSITIVITY ANALYSIS WITH SOBOL INDICES

After identifying the most influential parameters, a sensitivity analysis quantifies how each parameter, individually and in combination, affects the QoI. Sobol indices include:

- First-order: reflects the direct contribution of each parameter to the QoI
- Total: captures direct effects and interaction effects with other parameters.

***Figure 3*** shows first-order and total Sobol indices for an analysis that evaluates parameter sensitivity and interactions. The analysis shows that the length of the patch is more influential than the substrate's dielectric constant.

## UNCERTAINTY PROPAGATION WITH KERNEL DENSITY ESTIMATION (KDE)

Uncertainty propagation evaluates how variations in input parameters affect the $S_{11}$ distribution. A KDE plot shows a smoothed probability density function estimate of the QoI, illustrating how input parameter uncertainties influence the distribution. By depicting likely QoI values in a continuous manner, KDE provides clearer insight into probabilistic behavior and variability. This approach helps determine the probability of different outcomes, revealing the range of QoI values under inherent uncertainties. The KDE in ***Figure 4*** illustrates the probability density function of the QoI.

## RELIABILITY ANALYSIS

A reliability analysis calculates the probability of meeting a predefined performance criterion. It provides a probability value for conditions, indicating the fraction of scenarios falling below the threshold.

Example scenarios:

- Milling with loose anchoring: large tolerances on *l_patch* result in a 55 percent probability of $S_{11} < -10$ dB
- Non-high-precision PCB etching: reduced tolerances increase the probability of antennas passing to 86 percent.

Such findings highlight how tightening tolerances or employing more consistent manufacturing processes significantly raises the proportion of devices that meet the target specification.

## RESULTS AND DISCUSSION

Key takeaways from the UQ stud-

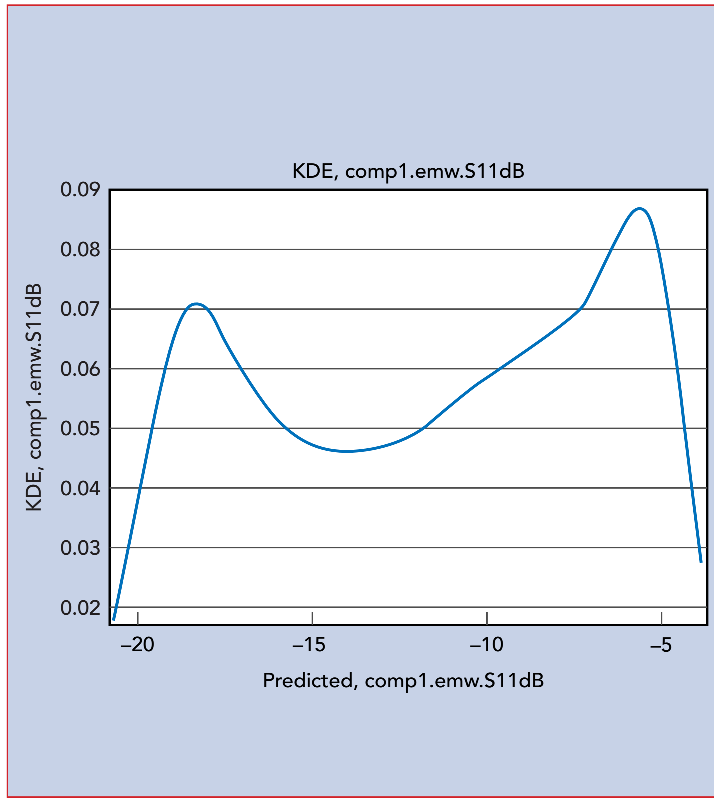


**Fig. 4** KDE plot.

ies include:

- MOAT screening frequently identifies *l_patch* and $d_k$ as primary drivers of $S_{11}$ variability
- Sobol indices confirm direct effects and the importance of interactions among parameters
- KDE plots display $S_{11}$ distribution, revealing whether most samples cluster around or deviate from the -10 dB threshold
- Reliability analysis quantifies the fraction of cases ≤ -10 dB, informing decisions on tolerance tightening and design adjustments.

Narrowband devices, particularly those operating at higher frequencies, are especially sensitive to slight geometric or material deviations. Even a minor 5 to 10 MHz shift in the resonant frequency can result in unacceptable return loss. By employing UQ, engineers can anticipate these shifts, optimize designs and determine when to tighten certain tolerances.

Integrating UQ into the design process helps engineers bridge the gap between simulation and reality, ensuring reliable performance across a range of manufacturing variations. For the 100 antennas, predicting that most will meet the -10 dB $S_{11}$ target provides a solid production foundation while offering refinement opportunities for the fraction not meeting the target. This continuous improvement loop elevates both design and manufacturing processes.

COMSOL Multiphysics is a registered trademark of COMSOL AB.

**COMSOL**
**Burlington, Mass.**
**www.comsol.com**

# Test Cables Work to 110 GHz

Pasternack has introduced a new line of high performance 1.0 mm test cable assemblies. These cable assemblies are specifically designed to meet the demands of industries such as test and measurement, aerospace and defense and telecommunications, where precision and reliability are critical. They deliver exceptional performance, ensuring signal clarity and durability, even in the most challenging testing environments.

Key features of the 1.0 mm test cable assemblies include a rugged armored coaxial design capable of withstanding extreme temperatures ranging from -55°C to 125°C. With frequency handling capabilities from DC to 110 GHz, these cables are ideal for advanced testing applications. They also provide low insertion loss and stable phase performance, minimizing signal interference and ensuring superior signal integrity for rigorous testing scenarios.

The new cable assemblies offer engineers and technicians reliable off-the-shelf solutions for high frequency testing. They are available with both male-to-male and male-to-female 1.0 mm connectors, offered in 12 in. lengths. These assemblies are ideal for environments requiring consistent performance and resilience.

In addition to being in stock and ready for same-day shipping to meet urgent project needs, custom versions of these RF cable assemblies can be built and shipped within two weeks. Custom cable lengths are also available by contacting a Pasternack sales representative. For added assurance, RF testing services can document the electrical performance of your specific cable assembly.

A leader in RF products since 1972, Pasternack is an ISO 9001:2015 certified manufacturer and supplier offering the industry's largest selection of active and passive RF, microwave and mmWave products available for same-day shipping.

VENDORVIEW

**Pasternack, an Infinite Electronics brand**
**Irvine, Calif.**
**www.pasternack.com**

---

# Antenna Range Spotlights 300 mm Apertures

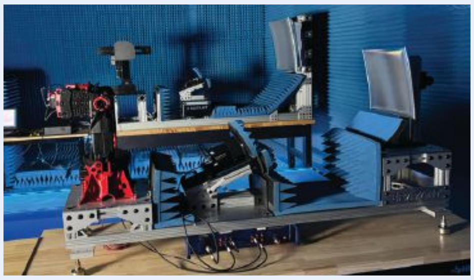

Building on its successful table-top Compact Antenna Test Range (CATR), Eravant offers a larger open-air CATR with a 600 x 600 mm rolled-edge reflector. Featuring a 300 mm diameter quiet zone for testing a variety of antenna types, the CATR includes a heavy-duty gimbal that supports loads up to 80 lbs. The gimbal provides ±72 arcsecond positioning accuracy with ±90-degree azimuth and elevation range.

The open-bed CATR is compatible with a variety of transmit and receive frequency extender modules using VNAs from vendors, including Copper Mountain, Anritsu, Keysight and Rohde & Schwarz. Eravant's VNA frequency extender modules cover full and extended waveguide bands from 20 to 330 GHz with dynamic ranges as high as 120 dB. The receive frequency extender connects to the antenna under test (AUT) and travels with it during measurements. The transmit frequency extender drives a feed horn projecting spherical waves onto the reflector to produce plane-wave signals within the quiet zone surrounding the AUT. Eravant offers a wide selection of compatible feed horns with optional polarizers and mode transitions.

Machined from a solid aluminum block, the reflector includes a protective chemical finish that prevents corrosion and maintains high surface conductivity. The support structure, built from T-slotted aluminum framing, provides a secure and versatile component mounting system. The configuration enables precise feed horn location and orientation to optimize the quiet zone quality.

The supplied software can control different-sized gimbals and various VNA brands and models. It can also be customized to control additional devices and supports a wide variety of automated measurements for various needs.

The 300 mm CATR is model STY-CATR-0300-OB-S1, while the 150 mm version is model STY-CATR-0150-OB-S1. Both systems are available for evaluation through Eravant's Antenna Measurement Services.

VENDORVIEW

**Eravant (formerly Sage Millimeter Inc.)**
**Torrance, Calif.**
**www.eravant.com**


# Quantum/Cryogenic Building Blocks

Quantum computers are being developed that could bring revolutionary capabilities to commercial, industrial and government sensing systems, radar, communications and radio astronomy. This rapidly advancing technology requires RF/microwave components to operate in the testing and manufacturing process within extremely cold temperature environments. To meet this demand, KRYTAR now offers a selection of components for your quantum and cryogenic designs using materials optimized for cryogenic environments to +85°C.

The new product line includes directional couplers, hybrid couplers, a two-way power divider and a 50 Ω coaxial termination:

- Directional coupler operates from 1.0 to 12.4 GHz: Model 101012410-Q-1006 with 10 dB coupling
- Directional couplers operating from 2.0 to 12.4 GHz: Model 102012410-Q-1006 with 10 dB coupling, Model 102012420-Q-1006 with 20 dB coupling and Model 102012430-Q-1006 with 30 dB coupling
- Directional couplers operating from 4.0 to 12.4 GHz: Model 104012410-Q-1006 with 10 dB coupling, Model 104012420-Q-1006 with 20 dB coupling and Model 104012430-Q-1006 with 30 dB coupling
- Hybrid couplers operating from 1.0 to 12.4 GHz: Model 3010124-Q-1006, a 90-degree hybrid with 3 dB coupling, Model 4010124-Q-1006, a 180-degree hybrid with 3 dB coupling
- Two-way power divider operates from 2.0 to 18 GHz: Model 6020180-Q-1006 is an MLDD design with > 19 dB isolation, ±0.3 dB of amplitude tracking and phase tracking of ±6 degrees
- 50 Ω coaxial termination operates from DC to 12.4 GHz: Model T1MA-Q-1006 with low VSWR and a 3.5 mm male connector

KRYTAR provides complete engineering services for custom designs that meet or exceed critical performance and/or packaging requirements. They are well known for quick-reaction capability, design responsiveness, flexibility, fast production turnaround and partnerships with customers. These components afford academia, industrial and government users the ability to operate cryogenic control electronics in their quantum computing product research, development and manufacturing process.

VENDORVIEW

**KRYTAR**
**Sunnyvale, Calif.**
**https://krytar.com/products/quantum-cryogenic-products/**

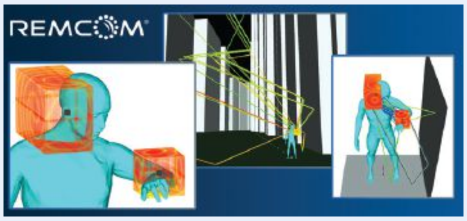


# Analysis of Mobility and Interactions with Body-worn Devices

Remcom has introduced a new Huygens surface capability that incorporates near-field antenna effects into simulations of antenna performance. This allows for the analysis of mobility, multipath and interactions with body-worn devices in realistic environments. The Huygens surface capability is integrated with dynamic mobility, enabling the movement of RF systems, vehicles and people through virtual wireless scenarios. Seamless interoperability between high-resolution near-field simulations and efficient 3D ray tracing supports applications such as GNSS, 6G connectivity, lunar missions and on-body communication while in motion.

Steady-state electric and magnetic field data for complex designs involving MCAD, ECAD, PCB, scatterers and circuit matching networks can be transferred from Remcom's XFdtd into Wireless InSite, where the Huygens configuration can be placed anywhere in the scene and moved through time via mobility options that reveal how motion or moving objects and people affect fading and shadowing.

The update supports several important applications:

- GNSS positioning: Accurate modeling of handheld devices on walking humans in urban environments, capturing multipath effects from 3D structures and signal losses from foliage, as observed from moving satellites
- NASA Artemis Program: Wireless channel simulation and coverage analysis for lunar environments, including simulation of MIMO antennas on spacesuits during moonwalks, digital elevation maps and analysis of network performance impacts from regolith dust, sub-surface scattering and blockage from rovers and craters
- 5G/6G connectivity for UAVs, automotive and robotics: Wireless InSite's mobility and accurate simulation of propagation and multipath provides training data to ML algorithms in AI-native 6G networks
- On-Body communications: Unique on-body communication modeling for wearables, including earbuds, smartwatches, UWB positioning tags, smart rings and more, allows RF engineers to analyze interactions between the human and the device and optimize wireless performance across wearable ecosystems.

VENDORVIEW

**Remcom Inc.**
**State College, Pa.**
**www.remcom.com**

## Robust Power Management Solutions from Analog Devices

Our robust power solutions support the most challenging industrial automation, aerospace and defense, automotive and digital healthcare applications.

**Analog Devices**

**www.analog.com/en/resources/media-center/videos/6361258972112.html**

## 800G for Field Applications

Anritsu's recent Test Talk blog post examines the processes required to ensure 800G networks perform optimally in the field, enhancing reliability and accelerating adoption.

**Anritsu**

**bit.ly/3DHa1Pc**

## Empower RF Celebrates 25th Anniversary

Entering 2025, Empower RF Systems announced the company's 25th anniversary and results from the previous year that included capacity expansion and record business results.

**Empower RF Systems**

**www.empowerrf.com**


## Qorvo Blog Series: LEO Satellites: Driving the Future of SATCOM


Explore how LEO satellites are revolutionizing communication in Qorvo's engaging blog series. Discover key trends, technologies and insights shaping the future of SATCOM.

**Qorvo**

**https://bit.ly/3BWVE90**

## New Layout Tool

Quantic X-Microwave's new Layout Tool provides an interactive design environment for part selection, layout and signal chain analysis using X-MWblocks. Featuring a newly expanded library, automated wall algorithms and robust export capabilities, this tool streamlines the design process.

**Quantic X-Microwave**

**https://layout.xmicrowave.com/configurator**


## Understanding RF Attenuators

This video provides a short overview of the different types of attenuators commonly used in RF test and measurement applications.

**Rohde & Schwarz**

**www.youtube.com/watch?v=BpQAoKivS7U**

# NEW PRODUCTS

FOR MORE NEW PRODUCTS, VISIT WWW.MWJOURNAL.COM/BUYERSGUIDE
FEATURING VENDORVIEW STOREFRONTS

## DEVICES/ COMPONENTS/MODULES

### Ultra-Low Loss Shielded Power Inductors


Coilcraft's compact XGL3020 Series molded power inductors offer the lowest DC losses and extremely low AC losses for a wide range of DC-DC converters, making them ideal for a variety of applications where space is limited and efficient power management is critical, including various non-isolated converter topologies, point-of-load, IoT devices and many others. Their 80 V voltage rating also makes them suitable for wide Vin DC-DC converters and applications. Additionally, their AEC qualification ensures reliability and robustness in automotive and other harsh environments.

**Coilcraft**
**www.coilcraft.com**

### RF and Microwave Switches


RF and microwave switches offer unparalleled control and versatility for your signal routing and manipulation. These switches offer fast response time and low insertion loss, ensuring optimal performance in high frequency applications. With a compact and robust connectorized design, it is the ideal choice for aerospace applications.

**ERZIA Technologies**
**www.erzia.com**

### 2-Way Divider

VENDORVIEW


KRYTAR's technological advances provide excellent operating performance of this new 2-way unit. The 2-way divider exhibits insertion loss of < 1.2 dB across the full frequency range. Maximum VSWR is 1.5. Input power rating is 10 watts with 2:1 load VSWRs. Units with tighter amplitude and phase tracking specifications can be supplied.

**Krytar Inc.**
**www.krytar.com**

### Coaxial Switch

This DC to 26.5 GHz SMA for your RF/ microwave requirements has a VSWR of 1.6:1 maximum, insertion loss of 0.6 dB maximum and isolation of 55 dB minimum. Weatherproof models are available.

**Logus Microwave**
**www.logus.com**

### Phase Shifter

VENDORVIEW


Quantic PMI Model PS-360-DC-3 OPTION 618-15D-10BIT is a 10-Bit, digitally controlled phase shifter operating over the 6 to 18 GHz frequency range. This high speed phase shifter has a range of 360 degrees, an insertion loss of 12 dB, an accuracy of 8.5 degrees, a PM/AM of ±2.5 dB, a carrier suppression of 18 dB, a sideband suppression of 15 dB and a power handling of +20 dBm. This phase shifter has SMA female connectors and is 1.85 × 1.75 × 0.50 in.

**Quantic PMI**
**www.quanticpmi.com**

### Wireless Filters

VENDORVIEW

Reactel has an extensive library of filters and multiplexers for wireless applications. These units cover all aspects of a wireless system: antennas, base stations, co-site interference, repeaters, point-to-point radios or any other function. These units are available in cavity, discrete component, ceramic, suspended substrate and tubular configurations. Packaging styles range from low-cost, drop-in to high-power connectorized and offer the option of weather resistant packaging for outdoor applications.

**Reactel**
**www.reactel.com**

### 50 GHz RF Switch

Teledyne HiRel Semiconductors announced the availability of its latest rad-tolerant wideband 50 GHz RF switch, model TDSW050A2T. This switch operates from true DC to 50 GHz, delivering excellent RF performance down to zero hertz, making this device ideal for many of today's complex space and defense applications. It has been developed in a 150 nm pHEMT Indium GaAs process and is available in a 1.15 × 1.47 × 0.1 mm die ideal for hybrid assembly products.

**Teledyne HiRel Semiconductors**
**www.teledynedefenseelectronics.com**

### Miniature Lumped Element Filters

Telonic Berkeley miniature lumped element filters include highpass, lowpass, bandpass, bandstop, diplexer, multiplexer and filter bank filters from 10 MHz to 20 GHz. Bandwidth 1 percent to multi-octave, surface-mount/connectorized package options available for broadcast, telecommunication, SATCOM, defense, IED jammers, space-level and commercial.

**Telonic Berkeley**
**www.telonicberkeley.com**

### Capacitors

VENDORVIEW

All SMT variants of the aluminum electrolyte and aluminum hybrid polymer capacitors from Würth Elektronik are now available in an extremely vibration-resistant version on request. Thanks to their enlarged solder pads and thicker base plate, the capacitors can withstand acceleration up to 30 g (294 m/s²). Electronics must continue to function reliably, even when exposed to strong mechanical stresses. This is the case with electronically controlled tools, industrial applications, construction machinery or drones, for example.

**Würth Elektronik**
**www.we-online.com**

## CABLES & CONNECTORS

### 1.0 mm Test Cable Assemblies

VENDORVIEW

Pasternack launched its new 1.0 mm test cable assemblies. These cables deliver exceptional performance in high frequency environments up to 110 GHz, addressing the critical needs of industries such as telecommunications, aerospace and defense, where precision and durability are paramount. The new line is designed for rigorous testing applications, offering signal clarity and robust performance even in the most challenging conditions.

**Pasternack**
**www.pasternack.com**

### Vertical Launch 0.8 mm Connectors

WithWave's vertical launch 0.8 mm connectors are specially designed for solderless vertical PCB launch on test and measurement boards. These connectors have

# New**Products**

excellent electrical transition performance up to 145 GHz, respectively, as well as reduce installation time by eliminating soldering.
**withwave co., ltd**
**www.with-wave.com**

## AMPLIFIERS

### 4 KW Solid-State C-Band Pulse Amplifier

VENDORVIEW

Exodus Advanced Communications' AMP2083P-4KW Pulse Amplifier is designed for pulse/HIRF, EMC/EMI Mil-Std 461/464 and radar applications. Providing superb pulse fidelity and up to 150 usec pulse widths. Duty cycles to 10 percent with a minimum 66 dB gain. Available monitoring parameters for forward/reflected power in watts and dBm, VSWR, voltage, current, temperature sensing for outstanding reliability and ruggedness in a compact 10U chassis.
**Exodus Advanced Communications**
**www.exoduscomm.com**

### Wideband, 0.01 - 20 GHz Low Noise Amplifier

Z-Communications Inc. announced the AWB1022A wideband, low noise amplifier spanning frequencies from 10 kHz to 20 GHz. The AWB1022A is a new product in Z-COMM's ever-expanding offerings in the low noise amplifier space for applications varying from test and measurement, lab bench and prototyping. The AWB1022A low noise amplifier complements Z-COMM's products in the RF frequency chain and compliments the company's existing frequency sources, such as the SSG22645LX wideband frequency synthesizer (45 MHz to 22 GHz) and family of phase locked oscillators.
**Z-Communications Inc.**
**www.zcomm.com**

## SYSTEMS & SUBSYSTEMS

### RF System-On-Module

VENDORVIEW

The ADRV9009-ZU11EG is a highly integrated RF system-on-module (RF-SOM) based on dual Analog Devices ADRV9009 wideband transceivers. When combined with the ADRV2CRR-FMC carrier board, this hardware platform can be used for prototyping and reducing time to market for application-specific designs, offering four Tx and Rx RF channels. With the AD-FMCOMMS8-EBZ a customer can extend this system to eight Tx and Rx RF channels.

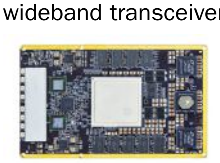

**Analog Devices**
**www.analog.com**

## SOURCES

### Phase Locked Dielectric Resonator Oscillators

VENDORVIEW

Quantic MWD, a business of Quantic Electronics, announced the launch of its new Whisper Series phase locked dielectric resonator oscillators (PLDROs). The new Whisper Series PLDROs are designed to deliver low phase noise performance and exceptional frequency stability, providing industry-leading performance in even the harshest environments. With fully customizable options — including phase locked loops and tuning — Whisper Series PLDROs meet and exceed the most stringent system requirements.
**Quantic MWD**
**www.quanticmwd.com**

## ANTENNAS

### UWB 5G External Antennas

Quectel Wireless Solutions has introduced three new 5G terminal mount antennas. The antennas, the YECT002W1A, YECT102WAAH and YECT103W7AH, offer high gain and efficiency as well as simplified design and deployment flexibility. All three antennas offer robust, ultra-wideband external 5G capabilities and backed by Quectel's comprehensive antenna design support. This includes simulation, testing and manufacturing for custom antenna solutions to meet customers' specific application needs. Quectel's regional R&D centers are located to ensure quick responses to customer requirements.
**Quectel Wireless Solutions**
**www.quectel.com**

## TEST & MEASUREMENT

### Noise Figure Measurement Service

VENDORVIEW


Utilizing in-house developed and calibrated noise sources, Eravant offers noise figure measurement services for amplifiers and receivers operating up to 320 GHz. The noise sources used are calibrated using reference terminations cooled with liquid nitrogen. Industry-standard noise analyzers are combined with custom frequency extenders to yield accurate noise figure measurements.
**Eravant**
**www.eravant.com**

### Spectrum Analyzers

Saelig Company Inc. has introduced the PX Series real-time spectrum analyzers with three models in the series: PXN-400 (9 kHz to 40 GHz), PXE-200 (9 kHz to 20 GHz) and PXE-90 (9 kHz to 9.5 GHz). With a superheterodyne receiver design and multi-segment preselected filtering, the PX Series offers an attractive combination of size, performance and cost. RF measurements and analysis from 9 kHz up to 40 GHz can now be carried out in a robust, compact instrument.
**Saelig Company Inc.**
**www.saelig.com**

## MICRO-ADS

Reviewed by: Ajay K. Poddar

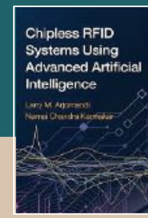


# Bookend

## Chipless RFID Systems Using Advanced Artificial Intelligence

**By: Larry M. Arjomandi and Nemai Chandra Karmakar**

This book is a comprehensive guide to developing hybrid mmWave chipless RFID systems. It encompasses chipless tags, reader hardware and detection algorithms that employ advanced image processing and ML techniques. This book distinguishes itself from existing literature with six chapters exploring a broad range of relevant topics. Each chapter in this book is structured to provide technical depth and accessibility, making it a valuable resource for engineers and researchers working on mmWave chipless RFID technologies. Readers will discover how to utilize cutting-edge AI detection techniques and cloud computing to significantly lower costs. Commencing with foundational concepts, the book equips readers with the necessary background to create chipless tag signatures that can be printed on standard plastic substrates. The book introduces cost-effective image construction methods aimed at reducing detection errors, to enhance overall system reliability. A key focus is on side-looking aperture radar (SLAR), where deep learning techniques improve the safety of chipless detection. The text emphasizes three principal areas of system development: tag design, reader design and formulating appropriate decoding algorithms.

Each chapter is rich with practical design examples, ensuring that readers can apply the concepts to real-world applications. With its emphasis on the mmWave band and a hands-on approach to designing chipless tags, reader hardware and detection algorithms, this book serves as an invaluable resource for industry engineers, design professionals and academic researchers alike. The inclusion of practical Q&A sections at the end of each chapter further enhances the reader's understanding of the content.

ISBN: 9781630819484
Pages: 240
To order this book, contact:
Artech House (2023)
us.artechhouse.com


# 2025 IEEE Texas Symposium on Wireless and Microwave Circuits and Systems
## April 8-9, 2025, Waco Texas

www.TexasSymposium.org

**Authors from academia, industry, government labs, and other organizations around the world are invited to submit papers in the areas listed below:**

- RF and microwave circuits and systems
- 5G/6G and millimeter-wave/THz wireless technologies
- Wireless technologies for biomedical applications
- Computational electromagnetics
- Antennas, propagation and electromagnetics
- Spectrum management and coexistence
- RF active and passive devices
- Microwave metrology
- Wireless power transfer
- Electromagnetic materials and modeling
- Wireless and optical communications
- Photonics
- Geophysical and subsurface modeling
- Radar and sensing
- Internet of Things
- Emerging wireless technologies

★ **2025 Special Session:**
**Artificial Intelligence (AI) Applied to RF/Microwave Design**

**Special Event:**
***Student Research Poster Competition***
**(please see the website for details)**

## Important Dates:

**Paper Submission Deadline: Feb 10, 2025**
**Author Notification: March 10, 2025**
**Final Manuscript Due: March 19, 2025**
**Advanced Registration Deadline: March 24, 2025**
**Conference Sessions: April 8-9, 2025**

**To learn more about the IEEE Texas Symposium on Wireless and Microwave Circuits and Systems please scan the QR code below:**

# Advertising**Index**


| Advertiser | Page No. |
|---|---|
| 3H Communication Systems | 15 |
| Aaronia AG | COV 3 |
| Anoison Electronics LLC | 80 |
| Anritsu Company | 67 |
| Artech House | 126 |
| B&Z Technologies, LLC | 23 |
| Cernex, Inc. | 64 |
| Ciao Wireless, Inc. | 36 |
| Coilcraft | 21 |
| COMSOL, Inc. | 27 |
| Copper Mountain Technologies | 61 |
| CPI Electron Device Business | 52 |
| Custom Cable Assemblies, Inc. | 106 |
| Dalicap | 33 |
| EDI CON Online 2025 | 115 |
| ERAVANT | 49 |
| ES Microwave, LLC | 125 |
| EuMW 2025 | 73, 119 |
| Exceed Microwave | 46 |
| Exodus Advanced Communications, Corp. | 29 |
| Fairview Microwave | 99 |
| FutureG for Defense Summit 2025 | 110 |
| G.T. Microwave Inc. | 68 |
| Greenray Industries, Inc. | 58 |
| Harogic Technologies | 65 |
| HASCO, Inc. | 104 |
| Herotek, Inc. | 62 |
| Huber + Suhner AG | 92 |
| HYPERLABS INC. | 24 |
| IEEE AP-S International Symposium 2025 | 117 |
| IEEE Texas Symposium 2025 | 127 |
| IEEE WAMICON 2025 | 118 |
| JQL Technologies | 3 |
| KYOCERA AVX | 51 |
| LadyBug Technologies LLC | 74 |
| LPKF Laser & Electronics | 32 |
| Marki Microwave, Inc. | 31 |
| Maury Microwave Corporation | 87 |
| MECA Electronics, Inc. | 26 |
| MIcable Electronic Technology Group | 47, 101 |
| *Microwave Journal* | 122 |
| Microwave Products Group (a Dover Company) | 70 |
| Miller MMIC | COV 2, 11 |
| Millimeter Wave Products Inc. | 53 |
| Mini-Circuits | 4-5, 16, 40, 83, 93, 107, 129 |
| Molex | 91 |
| Norden Millimeter Inc. | 22 |
| Nxbeam | 43 |
| OptEM Engineering Inc. | 84 |
| Parker Test Equipment | 46 |
| Pasternack | 13 |
| Pulsar Microwave Corporation | 34 |
| Qualwave Inc. | 72 |
| Quantic PMI | 9 |
| Quantic X-Microwave | 9 |
| Reactel, Incorporated | 39 |
| Remtec | 60 |
| RF-Lambda | 6, 35, 69, 111 |
| RFMW | 25 |
| RLC Electronics, Inc. | 19 |
| Rohde & Schwarz, Inc. | 85 |
| Safran Electronics & Defense | 38 |
| Samtec USA | 77 |
| Signal Hound | 55 |
| Smiths Interconnect | 97 |
| Southwest Microwave Inc. | 108 |
| Spectrum Control | 7 |
| Spectrum Instrumentation GmbH | 59 |
| SV Microwave, Inc. | 89 |
| Swift Bridge Technologies | 82 |
| Synergy Microwave Corporation | 45, 71 |
| Teledyne Storm Microwave | 81 |
| The Phoenix Company of Chicago, Inc. | 57 |
| Times Microwave Systems | 103 |
| Trans-Tech | 42 |
| TTE (iNRCORE Family of Brands) | 63 |
| Unmanned & Autonomous Systems Summit 2025 | 121 |
| Virginia Diodes, Inc. | 8 |
| Weinschel Associates | 30 |
| Wenteq Microwave Corporation | 125 |
| Werlatone, Inc. | COV 4 |


## Sales Representatives

**Eastern and Central Time Zones**
Carl Sheffres
*Group Director*
(New England, New York, Eastern Canada)
Tel: (781) 619-1949
csheffres@mwjournal.com

Michael Hallman
*Associate Publisher*
(NJ, Mid-Atlantic, Southeast, Midwest, TX)
Tel: (301) 371-8830
Cell: (781) 363-0338
mhallman@mwjournal.com

**Pacific and Mountain Time Zones**
Brian Landy
*Western Reg. Sales Mgr.*
(CA, AZ, OR, WA, ID, NV, UT, NM, CO, WY, MT, ND, SD, NE & Western Canada)
Tel: (831) 426-4143
Cell: (831) 713-9085
blandy@mwjournal.com

**International Sales**
Carl Sheffres
Tel: (781) 619-1949
csheffres@mwjournal.com

**Germany, Austria, and Switzerland (German-speaking)**
Victoria and Norbert Hufmann
victoria@hufmann.info
norbert@hufmann.info

**France**
Gaston Traboulsi
Tel: +44 207 596 8742
gtraboulsi@horizonhouse.com

**Korea**
Jaeho Chinn
JES MEDIA, INC.
Tel: +82 2 481-3411
corres1@jesmedia.com

**China**
*Shanghai*
Linda Li
ACT International
Tel: +86 136 7154 0807
lindal@actintl.com.hk

*Wuhan*
Phoebe Yin
ACT International
Tel: +86 134 7707 0600
phoebey@actintl.com.hk

*Shenzhen*
Annie Liu
ACT International
Tel: +135 9024 6961
*anniel@actintl.com.hk*

*Beijing*
Cecily Bian
ACT International
Tel: +86 135 5262 1310
cecilyb@actintl.com.hk

**Hong Kong**
Floyd Chun
ACT International
Tel: +852 28386298
floydc@actintl.com.hk

**Taiwan, Singapore**
Simon Lee
ACT International
Tel: +852 2838 6298
simonlee@actintl.com.hk

**Japan**
Katsuhiro Ishii
Ace Media Service Inc.
Tel: +81 3 5691 3335
amskatsu@dream.com

**Submitting ad material?**
Visit: www.adshuttle.com/mwj
(866) 774-5784
outside the U.S. call
+1-414-566-6940

Ed Kiessling
(781) 619-1963
ekiessling@mwjournal.com

Corporate Headquarters: 685 Canton Street, Norwood, MA 02062 • Tel: (781) 769-9750

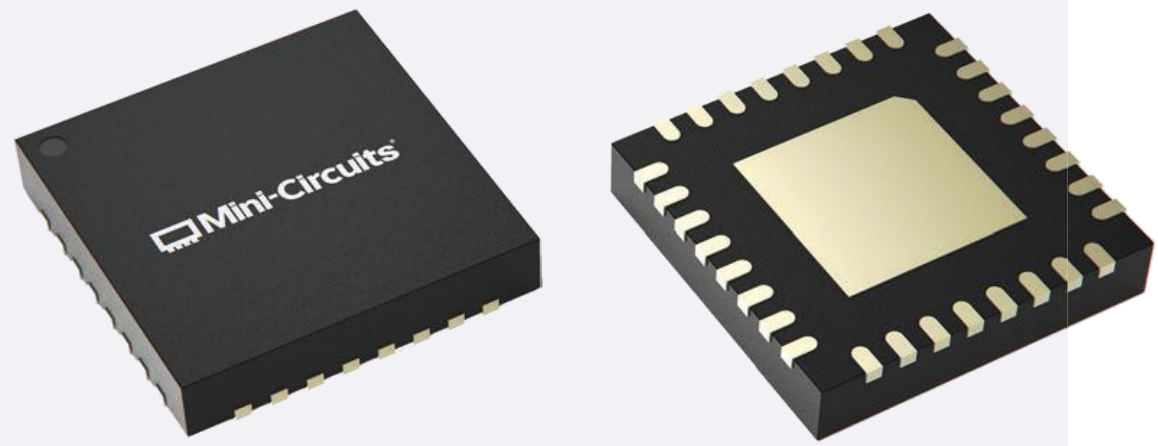
Mini-Circuits

# FABS and LABS

## Infineon IR HiRel Pioneers Advancing Power Management Technologies



International Rectifier (IR) is a well-recognized name in the electronics industry with a legacy of innovation. The company was established in the U.S. in 1947, primarily as a power management technology company. Since the 1950s, what became known as IR HiRel has been a pioneer in power management technology. In 1954, IR HiRel commercialized germanium rectifiers and they created the first silicon-based rectifier in 1959. In 1974, the company developed the first power and Darlington transistors, which used glass passivation. In 1979, IR HiRel introduced the first hexagonal power MOSFET. They followed that development with the first intelligent power integrated circuit in 1983, and in 1987, the company designed the first rad-hard MOSFET.

In 2015, Infineon Technologies acquired IR in a deal that provided synergistic benefits for both companies. Infineon is a global leader in semiconductor technology and acquiring IR allowed it to broaden its product offerings and increase its footprint in high-growth markets, including automotive, industrial and consumer electronics, where power efficiency is a critical factor. IR had made significant investments in GaN and SiC power technologies, so this acquisition positioned Infineon as a leader in wide-bandgap semiconductor materials. From the IR standpoint, they had a significant presence in North America, which helped Infineon, but IR benefited from Infineon's global reach and broader market presence and this gave the IR HiRel products access to new markets.

While the combined company maintains facilities around the world, it operates in several locations across the U.S., with a key manufacturing facility in Leominster, Mass., not too far from the Microwave Journal corporate offices. The Leominster site houses HiRel R&D and Operations with annual production volumes of approximately 300,000 to 500,000 pieces per year. These hermetic devices consist primarily of discrete power products. Because of the unique nature of these devices and the harsh environments they operate in, the facility is certified by the Defense Logistics Agency to meet MIL-PRF-19500/MIL-STD-750, MIL-PRF-38534/MIL-STD-883 and MIL-PRF-38535/MIL-STD-883 quality standards.

In addition to decades of contributions to developing products and advancing the state-of-the-art in power management, IR HiRel is probably best known for their world-leading radiation-hardened power products that have been part of America's quest to explore the universe for over 50 years. Space and other harsh environment applications create challenges for system designers. Electronics in these systems must be able to withstand severe thermal, mechanical and radiation conditions with expected lifespans measured in decades. To meet these challenges, Infineon offers a portfolio of high-reliability, rad-hard memory, power and RF solutions for extreme conditions, such as those found in space, aviation, defense and other extreme environment industries. The portfolio includes secure, rad-hard and high-reliability memories; high-reliability and rad-hard power MOSFETs and ICs; RF and microwave transistors and diodes; rad-hard solid-state relays; space Schottkys and rectifiers; custom high-reliability solutions including die and wafer sales, extreme environment solutions; custom-screened products and RF foundry services.

From their earliest roots in IR as pioneers advancing power management technologies on spacecraft from Voyager 1 to today, IR HiRel and now Infineon power products continue to enable humankind to explore the far reaches of the universe.

**www.infineon.com/hirel**


WERLATONE
THE RIGHT COMBINATION
HI-REL MISSION CRITICAL RADIAL COMBINER SOLUTIONS
HIGH-POWER OPERATION FOR ISM, RADAR, AND EW SYSTEMS
3-WAY TO 32-WAY | VHF THROUGH X-BAND | UP TO 10:1 BANDWIDTH
WERLATONE® HIGH POWER RADIAL COMBINERS AND DIVIDERS ARE READY FOR YOUR ISM, RADAR, AND EW SYSTEMS.
OUR COMBINERS AND DIVIDERS ARE IN-PHASE RADIAL TRANSMISSION LINE STRUCTURES - COMBINING OR DIVIDING IN A SINGLE STAGE AT LOWER LOSSES AND AT POWER LEVELS TO 64 KW CW AND 200 KW PEAK.
OUR CUSTOM COMBINING METHODS ALLOW FOR HIGHER FREQUENCY OPERATION AND EXCELLENT RELIABILITY, WHILE SUPPORTING A SOLID STATE APPROACH.
CUSTOM DESIGNS ARE AVAILABLE
CHECK OUT OUR CATALOG
BRING US YOUR CHALLENGE | WWW.WERLATONE.COM
WERLATONE
LEARN MORE

eXclusive Digital Content

# High-Selectivity SIW Filters with Controllable Transmission Zeros

Qingqing Ye
*Institute of Microelectronics of the Chinese Academy of Sciences, Beijing, China*
*University of the Chinese Academy of Sciences, Beijing, China*

Anmou Liao and Rui Guo
*Institute of Microelectronics of the Chinese Academy of Sciences, Beijing, China*

Zheng Wang and Yongwen Gong
*Beijing Smart-Chip Microelectronics Technology Co. Ltd., Beijing, China*

Chong Li and Juchuan Guo
*State Grid Hebei Marketing Service Center, Shijiazhuang, China*

Substrate integrated waveguide (SIW) filters based on the theory of mixed cross-coupling improve selectivity. With the introduction of slots on the top metal plane of two adjacent SIW cavities, electric coupling (EC) and magnetic coupling (MC) can be separately controlled by adjusting the slot widths and the inductive window, producing a controllable transmission zero above or below the passband. High-selectivity filters with multiple controllable transmission zeros (TZs) can be implemented by cascading the structure or combining it with a coplanar waveguide (CPW). Three prototypes have been designed, fabricated and measured. Measurements verify the predicted selectivity.

SIW technology is widely used in microwave and mmWave circuits for 5G and beyond 5G communications, automotive radars and satellite systems.[1] SIW antennas, bandpass filters (BPFs) and multiplexers, as indispensable constituent modules, are designed for these systems. SIW BPFs are attractive for their characteristic low loss, low radiation, high-quality factor and high power-handling capability.[2] Over the past two decades, much work has been done to improve SIW filter tunability, ultra-wide bandwidth performance, wide stopband performance and selectivity.[3-9]

Elliptic or quasi-elliptic filters achieve good selectivity, which enables superior filtering characteristics. The synthesis of elliptic filtering functions can introduce finite TZs by providing multiple coupling paths between nonadjacent resonators, which generates different phase shifts. Common methods to realize elliptic or quasi-elliptic filters are bypass coupling, cross-coupling and source-load coupling. Filters employing bypass coupling are restricted to inline topologies.[10] Cross-coupling produces phase shift differences via EC with open slots[11] or S-shaped slots.[12,13] However, these structures reduce the surface current of the TE10 mode, which causes high radiation losses and degrades the quality factor. Source-load coupling can be unrealizable in some structures and it degrades isolation between the ports as well.

Mixed coupling, in which EC and MC coexist, provides an effective choice for the design of quasi-elliptic filters because it can also achieve dual-coupling paths to produce TZs controlled by adjusting the mixed-coupling coefficients between two adjacent resonators. Mixed coupling has been used in filter design, including open-loop structures and rectangular waveguides.[14] It has emerged in SIW filter structures in recent years. For a multilayer structure, however, etching slots

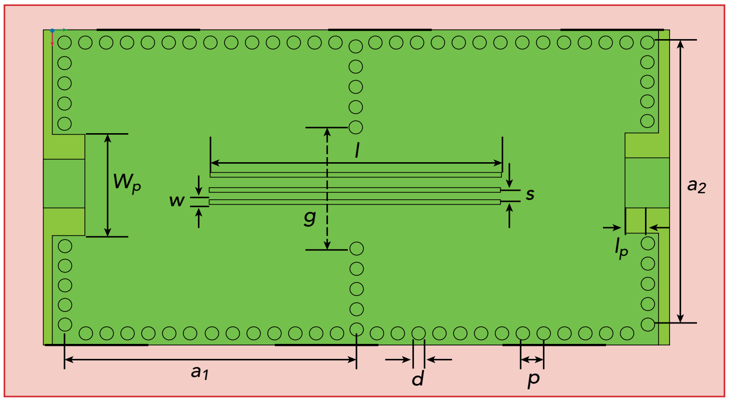


**Fig. 1** SIW filter structure with mixed coupling.

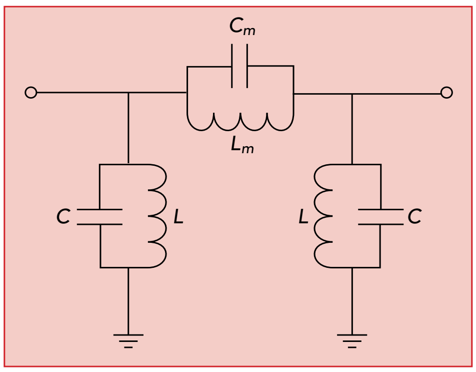


**Fig. 2** Mixed coupling equivalent circuit.

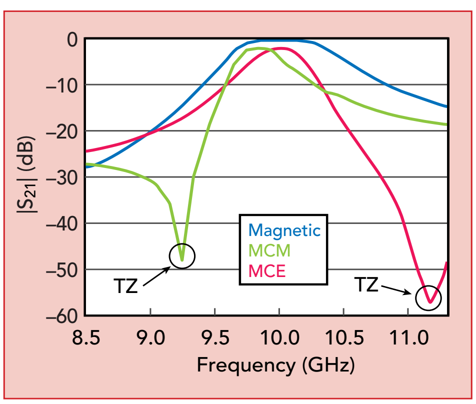


**Fig. 3** Responses of mixed and magnetic coupling structures.

introduce significant radiation losses, degrade structural shielding and reduce the quality factor.[15,16]

To solve these problems, new types of multiple TZ SIW filters with controllable mixed EC and MC are introduced in this work. First, a quasi-elliptic filter is designed using mixed coupling to realize high selectivity. Two more filters are then introduced that combine a mixed-coupling structure with CPW. It is shown that the TZs can be controlled and located below and above the passband corresponding to MC or EC dominance, which increases design flexibility. Prototype filters are designed, simulated and fabricated. Measured results show good agreement with the simulation. The filters exhibit good selectivity, are low-cost and are easy to fabricate and integrate with other planar circuits.

## MODELING AND SIMULATION

### Mixed Coupling

***Figure 1*** shows the structure of a mixed-coupling filter. It consists of two parts: the first is a second-order SIW filter producing MC with an inductive window and the second part introduces EC by etching three slot lines on the top metal plane. MC is controlled by adjusting the width of the inductive window, *g*, while the width of slots, *w*, the length of slots, *l*, and the distance between slots, *s*, determine EC strength. Therefore, mixed coupling is created by coexistent EC and MC. The equivalent mixed-coupling circuit is shown in ***Figure 2***.

In addition, like the CPW filter described by Su et al.,[17] the three slots almost do not have an open end perpendicular to the direction of the surface current of the TE101 mode. There is little radiation loss and no degradation of the structural shielding or quality factor.

Now, the coupling mechanism can be explored. The mixed-coupling coefficient, *k*, can be extracted as shown in ***Equation 1***:

$$k = \frac{\omega_{odd}^2 - \omega_{even}^2}{\omega_{odd}^2 + \omega_{even}^2} = \frac{M_c - E_c}{1 - M_c E_c}$$

$$M_c = \frac{L_m}{L}; E_c = \frac{C}{C_m} \qquad (1)$$

Where $\omega_{odd}$ and $\omega_{even}$ represent the odd-mode and even-mode resonant frequencies and $M_c$ and $E_c$ are the coefficients of MC and EC, respectively.

The relationship between the resonant frequency, $\omega_0 = (LC)^{-1/2}$ and the TZ frequency, $\omega_m = (L_m C_m)^{-1/2}$, is shown in ***Equation 2***:

$$\frac{\omega_m}{\omega_0} = \sqrt{\frac{E_c}{M_c}} \qquad (2)$$

When MC is dominant, $\omega_{odd} > \omega_{even}$, the coefficient *k* can be calculated from Equation 1 and $k > 0$. When EC is dominant, $\omega_{odd}$ has a lower resonant frequency than $\omega_{even}$ and $k < 0$. The specific values of $M_c$ and $E_c$ can be extracted by combining Equations 1 and 2.

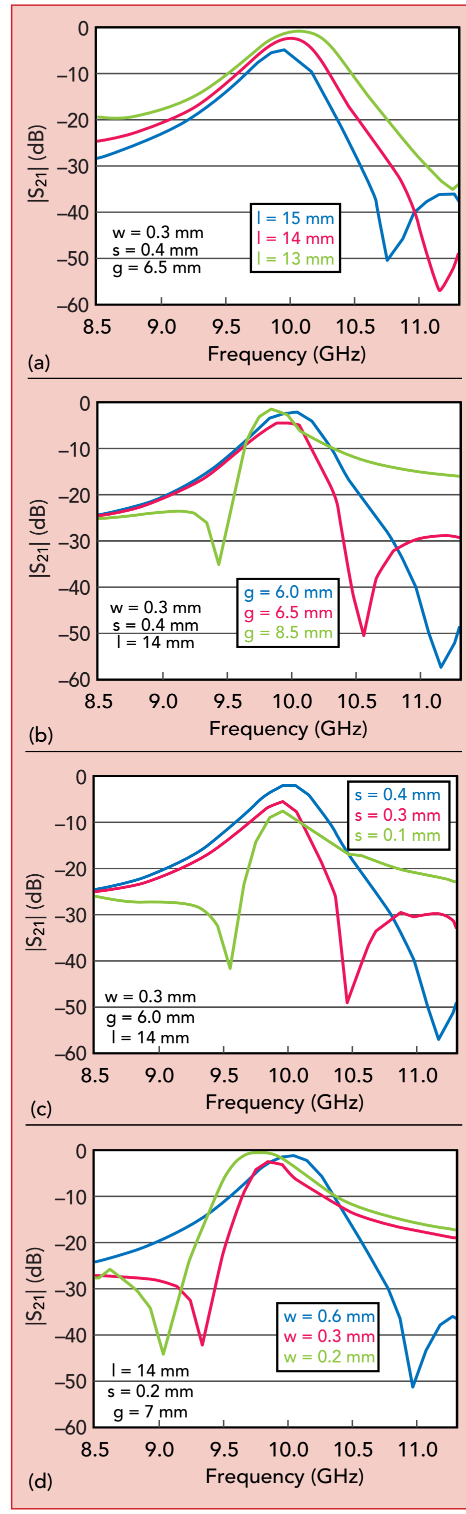


**Fig. 4** Response of the mixed-coupling structure with *g* (a), *l* (b), *s* (c) and *w* (d).

The responses of the mixed-coupling structure and traditional magnetic structure are plotted in ***Figure 3***. Compared with the traditional MC structure, a TZ can be produced in the

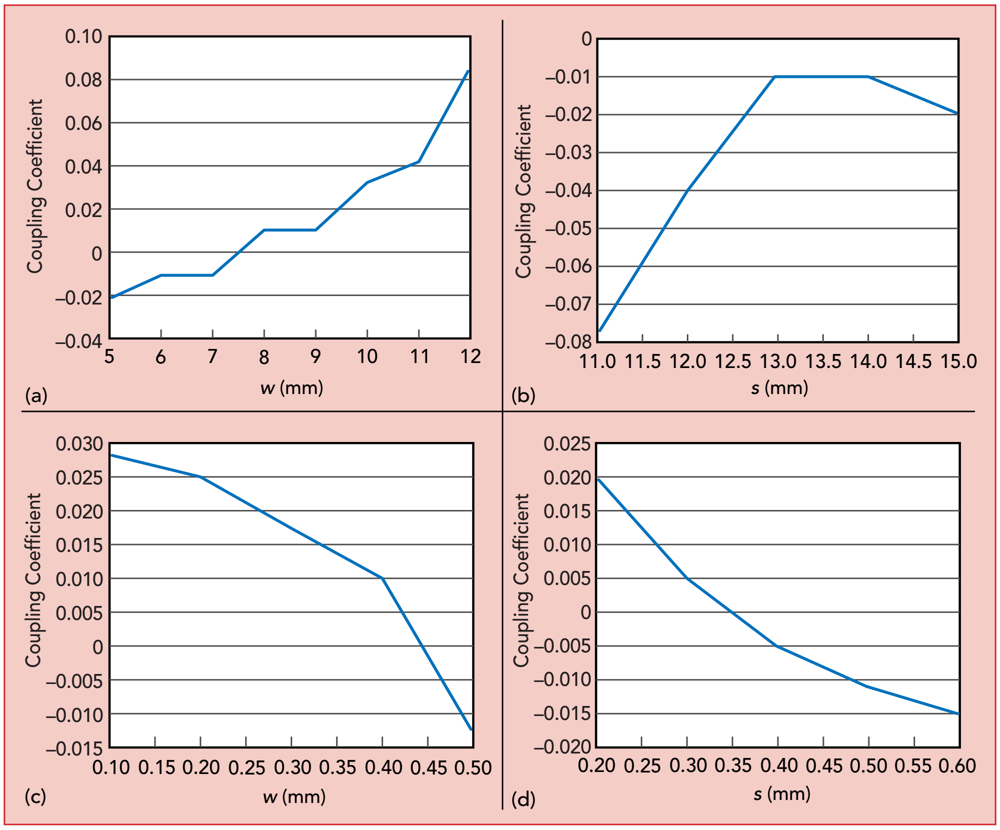


▲ Fig. 5 Coupling coefficient of the mixed coupling structure as a function of *g* (a), *l* (b), *s* (c) and *w* (d).

lower band when MC dominates the mixed coupling (MCM) and a TZ can be created in the upper band when EC dominates the mixed coupling (MCE).

***Figures 4a*** to ***4d*** show how the response of the mixed-coupling structure varies with *g*, *l*, *s* and *w*. The dominance of the mixed coupling (MCM or MCE) and the TZ can be controlled by adjusting these parameters. When *g* is varied from 6 to 8.5, MCE changes to MCM and the TZ moves from the upper band to the lower band, as shown in Figure 4a. Figure 4b shows that *l* does not affect the dominant coupling mechanism but changes the TZ location; a longer *l* corresponds with a lower ω*m*. Slot width, *w*, also controls the coupling, as shown in Figure 4c. When *w* is a small value, MC is dominant; however, when *w* increases to 0.6, EC dominates. As shown in Figure 4d, as the distance between slots, *s*, varies from 0.1 to 0.4, coupling changes from MCM to MCE.

## Filter Design

The coupling coefficient, *k*, of the mixed-coupling structure, is extracted from ***Figure 5***. EC is dominant when $k < 0$, while $k > 0$ represents MC being dominant. The parameters *g*, *l*, *s* and *w* affect the value of *k*, with the trends shown in Figure 4. Figure 5 determines the initial filter size.

***Figure 6*** shows the extracted values of the external quality factor, $Q_e$, versus the physical dimensions, $w_p$ and $l_p$. It can be observed that $Q_e$ gradually decreases as $w_p$ and $l_p$ increase.

Based on the mixed-coupling structure, an inline quasi-elliptic filter with high selectivity is chosen for prototyping. This is shown in ***Figure 7***. The cascade of an MCM and an MCE produces two TZs, one in the upper band and the other in the lower band.

Two high-selectivity filters with multiple TZs, as shown in ***Figure 8***, are also fabricated. The mixed-coupling structure is combined with CPW to form a hybrid structure. There are three TZs in the upper band when EC is dominant. When

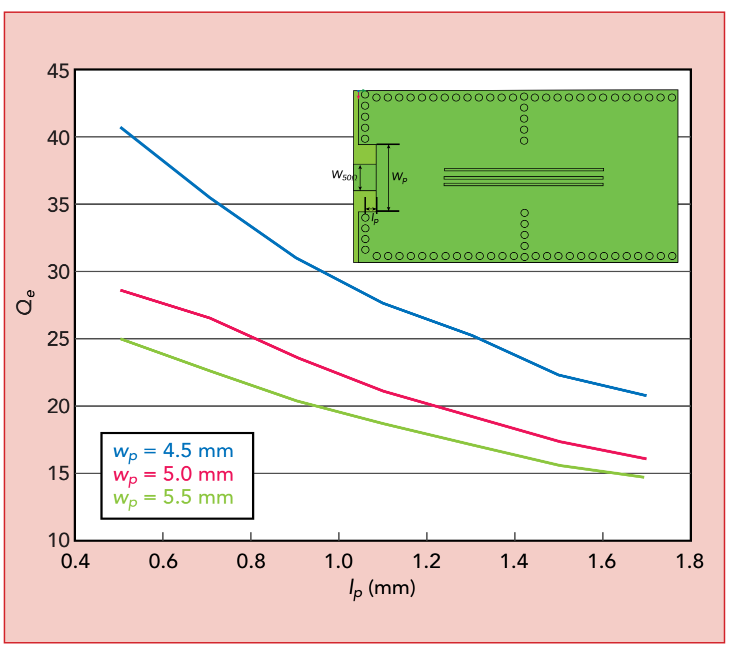


▲ Fig. 6 External quality factor $Q_e$ versus $w_p$ and $l_p$.

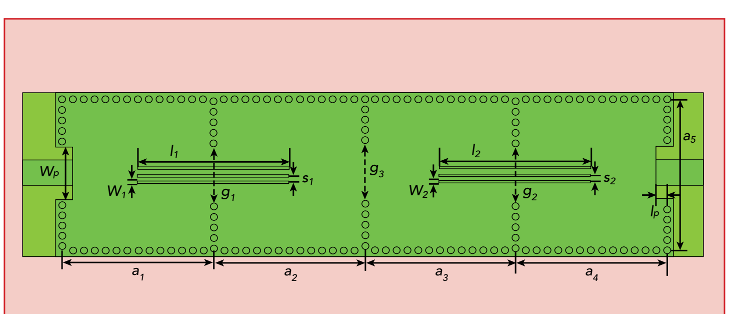

▲ Fig. 7 Inline quasi-elliptic filter based on mixed coupling.

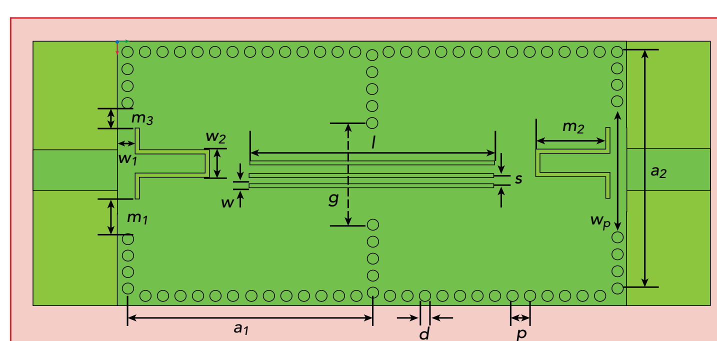

▲ Fig. 8 Multiple transmission zeros filter based on mixed coupling.

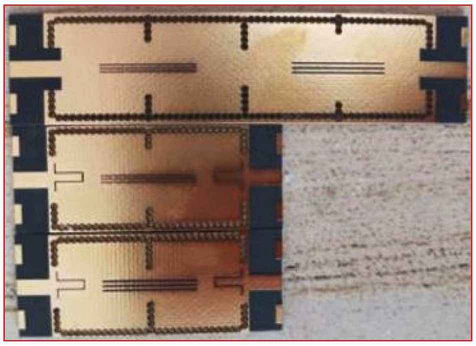

Fig. 9 Photograph of the prototype mixed-coupling filters.

## TABLE 1
### QUASI-ELLIPTICAL FILTER DIMENSIONS

| Parameter | Value (mm) | Parameter | Value (mm) |
|---|---|---|---|
| $\alpha_1$ | 14 | $g_3$ | 6.331 |
| $\alpha_2$ | 14 | $w_1/w_2$ | 0.2/0.3 |
| $\alpha_3$ | 14 | $g_1/g_2$ | 8.796/11.25 |
| $\alpha_4$ | 14 | $l_1/l_2$ | 14/14 |
| $\alpha_5$ | 14.5 | $s_1/s_2$ | 0.3/0.4 |
| $l_p$ | 1.5 | $d$ | 0.6 |
| $w$ | 6.265 | $p$ | 1 |

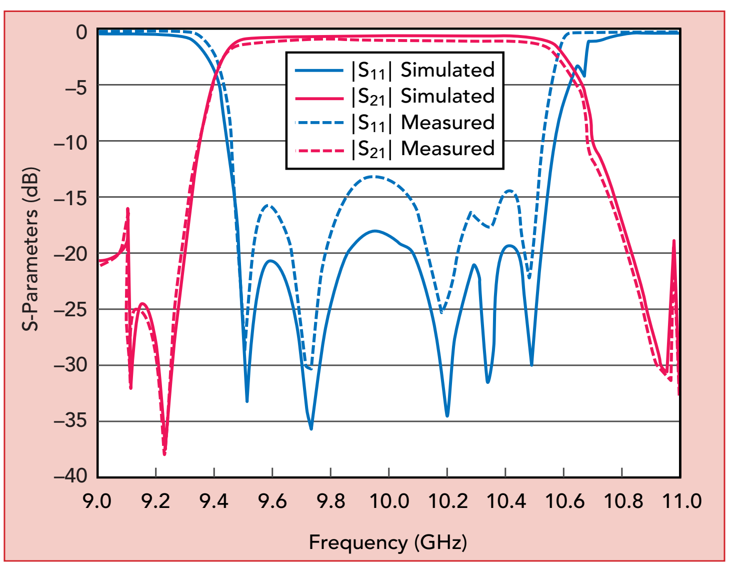


Fig. 10 S-parameters of the quasi-elliptic filter.

## TABLE 2
### MULTIPLE TRANSMISSION FILTERS (MCM/MCE) DIMENSIONS

| Parameter | Value (mm) MCM/MCE | Parameter | Value (mm) MCM/MCE |
|---|---|---|---|
| $m_1$ | 4.88/4.88 | $g$ | 7/6 |
| $m_2$ | 4/4 | $l$ | 14/14 |
| $m_3$ | 1.5475/1.8958 | $s$ | 0.3/0.4 |
| $w_1$ | 1/1 | $\alpha_2$ | 14.5/14.5 |
| $w$ | 6.9092/6.22685 | $\alpha_1$ | 14/14 |
| $w_2$ | 1.54/1.54 | $d$ | 0.6/0.6 |
| $w$ | 0.2/0.3 | $p$ | 1/1 |

the MC is dominant, one TZ is in the lower band and two TZs are in the upper band.

## MEASUREMENTS

The filters are fabricated on 0.787 mm Rogers RT/duroid 5880 with εr = 2.2 and tanδ = 0.0009. These are shown in ***Figure 9***. The dimensions of the quasi-elliptic filter are listed in ***Table 1***. Measurements are performed with an Agilent N5227A network analyzer and an Anritsu test fixture.

Measured results agree closely with the simulation as shown in ***Figure 10***. The center frequency is 9.9 GHz with a fractional bandwidth of 11 percent and zeros at 9.2 and 10.9 GHz. The measured insertion loss is about 1.2 dB.

The dimensions of the high-selectivity filters with multiple TZs are listed in ***Table 2***. Measured results are shown in ***Figure 11*** (for the MCE) and ***Figure 12*** (for the MCM). The MCE filter produces three TZs in the upper stopband and provides good selectivity. The center frequency is 9.7 GHz with a fractional bandwidth of 8 percent and three zeros at 10.5, 10.7 and 10.9 GHz. The measured insertion loss is about 1.1 dB. The MCM filter has a controllable TZ at 9.4 GHz and two additional TZs at 10.6 and 10.8 GHz. The center frequency is 9.8 GHz, and the fractional bandwidth is 8 percent. The measured insertion loss is about 1.1 dB.

Compared to other similar work shown in ***Table 3***, the proposed three filters have good characteristics with greater flexibility. The quasi-elliptic filter, which has almost no radiation loss, does not degrade structural shielding or the quality factor. The MCE and MCM filters further increase the number of TZs, which can be controlled by adjusting the mixed coupling. Design flexibility and selectivity are improved. As inline structures, these filters can all be used as universal SIW filter modules to realize high selectivity.

## CONCLUSION

Three high-selectivity filters are designed based on a mixed-coupling structure. The center frequency of the quasi-elliptic filter is 9.9 GHz with a fractional bandwidth of 11 percent and two TZs at 9.2 and 10.9 GHz. The measured insertion loss is about 1.2 dB. Compared with traditional Chebyshev filters, it exhibits improved selectivity. The center frequency of the MCE filter is 9.7 GHz with a fractional bandwidth of 8 percent and three zeros at 10.5, 10.7 and 10.9 GHz. The measured insertion loss is about 1.1 dB. It produces three TZs in the upper stopband for improved selectivity. The MCM filter also demonstrates high selectivity with a controllable TZ at 9.4 GHz and another two TZs at 10.6 and 10.8 GHz. Its center frequency is 9.8 GHz with a fractional bandwidth of 8 percent. The measured insertion loss is about 1.1 dB. The proposed filters are suitable for integration with other planar RF components due to their compact sizes, good selectivity, low-cost and ease of fabrication. ■

## ACKNOWLEDGMENTS

This work is supported by the STATE GRID Corporation of China for the project, "Research on Electromagnetic Wave Power Sensor Chip for Active Warning Function of Secondary Equipment in Power Grid," (No. 5700-202341262A-1-1-ZN).

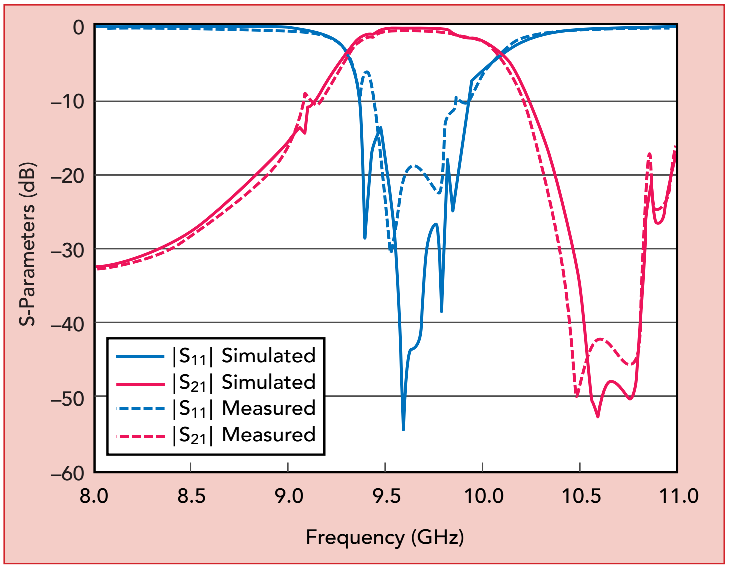


**Fig. 11** S-parameters of the MCE multiple transmission zeros filter.

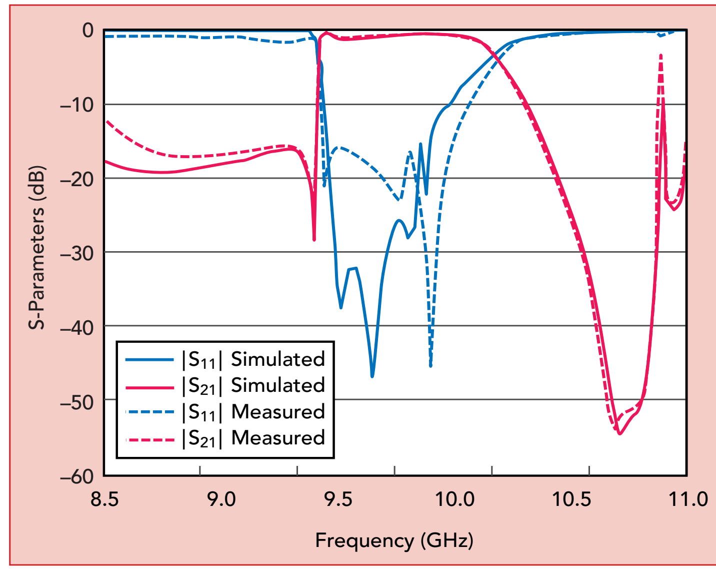


**Fig. 12** S-parameters of the MCM multiple transmission zeros filter.

## References


1. K. Wu, M. Bozzi and N. J. G. Fonseca, "Substrate Integrated Transmission Lines: Review and Applications," *IEEE Journal of Microwaves*, Vol. 1, No. 1, January 2021, pp. 345–363.
2. M. Bozzi, A. Georgiadis and K. Wu, "Review of Substrate-Integrated Waveguide Circuits and Antennas," *IET Microwaves, Antennas & Propagation*, Vol. 5, No. 8, June 2011, pp. 909—920.
3. E. M. Messaoudi, J. D. M. Perez and V. E. Boria, "Compact Substrate Integrated Waveguide Wideband Bandpass Filter with Post-Manufacturing Tuning Capabilities," *IEEE Access*, Vol. 11, January 2023, pp. 2327–2341.
4. A. Augustine and K. J. Vinoy, "A Wideband Substrate Integrated Waveguide Bandpass Filter for 5G Millimeter Wave Transceiver," *IEEE Microwaves, Antennas and Propagation Conference*, December 2022.
5. P. Chu, J. Feng, L. Guo, L. Zhang, W. -W. Yang, L. Liu, F. Xu and K. Wu, "Using Mixed Coupling to Realize Wide Stopband Multilayer Substrate Integrated Waveguide Filter," *IEEE Transactions on Circuits and Systems II: Express Briefs*, Vol. 70, No. 8, August 2023, pp. 2744–2748.
6. Y. Zhu and Y. Dong, "A Novel Compact Wide-Stopband Filter with Hybrid Structure by Combining SIW and Microstrip Technologies," *IEEE Microwave and Wireless Components Letters*, Vol. 31, No. 7, July 2021, pp. 841–844.
7. X. Liu, Y. Liu, T. Zhang, Q. Lu and Z. Zhu, "Substrate-Integrated Waveguide Band-Pass Filter and Diplexer with Controllable Transmission Zeros and Wide-Stopband," *IEEE Transactions on Circuits and Systems II: Express Briefs*, Vol. 70, No. 2, February 2023, pp. 526–530.
8. X. Liu, N. Liu, C. Fan, Y. Liu, Y. Yang and Z. Zhu, "SIW Bandpass Filter with Wide Stopband Using Harmonic Interleaving and Orthogonal Transmission Techniques," *IEEE Transactions on Components, Packaging and Manufacturing Technology*, Vol. 12, No. 11, November 2022, pp. 1841–1848.
9. F. Zhu, Y. Wu, P. Chu, G. Q. Luo and K. Wu, "Single-Layer Substrate-Integrated Waveguide Inline Filters with Flexible Transmission Zeros," *IEEE Microwave and Wireless Components Letters*, Vol. 32, No. 6, June 2022, pp. 495–498.
10. S. -W. Wong, R. -S. Chen, J. -Y. Lin, L. Zhu and Q. -X. Chu, "Substrate Integrated Waveguide Quasi-Elliptic Filter Using Slot-Coupled and Microstrip-Line Cross-Coupled Structures," *IEEE Transactions on Components*, Packaging and Manufacturing Technology, Vol. 6, No. 12, December 2016, pp. 1881–1888.
11. S. Sirci, J. D. Martinez, J. Vague and V. E. Boria, "Substrate Integrated Waveguide Diplexer Based on Circular Triplet Combline Filters," *IEEE Microwave and Wireless Components Letters*, Vol. 25, No. 7, July 2015, pp. 430–432.
12. L. Szydlowski, A. Jedrzejewski and M. Mrozowski, "A Trisection Filter Design with Negative Slope of Frequency-Dependent Crosscoupling Implemented in Substrate Integrated Waveguide (SIW)," *IEEE Microwave and Wireless Components Letters*, Vol. 23, No. 9, September 2013, pp. 456–458.
13. Y. Uemichi, O. Nukaga, K. Nakamura, Y. Hasegawa, X. Han, R. Hosono, K. Kobayashi and N. Guan, "A 60-GHz Six-Pole Quasi-Elliptic Bandpass Filter with Novel Feeding Mechanisms Based on Silica-Based Post-Wall Waveguide," *IEEE MTT-S International Microwave Symposium*, June 2017.
14. K. Ma, J. -G. Ma, K. S. Yeo and M. A. Do, "A Compact Size Coupling Controllable Filter with Separate Electric and Magnetic Coupling Paths," *IEEE Transactions on Microwave Theory and Techniques*, Vol. 54, No. 3, March 2006, pp. 1113–1119.
15. A. Iqbal, J. J. Tiang, C. K. Lee and B. M. Lee, "Tunable Substrate Integrated Waveguide Diplexer with High Isolation and Wide Stopband," *IEEE Microwave and Wireless Components Letters*, Vol. 29, No. 7, July 2019, pp. 456–458.
16. Z. L. Su, B. W. Xu, S. Y. Zheng, H. W. Liu and Y. L. Long, "High Isolation and Wide-Stopband SIW Diplexer Using Mixed Electric and Magnetic Coupling," *IEEE Transactions on Circuits and Systems II: Express Briefs*, Vol. 67, No. 1, January 2020, pp. 32–36.
17. P. Chu, J. Feng, L. Guo, L. Zhang, F. Zhu, L. Liu, G. Q. Luo and K Wu, "Substrate Integrated Waveguide Filter with Flexible Mixed Coupling," *IEEE Transactions on Microwave Theory and Techniques*, Vol. 71, No. 9, September 2023, pp. 4003–4011.
18. W. Shen, W. -Y. Yin, X. -W. Sun and J. -F. Mao, "Compact Coplanar Waveguide-Incorporated Substrate Integrated Waveguide (SIW) Filter," *Journal of Electromagnetic Waves and Applications*, Vol. 24, No. 7, May 2010, pp. 871–879.
19. Y. Zheng, Y. Zhu, Z. Wang and Y. Dong, "Compact, Wide Stopband, Shielded Hybrid Filter Based on Quarter-Mode Substrate Integrated Waveguide and Microstrip Line Resonators," *IEEE Microwave and Wireless Components Letters*, Vol. 31, No. 3, March 2021, pp. 245–247.
20. Y. Zhu and Y. Dong, "A Compact Dual-Band Quasi-Elliptic Filter Based on Hybrid SIW and Microstrip Technologies," *IEEE Transactions on Circuits and Systems II: Express Briefs*, Vol. 69, No. 3, March 2022, pp. 719–723.
21. G. Lin and Y. Dong, "A Compact, Hybrid SIW Filter with Controllable Transmission Zeros and High Selectivity," *IEEE Transactions on Circuits and Systems II: Express Briefs, Vol. 69, No. 4, April 2022, pp. 2051–2055.*


**TABLE 3**

**COMPARISON WITH OTHER WORK**

| Reference | f (GHz), FBW (%) | IL (dB), Order | TZs Below, Above f | Single Layer | Degrade $Q_e$ | Inline |
|---|---|---|---|---|---|---|
| 15 | 10.5, 3.7 | 1.3, 2 | 0, 1 | × | × | √ |
| 16 | 9.5, 3.2 | 2.6, 2 | 0, 1 | × | × | √ |
| 18 | 5.2, 5.8 | 2.1, 3 | 0, 1 | √ | × | √ |
| 19 | 10, 22.7 | 1.2, 4 | 1, 1 | √ | √ | × |
| 20 | 8, 8.8 | 1.8, 4 | 1, 1 | √ | √ | × |
| 21 | 11.5, 6.8 | 1.4, 4 | 1, 1 | √ | √ | × |
| Quasi-elliptic | 9.9, 11 | 1.2, 4 | 1, 1 | √ | × | √ |
| MCE | 9.7, 8 | 1.1, 4 | 0, 3 | √ | √ | √ |
| MCM | 9.8, 8 | 1.1, 4 | 1, 2 | √ | √ | √ |

eXclusive Digital Content >>>

REVIEW BOARD MWJ APPROVED

# Slotline Radial Stubs Improve the Bandwidth of Balun Bandpass Filters

Yubo Wang, Mi Lin and Guohua Liu
*School of Electronics and Information, Hangzhou Dianzi University, Hangzhou, China*

The bandwidth of an ultra-wideband, high-selectivity balun bandpass filter (BPF) is improved by using slotline radial stubs. At the same time, selectivity is enhanced with a short-circuit microstrip stub at the input port. The center frequency of the design is 7.93 GHz with a relative bandwidth of 131 percent. Phase imbalance (PI) within the passband is less than 180 ± 5 degrees, with amplitude flatness better than 0.5 dB. Transmission zero depth at the cutoff frequency is less than -40 dB.

Balun BPFs can achieve balanced-to-unbalanced conversion and filtering functions while meeting miniaturization requirements. Balun BPFs are widely used in RF communication systems. They find use in components like antennas[1] and push-pull power amplifiers.[2] To be useful in multiple applications, the bandwidth of these devices is usually designed to be very broad.

In recent years, various broadband and ultra-wideband balun filters have been proposed. A branch-line broadband balun BPF was designed by introducing a quarter-wavelength shorted stub at one of its output ports.[3] A branch-line balun based on an entirely artificial fractal-shaped composite right/left-handed transmission line (CRLH TL) further improved bandwidth.[4]

Balun BPFs designed with slotline-microstrip composite structures can maintain excellent phase and amplitude balance over a wide passband. Tseng and Hsiao[5] showed that a broadband Marchand balun based on slot-coupled microstrip lines can improve bandwidth by enhancing the coupling coefficient of the top and bottom quarter-wavelength coupling lines.[5] Chen et al.[6] demonstrated a wideband balun filter based on a triple-mode slotline resonator with controllable bandwidth.

A compact wideband filtering balun based on stacked composite resonators can reduce the size of a balun filter while expanding its bandwidth.[7] However, expanding the bandwidth often decreases selectivity. A new slotline-to-microstrip transition dual-mode balun BPF has been proposed to improve balun BPF selectivity by changing the resonant structure and generating four transmission zeros outside the passband.[8] However, this structure cannot be designed for wideband balun BPFs.

To achieve the wide bandwidth and high selectivity, Zeng et al.[9] proposed a dual-band balun filter. This filter is based on a novel slotline multi-mode, T-line-loaded, middle-shorted, complementary split-ring resonator (TLMS-CSRR). Coupled with τ-shaped and

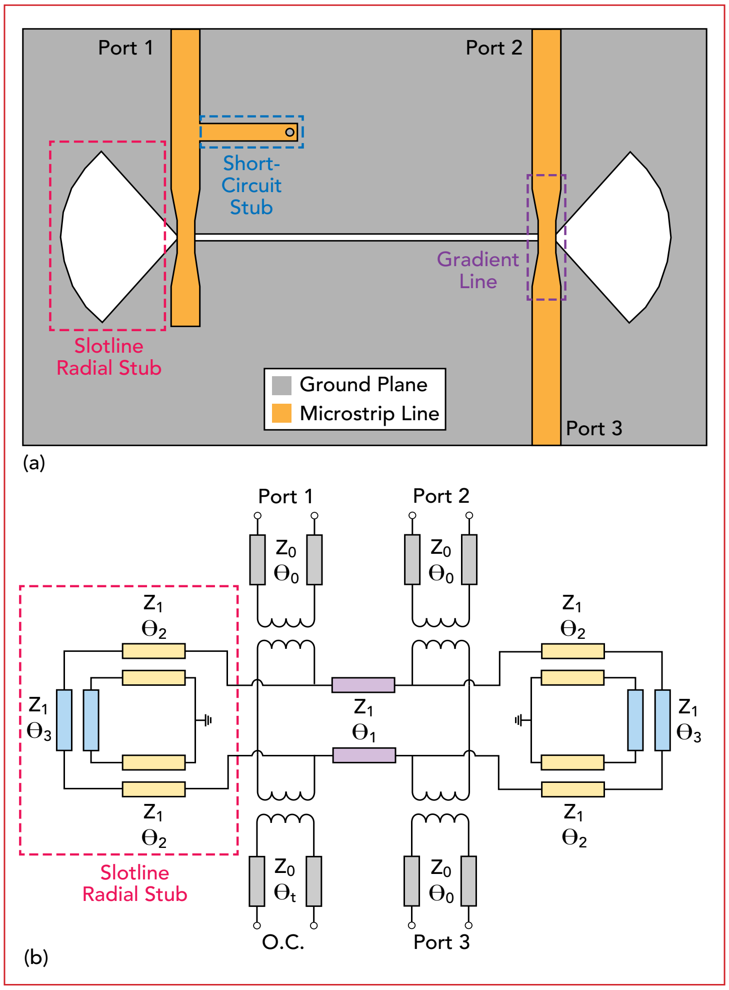


Fig. 1 UWB balun BPF circuit configuration (a) and equivalent circuit schematic (b).

π-shaped slotline stubs as the input and output microstrip-slotline transition structures, respectively, designers have realized devices with high rejection between two passbands and at harmonic frequencies.

Uniplanar, wideband, high-selectivity, full-band isolation baluns using two different types of out-of-phase matching phase shifters were also proposed by Wang et al.[10] To obtain high selectivity, half-wavelength open-circuit stubs were introduced. However, there is still room for improving selectivity and expanding the bandwidth.

In this work, slotline radial stubs are used to achieve ultra-wide bandwidth and high selectivity with an impedance transformation and an input short-circuit stub for matching. First, the slotline radial stub structure is analyzed. Its equivalent is approximated as a short-circuit stub, which simplifies the calculation when analyzing the frequency response. Five transmission poles (TPs) are designed within the passband to improve transmission performance. Then, the matching circuit is designed and optimized with an impedance transformation of a short-circuit stub. In addition, a short-circuit stub of appropriate length generates a transmission zero at the cutoff frequency, which improves balun selectivity. Finally, the design is verified through prototype testing.

## ANALYSIS AND DESIGN

The design employs a slotline radial stub structure, as shown in ***Figure 1a***. This enhances the filter's resonance depth and reduces insertion loss while expanding the bandwidth. The slotline radial stub structure is equivalent to cascading terminally-grounded transmission lines. The coupling between microstrip and slotline is comparable to a transformer with the circuit diagram shown in ***Figure 1b***.[11]

### Slotline Radial Stub Analysis

The slotline radial stub in Figure 1b is represented by a two-port network. The cascading connection of the three sections forming the stub is shown in ***Figure 2a***. The four ports are defined as $P_1$ through $P_4$ for subsequent analysis. The ABCD matrix of the transmission lines is given by ***Equation 1***:

$$M_i = \begin{bmatrix} \cos\theta_i & jZ_1\sin\theta_i \\ \dfrac{j\sin\theta_i}{Z_1} & \cos\theta_i \end{bmatrix} \quad i = 2,3 \qquad (1)$$

Then, the ABCD matrix of the cascaded two-port network is shown in ***Equation 2***:

$$\begin{bmatrix} A & B \\ C & D \end{bmatrix} = M_2 M_3 M_2 = \qquad (2)$$

$$\begin{bmatrix} \cos(2\theta_2+\theta_3) & jZ_1\sin(2\theta_2+\theta_3) \\ \dfrac{j\sin(2\theta_2+\theta_3)}{Z_1} & \cos(2\theta_2+\theta_3) \end{bmatrix}$$

As shown in ***Figure 2b***, $P_3$ and $P_4$ in Figure 2a are grounded together. The current and voltage expressions of the two-port network shown in Figure 2b are described in ***Equation 3*** and ***Equation 4***:

$$V_1 = AV_2 - BI_2 \qquad (3)$$

$$I_1 = CV_2 - DI_2 \qquad (4)$$

The ideal transmission line has no loss. This means the input current, $I_1$, of $P_1$ and the output current, $I_2$, of $P_2$ are equal in magnitude ($I_1 = -I_2$). Therefore, the current and voltage relationship between $P_1$ and $P_2$ is shown in ***Figure 2c***. The current is $I_1$ and the voltage is the difference between $V_1$ and $V_2$. The equivalent impedance is described in ***Equation 5***:

$$Z_r = \frac{V_1 - V_2}{I_1} \qquad (5)$$

Combining Equations 3, 4 and 5 yields the expression in ***Equation 6***:

$$Z_r = \frac{(A-1)(1-D)}{C} + B \qquad (6)$$

Substituting $A$, $B$, $C$ and $D$ from Equation 2 into Equation 6 yields the equivalent impedance of the slotline radial stub, as shown in

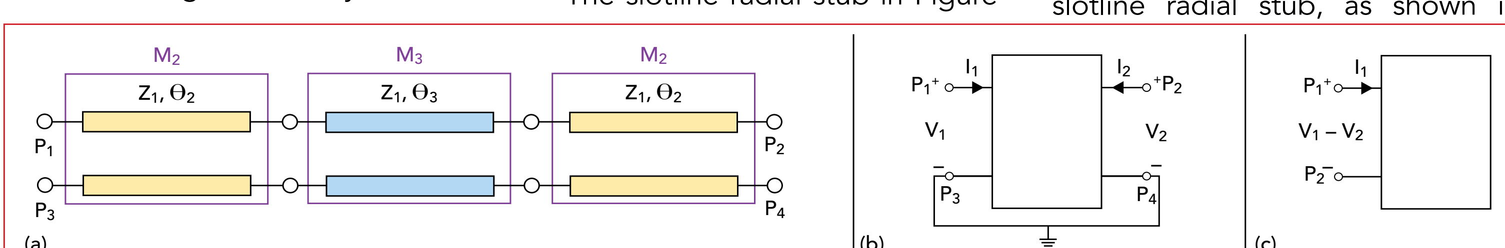


Fig. 2 Slotline radial stub (a), two-port network (b), and current/voltage relationship between $P_1$ and $P_2$ (c).

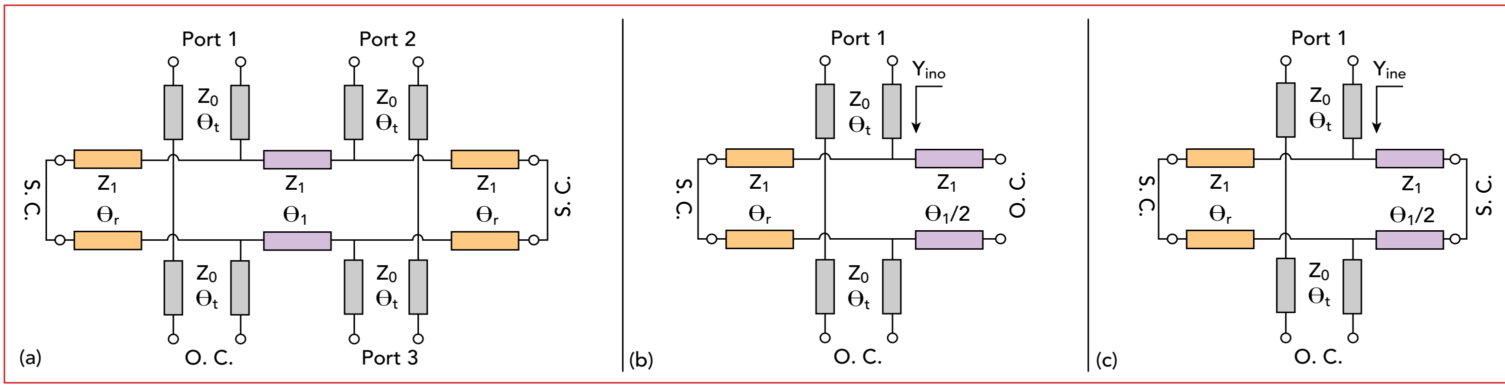


Fig. 3 Simplified transmission line equivalent circuit (a), odd-mode equivalent circuit (b), and even-mode equivalent circuit (c).

***Equation 7***:

$$Z_r = j2Z_1 \tan\theta_r \quad (7)$$

Where: $\theta_r$ is described in ***Equation 8***:

$$\theta_r = \frac{2\theta_2 + \theta_3}{2} \quad (8)$$

Equation 7 implies that the slotline radial stub is equivalent to a short-circuit transmission line with an electrical length of $\theta_r$ and characteristic impedance $2Z_1$ when conducting frequency response analysis. This equivalence simplifies the analysis.

### Ultra-Wideband Balun BPF Frequency Response

For a simple and concise synthesis procedure, the transformer can be treated as a short circuit.[12] ***Figure 3a*** shows a simplified equivalent circuit of the ultra-wideband balun BPF. Since the change of the input and output electrical lengths, $\theta_0$, does not affect the frequency response, let $\theta_0 = \theta_t$. The equivalent circuit is symmetric, so it can be further simplified using even-odd mode analysis. The odd mode impedance of the circuit is shown in ***Figure 3b*** and described in ***Equation 9***:

$$Z_{ino} = jZ_0 \frac{k + \left(\tan\frac{\theta_1}{2} - \frac{\cot\theta_r}{2}\right)(\cot\theta_t - \tan\theta_t)}{2\left(\tan\frac{\theta_1}{2} - \frac{\cot\theta_r}{2}\right) + k\tan\theta_t} \quad (9)$$

The even mode impedance of the circuit shown in ***Figure 3c*** is described in ***Equation 10*** as:

$$Z_{ine} = jZ_0 \frac{-k + \left(\cot\frac{\theta_1}{2} + \frac{\cot\theta_r}{2}\right)(\cot\theta_t - \tan\theta_t)}{2\left(\cot\frac{\theta_1}{2} + \frac{\cot\theta_r}{2}\right) - k\tan\theta_t} \quad (10)$$

Where: $k$ is described in ***Equation 11*** as:

$$k = \frac{Z_1}{Z_0} \quad (11)$$

Based on Equations 9 and 10, $S_{11}$ of the equivalent circuit of Figure 3a can be expressed as shown in ***Equation 12***:

$$S_{11} = \frac{Z_{ine}Z_{ino} - Z_0^2}{(Z_{ine} + Z_0)(Z_{ino} + Z_0)} \quad (12)$$

Five TPs are placed within the passband to ensure low transmission loss. ***Figure 4*** compares the calculated and simulated S-parameters. Five TPs are generated within the ultra-wideband range.

### Improving the Transmission Performance and Selectivity

The previous section simplifies the slotline radial stub, treating it as a short-circuit stub for ease of analysis. However, the slotline radial stub structure offers more flexibility. It allows adjustments of $\theta_2$ and $\theta_3$ to achieve better performance in combination with an impedance transformation and input open-circuit stub.

Full-wave electromagnetic field simulations of the ultra-wideband balun BPF with different configurations are shown in ***Figure 5***. Configuration A is the slotline-microstrip line structure without the radial stubs. $TP_3$ is not excited effectively and the resonance depths of the other TPs are shallow. Configuration B adds slotline radial stubs. $TP_4$ is excited, but the other TPs are not adequately excited. In Configuration C, an impedance transformation is added and a gradient line is used for the connection. The TPs are weakly excited. Configuration D represents the final design with the addition of an open-circuit stub. In this design, all five TPs are strongly excited. The introduction of an input open-circuit stub not only improves the transmission performance of the ultra-wideband balun BPF, but also allows control over its passband width and selectivity.

***Figure 6*** shows the influence of different lengths of the short-circuit stub on transmission zeros at the cutoff frequency. The simulation results indicate that a short-circuit stub with a length of 1.74λ improves selectivity. It also shows that the resonance depth at the transmission zero is below -40 dB.

## RESULTS AND DISCUSSION

A prototype has been constructed on a substrate with a thickness of 0.762 mm, a relative permittivity of 3.66 and a loss tangent of 0.0037. The layout is shown in ***Figure 7***, with the following dimensions: $L_s$ = 20 mm, $W_s$ = 0.46 mm, $R_{rr}$ = 6.7 mm, $\theta_{rr}$ = 100 degrees, $L_{st}$ = 6.2 mm, $W_{st}$ = 1 mm, $L_g$ = 2 mm, $W_g$

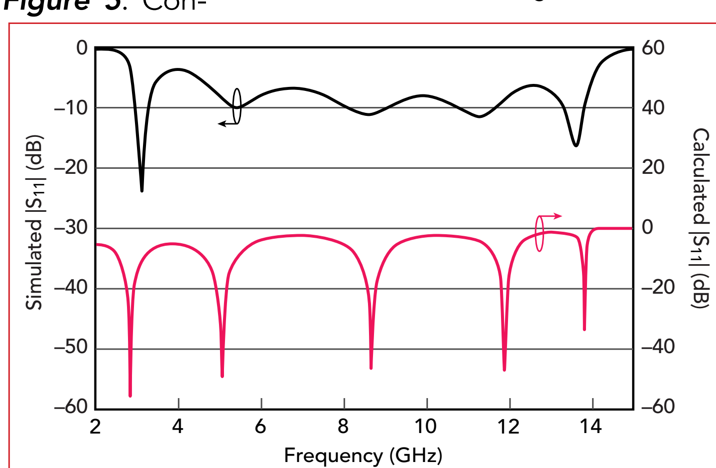


Fig. 4 Comparison of simulated with calculated $|S_{11}|$.

=1.1 mm, $L_t$ = 2.3 mm and $L_{gs}$ = 2 mm. Photographs of the prototype are shown in ***Figure 8***.

Measurements are in good agreement with electromagnetic simulation in the frequency range of 1 to 15 GHz. The center frequency is 7.93 GHz, with an absolute bandwidth of 10.38 GHz and a relative bandwidth of 131 percent. Five TPs are shown in ***Figure 9a***, which is consistent with the model. The measured amplitude imbalance (AI) is -0.39 to 0.50 dB and the PI, shown in ***Figure 9b***, is within 180 ± 5 degrees.

***Table 1*** provides a performance comparison of this work with other designs. This design achieves the highest absolute bandwidth, from 2.74 to 13.12 GHz. Furthermore, it demonstrates excellent selectivity, with a transmission zero depth at the cutoff frequency of less than -40 dB.

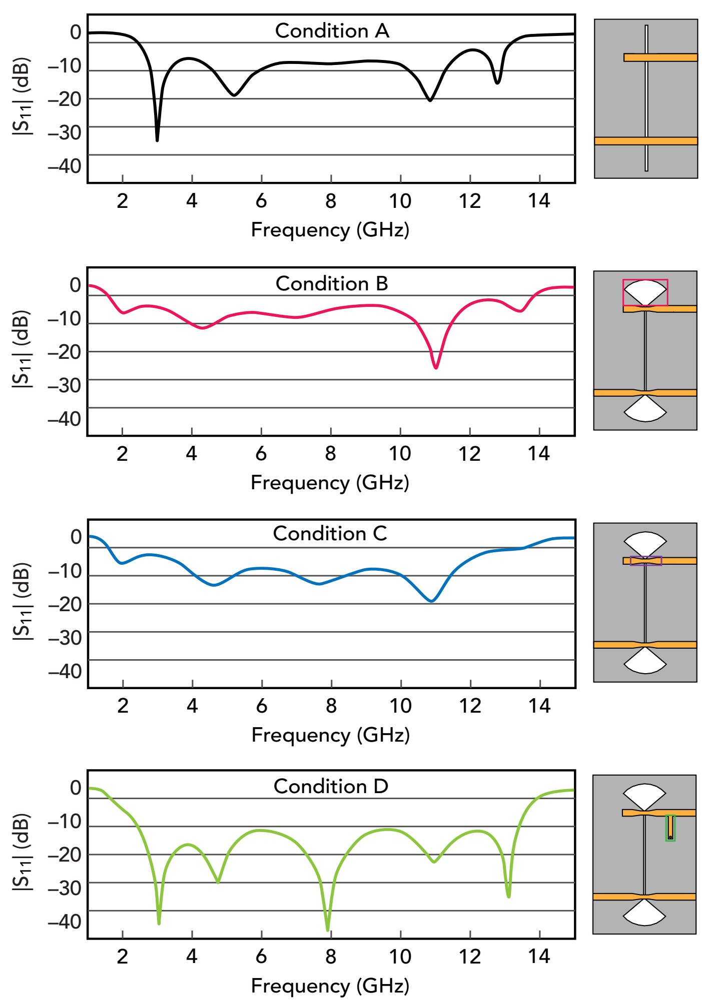


**Fig. 5** |$S_{11}$| versus frequency for different balun configurations.

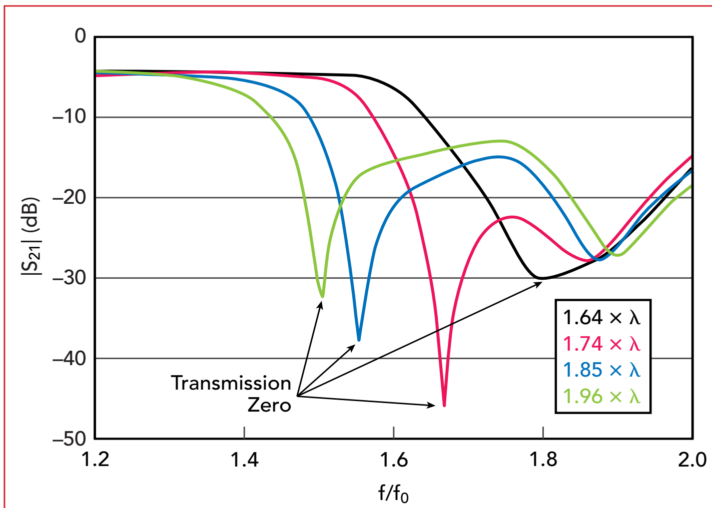


**Fig. 6** The influence of different lengths of short-circuit stubs on transmission zeros at the cut-off frequency.

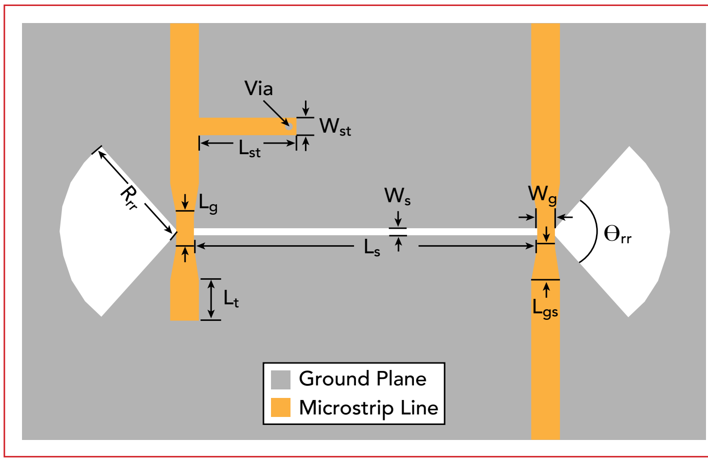


**Fig. 7** Ultra-wideband balun BPF prototype layout.

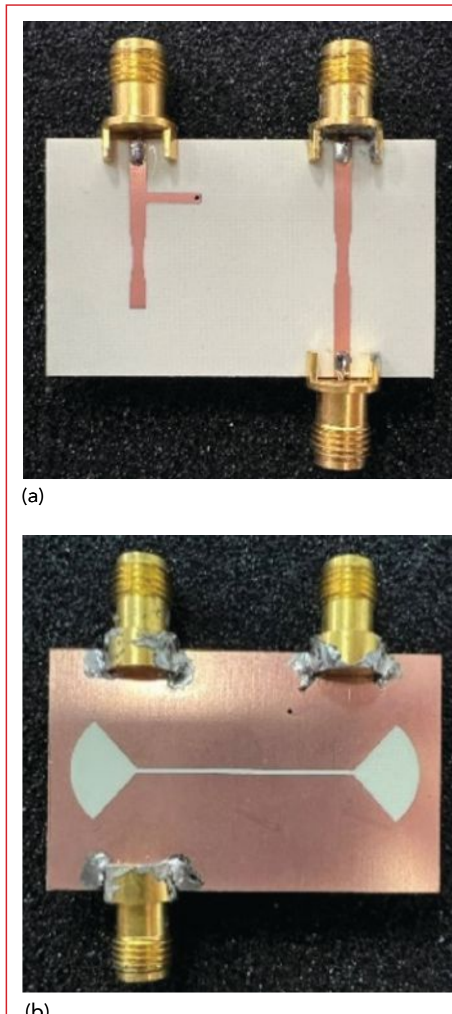


**Fig. 8** Photograph of the UWB balun BPF: top view (a) and bottom view (b).

## CONCLUSION

The use of a slotline radial stub structure is a new approach for the design of an ultra-wideband balun filter. The frequency response characteristics of the slotline radial stub are analyzed and determined to provide superior resonance effects. Additionally, the introduction of an input short-circuit stub enhances selectivity by generating transmission zeros at the cutoff frequency. Prototype test results are in good agreement with the simulation, verifying the effectiveness of the slotline radial stubs for improving in-band transmission and the input short-circuit stub for enhancing selectivity. ■

## References

1. Y. Wang, D. Zhang and Q. Wu, "A Broadband Balun with Tunable Phase-Shifting Function for Low-Cost Phased Array," *IEEE Trans-*

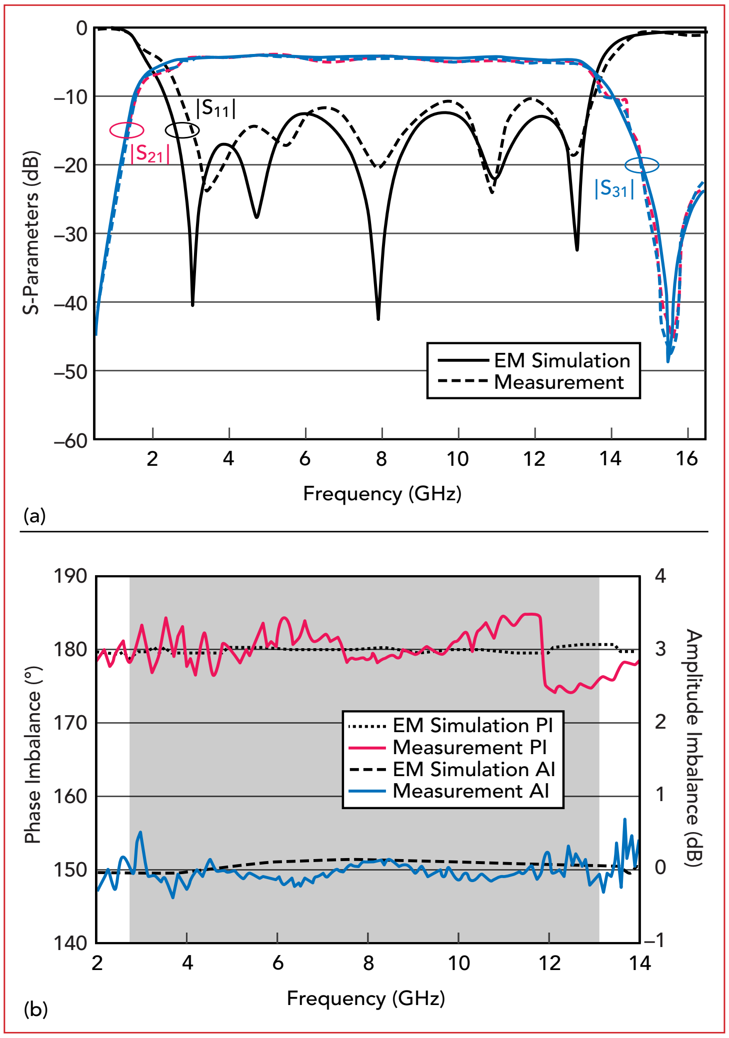


**Fig. 9** **Comparison of EM simulation results with the measurements: S-parameters (a) and AI and PI (b).**

**TABLE 1**

**PERFORMANCE COMPARISON WITH OTHER DESIGNS**

| *Ref.* | $f_0$ *(GHz)* | *FBW (%)* | *AI (dB)* | *PI (⁰)* | *TZD* (dB)* |
|---|---|---|---|---|---|
| 13 | 7.3 | 123 | 0.2 | 3.1 | -15 |
| 14 | 3.65 | 175 | 0.5 | 10 | N/A |
| 15 | 4.74 | 122 | 0.08 | 4.9 | -25 |
| 16 | 1.55 | 135 | 0.75 | 7 | -25 |
| This work | 7.93 | 131 | 0.5 | 5 | -40 |

*TZD is the transmission zero depth at the cutoff frequency.


*actions on Antennas and Propagation*, Vol. 70, No. 1, January 2022, pp. 278–287.

2. M. H. Maktoomi, H. Ren, M. N. Marbell, V. Klein, R. Wilson and B. Arigong, "A Wideband Isolated Real-to-Complex Impedance Transforming Uniplanar Microstrip Line Balun for Push–Pull Power Amplifier," *IEEE Transactions on Microwave Theory and Techniques*, Vol. 68, No. 11, November 2020, pp. 4560–4569.
3. J. L. Li, S. W. Qu and Q. Xue, "Investigation of a Compact and Broadband Balun," *Microwave and Optical Technology Letters*, Vol. 50, No. 5, May 2008, pp. 1380–1384.
4, H. -X. Xu, G. -M. Wang, X. Chen and T. -P. Li, "Broadband Balun Using Fully Artificial Fractal-Shaped Composite Right/Left-Handed Transmission Line," *IEEE Microwave and Wireless Components Letters*, Vol. 22, No. 1, January 2012, pp. 16–18.
5. C. -H. Tseng and Y. -C. Hsiao, "A New Broadband Marchand Balun Using Slot-Coupled Microstrip Lines," *IEEE Microwave and Wireless Components Letters*, Vol. 20, No. 3, March 2010, pp. 157–159.
6. D. Chen, L. Zhu, H. Bu and C. Cheng, "A Wideband Balun Filter on a Triple-Mode Slotline Resonator with Controllable Bandwidth," *IEEE Microwave and Wireless Components Letters*, Vol. 27, No. 6, June 2017, pp. 569–571.
7. L. -P. Feng and L. Zhu, "Compact Wideband Filtering Balun Using Stacked Composite Resonators," *IEEE Access*, Vol. 6, June 2018, pp. 34651–34658.
8. H. Xu, J. Wang, L. Zhu, F. Huang and W. Wu, "Design of a Dual-Mode Balun Bandpass Filter With High Selectivity," *IEEE Microwave and Wireless Components Letters*, Vol. 28, No. 1, January 2018, pp. 22–24.
9. X. Zeng, X. Bi, Z. Cao, R. Wan and Q. Xu, "High Selectivity Dual-Wideband Balun Filter Utilizing a Multimode T-line Loaded Middle-Shorted CSRR," *IEEE Transactions on Circuits and Systems II: Express Briefs*, Vol. 67, No. 11, November 2020, pp. 2447–2451.
10. W. Wang, Y. Zheng, Y. Wu and J. Ran, "Uniplanar Wideband High-Selectivity Filtering Full-Band-Isolation Baluns Using Novel Out-of-Phase Matching Phase Shifters," *IEEE Transactions on Circuits and Systems II: Express Briefs*, Vol. 69, No. 3, March 2022, pp. 954–958.
11. S. Guan, X. Bi, Q. Ma and Q. Xu, "A Wideband Balun Filter Based on Folded Ring Slotline Resonator and Dual-Feedback Stubs with >17.8 f0 Stopband Rejection," *IEEE Transactions on Circuits and Systems II: Express Briefs*, Vol. 70, No. 2, February 2023, pp. 466–470.
12. H. Zhu, Z. Cheng and Y. J. Guo, "Design of Wideband In-Phase and Out-of-Phase Power Dividers Using Microstrip-to-Slotline Transitions and Slotline Resonators," *IEEE Transactions on Microwave Theory and Techniques*, Vol. 67, No. 4, April 2019, pp. 1412–1424.
13. F. Zhu, W. Hong, J. -X. Chen and K. Wu, "Ultra-Wideband Single and Dual Baluns Based on Substrate Integrated Coaxial Line Technology," *IEEE Transactions on Microwave Theory and Techniques*, Vol. 60, No. 10, October 2012, pp. 3062–3070.
14. K. -C. Lin and Y. -C. Lin, "A Simple Printed Compensated Balun for Enhanced Ultra-Wideband Performances," *IEEE Microwave and Wireless Components Letters*, Vol. 24, No. 1, January 2014, pp. 5–7.
15. L. P. Feng and L. Zhu, "Wideband Balun Filter on Multi-Mode Resonator with Good Performance in Magnitude and Phase," *IEEE MTT-S International Wireless Symposium*, May 2018.
16. A. K. Sahoo and K. Rawat, "Design of an Ultrawideband Planar Guanella Balun," *IEEE Transactions on Instrumentation and Measurement*, Vol. 71, January 2022.